5-1-1994

Comparing color appearance models using pictorial images

Taek Gyu Kim

Comparing Color Appearance Models Using Pictorial Images

Taek Gyu Kim

B.S. Yon Sei University, Seoul, Korea (1981)
B.S. Rochester Institute of Technology (1986)

A thesis submitted for partial fulfillment
of the requirements for the degree of
Master of Science in Imaging Science in the
Center for Imaging Science in the
College of Imaging Arts & Sciences of the
Rochester Institute of Technology

May 1994

Signature of the Author

Taek Gyu Kim

Accepted by

Dana G. Marsh June 1, 1994

Coordinator, M.S. Degree Program

College of Imaging Arts & Sciences
Rochester Institute of Technology
Rochester, New York

CERTIFICATE OF APPROVAL

M.S. DEGREE THESIS

The M.S. Degree Thesis of Taek Gyu Kim
has been examined and approved
by the thesis committee
as satisfactory for the requirement for the
Master of Science degree

Dr. Roy Berns, Thesis Advisor

Dr. Mark Fairchild

Dr. Arthur J. Taggi

Ms. Lisa. Reniff

THESIS RELEASE PERMISSION FORM

Rochester Institute of Technology
Center for Imaging Science

Title of Thesis : **Comparing Color Appearance Models Using Pictorial Images**

I, Taek Gyu Kim, hereby grant permission to the Wallace Memorial Library of R.I.T. to reproduce my thesis in whole or in part. Any reproduction will not be for commercial use or profit.

Signature _____

Date 5-15-96

Comparing Color Appearance Models Using Pictorial Images

Taek Gyu Kim

Submitted for partial fulfillment
of the requirements for the degree of
Master of Science in Imaging Science in the
Center for Imaging Science in the
College of Imaging Arts & Sciences of the
Rochester Institute of Technology

ABSTRACT

Eight different color appearance models were tested using pictorial images. A psychophysical paired comparison experiment was performed where 30 color-normal observers judged reference and test images via successive-Ganzfeld haploscopic viewing such that each eye maintained constant chromatic adaptation and inter-ocular interactions were minimized. It was found that models based on von Kries had best performance, specifically CIELAB, HUNT, RLAB, and von Kries.

ACKNOWLEDGMENTS

I am very appreciative of the following sources for support in completion of this thesis:

E. I. Du Pont Company for supporting the work in every way;

Dr. Roy Berns, of RIT Center for Imaging Science, for guidance and patience;

Dr. Mark Fairchild, of RIT Center for Imaging Science, for expert advice and patience;

Dr. Arthur Taggi, of Du Pont, for guidance and editing;

Mr. Toru Hoshino, of Konica, for sharing his calibration software and data;

Mr. Tim Gallagher, of RIT Center for Imaging Science, for technical support;

each of my observers who have spent many hours judging images; and

My parents and Dukyu Kim for their endless support.

TABLE OF CONTENTS

LIST OF FIGURES

LIST OF TABLES

1. INTRODUCTION

Color appearance models must be incorporated into the color WYSIWYG (What You See Is What You Get) chain when images are viewed under dissimilar conditions such as illumination spectral power distribution and luminance, surround relative luminance, and media type where cognition is affected. These differing conditions often occur when comparing Cathode Ray Tube (CRT) and printed images, CRT and projected slides, or rear-illuminated transparencies and CRT or printed images.

Testing color-appearance models involves generating corresponding colors (in this case corresponding images) under a test and reference set of conditions. An appearance model will predict the tristimulus values for a pair of stimuli such that when each is viewed in its respective illuminating and viewing conditions, the stimuli will match in appearance for a CIE standard observer.

A psychophysical experiment was performed to test a variety of color-appearance models described in the literature. Some of these models were developed for only object colors while some were developed for use in many modalities. The following models were tested: von Kries, CIELAB, CIELUV, LABHNU (Richter), Reilly-Tannenbaum (DuPont), Hunt, Nayatani, and RLAB (Fairchild-Berns).

In practice, different devices have different spatial (resolution and image microstructure) and colorimetric (gamut) properties. It was appropriate, therefore, to first test these appearance models such that these differences were eliminated. This was accomplished by using a single device, a continuous-tone dye-diffusion thermal-transfer printer. The requisite

samples can be generated by colorimetrically characterizing the printer for both conditions.

The overview of the data flow to generate the samples is shown in Fig. 1.1.

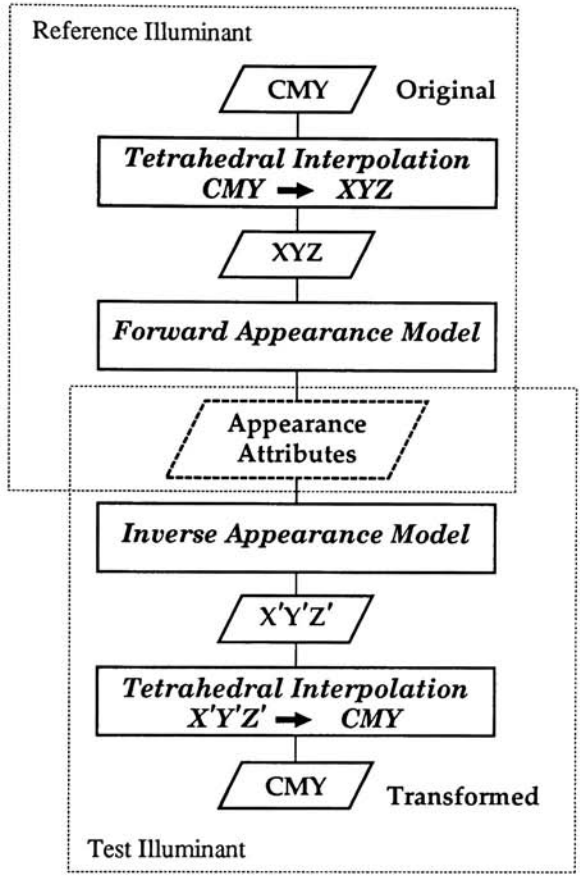

Fig. 1.1 Overview and data flow of the experiment

Selected originals in CMY (Cyan, Magenta and Yellow, See 2.2 for explanation of using CMY versus CMYK) information is transformed into tristimulus values (TSVs) for the reference illuminant using tetrahedral interpolation. The appearance attributes are calculated from the TSVs using the appearance models being tested. TSV for the test illuminant, which is the corresponding

color to the TSVs for the reference illuminant, are calculated using the inverse of the appearance model. CMY values for the given TSVs under a test illuminant are calculated using TSV to CMY tetrahedral interpolation. The steps described can be simplified by equating appearance attributes and solving for the TSV under a test illuminant. All other parameters such as white references both for the reference (X_n, Y_n, Z_n) and test illuminant (X_n', Y_n', Z_n') must be known. Hunt, Nayatani and RLAB require other parameters such as luminance level and background.

Terminology

Reference field : The reference field consists of a nonselective background and a reference sample on it. The reference field is uniformly illuminated by a specified illuminant at a specified illuminance. A medium-gray surface is used as the background.

Test field : The test field has the same gray background as the reference field. The test field is uniformly illuminated by a given illuminant at a given illuminance.

X, Y, Z or X_{ref}, Y_{ref}, Z_{ref} : Tristimulus values measured or calculated using reference illuminant.

X', Y', Z' or X_{test}, Y_{test}, Z_{test} : Tristimulus values measured or calculated using test illuminant.

X_n, Y_n, Z_n or $X_{n,ref}$, $Y_{n,ref}$, $Z_{n,ref}$: Tristimulus values of a white reference measured or calculated using reference illuminant.

X_n', Y_n', Z_n' or $X_{n,test}$, $Y_{n,test}$, $Z_{n,test}$: Tristimulus values of a white reference measured or calculated using test illuminant.

1.1 Color Appearance Models

1.1.1 von Kries

The von Kries model is the best-known simple chromatic adaptation model. It is known as the proportionality rule. In this model the cone signals are scaled by factors proportional to their excitation. The cone signals as a function of cone excitations can be expressed as:

$$\begin{aligned} L' &= k_L \cdot L \\ M' &= k_M \cdot M \\ S' &= k_S \cdot S \end{aligned} \qquad (1.1.1.1)$$

or

$$\begin{aligned} L' &= \frac{L'_n}{L_n} \cdot L \\ M' &= \frac{M'_n}{M_n} \cdot M \\ S' &= \frac{S'_n}{S_n} \cdot S \end{aligned} \qquad (1.1.1.2)$$

where L, M, and S represent the excitations of the long-, middle-, and short-wavelength sensitive cones; L', M', and S' represent the post-adaptation cone signals; L_n, M_n, S_n, L'_n, M'_n, and S'_n represent cone signals for the reference whites in reference and test fields; and k_L, k_M, and k_S , are the multiplicative factors, generally taken to be the inverse of the respective maximum cone excitations for the illuminating condition (Fairchild, 1990, 1991). The calculation of the cone fundamentals is a linear transformation of CIE tristimulus values. In this case the Stiles-Estévez-Hunt-Pointer fundamentals (Fig. 1.2) were used (see section 1.1.8.1). (These are also used in the Hunt, Nayatani, and RLAB models.)

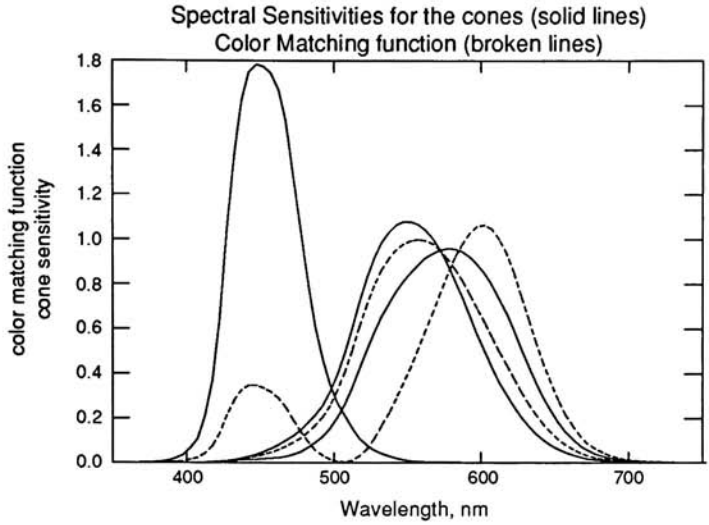

Fig. 1.2 Comparison of cone sensitivity and 1931 color matching functions

Equations used for the experiment.

Knowns for calculation.

M_{E-H-P} : Estévez-Hunt-Pointer Primaries

$X_{n,ref}$, $Y_{n,ref}$, $Z_{n,ref}$: White reference TSV for the reference field

$X_{n,test}$, $Y_{n,test}$, $Z_{n,test}$: White reference TSV for the test field

X_{ref}, Y_{ref}, Z_{ref} : TSV of corresponding color for the reference field

Unknowns are X_{test}, Y_{test}, Z_{test}

Pre-calculation

(1) Calculate cone excitations, L, M, S for the reference white

$$\begin{bmatrix} L_{n,ref} \\ M_{n,ref} \\ S_{n,ref} \end{bmatrix} = M_{E-H-P} \cdot \begin{bmatrix} X_{n,ref} \\ Y_{n,ref} \\ Z_{n,ref} \end{bmatrix} \begin{bmatrix} L_{n,test} \\ M_{n,test} \\ S_{n,test} \end{bmatrix} = M_{E-H-P} \cdot \begin{bmatrix} X_{n,test} \\ Y_{n,test} \\ Z_{n,test} \end{bmatrix} \qquad (1.1.1.3)$$

(2) Calculate von Kries multiplicative factors k_L, k_M, k_S

$$\begin{bmatrix} k_L \\ k_M \\ k_S \end{bmatrix} = \begin{bmatrix} L_{n,test} / L_{n,ref} \\ M_{n,test} / M_{n,ref} \\ S_{n,test} / S_{n,ref} \end{bmatrix} \tag{1.1.1.4}$$

Main-calculation

(1) Calculate cone excitations, L, M, S

$$\begin{bmatrix} L_{ref} \\ M_{ref} \\ S_{ref} \end{bmatrix} = M_{E-H-P} \cdot \begin{bmatrix} X_{ref} \\ Y_{ref} \\ Z_{ref} \end{bmatrix} \tag{1.1.1.5}$$

(2) Calculate cone excitations, L, M, S in test field by multipling von Kries multiplicative factors k_L, k_M, k_S from precalculation (2).

$$\begin{bmatrix} L_{test} \\ M_{test} \\ S_{test} \end{bmatrix} = \begin{bmatrix} k_L \cdot L_{ref} \\ k_M \cdot M_{ref} \\ k_S \cdot S_{ref} \end{bmatrix} \tag{1.1.1.6}$$

(3) Calculate tristimulus values from cone excitations, L, M, S

$$\begin{bmatrix} X_{test} \\ Y_{test} \\ Z_{test} \end{bmatrix} = M_{E-H-P}^{-1} \cdot \begin{bmatrix} L_{test} \\ M_{test} \\ S_{test} \end{bmatrix} \tag{1.1.1.7}$$

1.1.2 CIELAB 1976

The CIELAB space was recommended by the Commission Internationale de l'Eclairage (CIE) in 1976 for use as a color-difference metric (CIE, 1978). While CIELAB was developed to describe color differences, it also incorporates fundamental metrics of color appearance through the cylindrical specification of lightness(L^*), chroma(C_{ab}^*), and hue angle(h_{ab}) and the

inclusion of a modified form of the von Kries model of chromatic adaptation $(\frac{X}{X_n}, \frac{Y}{Y_n}, \frac{Z}{Z_n})$.

A three dimensional, approximately uniform, color space is produced by plotting the quantities L^*, a^*, b^* in rectangular coordinates. L^*, a^*, b^* are defined by the equations:

$$L^* = \begin{cases} 116\left(\frac{Y}{Y_n}\right)^{\frac{1}{3}} - 16, & \frac{Y}{Y_n} > 0.008856 \\ 903.3\left(\frac{Y}{Y_n}\right), & \frac{Y}{Y_n} \le 0.008856 \end{cases} \tag{1.1.2.1}$$

$$a^* = 500\left[f\left(\frac{X}{X_n}\right) - f\left(\frac{Y}{Y_n}\right)\right] \tag{1.1.2.2}$$

$$b^* = 200\left[f\left(\frac{Y}{Y_n}\right) - f\left(\frac{Z}{Z_n}\right)\right] \tag{1.1.2.3}$$

where

$$f(\rho) = \begin{cases} \rho^{\frac{1}{3}}, & \rho > 0.008856 \\ 7.787\rho + \frac{16}{116}, & \rho \le 0.008856 \end{cases} \tag{1.1.2.4}$$

where X, Y, Z, describe the color stimulus considered and X_n, Y_n, Z_n, describe a specified white object color stimulus.

The color difference between two stimuli can be calculated as an Euclidean distance between the points in the space.

$$\Delta E^*_{ab} = \left[(\Delta L^*)^2 + (\Delta a^*)^2 + (\Delta b^*)^2\right]^{\frac{1}{2}} \tag{1.1.2.5}$$

Correlates of lightness, chroma, and hue, are calculated.

CIE 1976 Lightness, L^*

$$L^* = \begin{cases} 116\left(\frac{Y}{Y_n}\right)^{\frac{1}{3}} - 16, & \frac{Y}{Y_n} > 0.008856 \\ 903.3\left(\frac{Y}{Y_n}\right), & \frac{Y}{Y_n} \le 0.008856 \end{cases} \quad (1.1.2.6)$$

CIE 1976 a, b chroma, C^*_{ab}

$$C^*_{ab} = \left(a^{*2} + b^{*2}\right)^{\frac{1}{2}} \quad (1.1.2.7)$$

CIE 1976 a, b hue-angle, h_{ab}

$$h_{ab} = \arctan\left(\frac{b^*}{a^*}\right) \quad (1.1.2.8)$$

CIE 1976 a, b hue-difference, ΔH^*_{ab}

$$\Delta H^*_{ab} = \left[\left(\Delta E^*_{ab}\right)^2 - \left(\Delta L^*\right)^2 - \left(\Delta C^*_{ab}\right)^2\right]^{\frac{1}{2}} \quad (1.1.2.9)$$

Equations used for the experiment.

Knowns for calculation.

$X_{n,ref}$, $Y_{n,ref}$, $Z_{n,ref}$: White reference TSV for the reference field

$X_{n,test}$, $Y_{n,test}$, $Z_{n,test}$: White reference TSV for the test field

X_{ref}, Y_{ref}, Z_{ref} : TSV of corresponding color for the reference field

Unknowns are X_{test}, Y_{test}, Z_{test}

Condition

$$\begin{bmatrix} L_{test} \\ a^*_{test} \\ b^*_{test} \end{bmatrix} = \begin{bmatrix} L_{ref} \\ a^*_{ref} \\ b^*_{ref} \end{bmatrix} \tag{1.1.2.10}$$

(1) Calculate Y

From the condition (1.1.2.10), $L_{test} = L_{ref}$,

$$Y_{test} = \frac{Y_{n,test}}{Y_{n,ref}} \cdot Y_{ref} \tag{1.1.2.11}$$

(2) Calculate X and Z

From the condition (1.1.2.10), $a^*_{test} = a^*_{ref}$ and $b^*_{test} = b^*_{ref}$

$$f_{test}\left(\frac{X}{X_n}\right) = f_{ref}\left(\frac{X}{X_n}\right) - f_{ref}\left(\frac{Y}{Y_n}\right) + f_{test}\left(\frac{Y}{Y_n}\right) \tag{1.1.2.12}$$

$$f_{test}\left(\frac{Z}{Z_n}\right) = f_{test}\left(\frac{Y}{Y_n}\right) - f_{ref}\left(\frac{Y}{Y_n}\right) + f_{ref}\left(\frac{Z}{Z_n}\right) \tag{1.1.2.13}$$

where $f(\rho)$ is defined in (1.1.2.4)

$$X_{test} = \begin{cases} f_{test}\left(\frac{X}{X_n}\right)^3 \cdot X_{n,test}, & f_{test}\left(\frac{X}{X_n}\right) > 0.008856^{\frac{1}{3}} \\ \dfrac{f_{test}\left(\frac{X}{X_n}\right) - \frac{16}{116}}{7.78 \cdot 0.008856}, & f_{test}\left(\frac{X}{X_n}\right) \le 0.008856^{\frac{1}{3}} \end{cases} \tag{1.1.2.14}$$

$$Z_{test} = \begin{cases} f_{test}\left(\frac{Z}{Z_n}\right)^3 \cdot Z_{n,test}, & f_{test}\left(\frac{Z}{Z_n}\right) > 0.008856^{\frac{1}{3}} \\ \dfrac{f_{test}\left(\frac{Z}{Z_n}\right) - \frac{16}{116}}{7.78 \cdot 0.008856}, & f_{test}\left(\frac{Z}{Z_n}\right) \le 0.008856^{\frac{1}{3}} \end{cases} \tag{1.1.2.15}$$

1.1.3 CIELUV 1976

The CIELUV space was recommended by the CIE in 1976 at the same time as CIELAB (CIE, 1978). Although it has similar perceptual metrics to CIELAB, it differs significantly in its chromatic adaptation model $(u'-u'_n,\ v'-v'_n)$.

The CIELUV formula incorporates a chromaticity diagram which is a projective transformation of the CIE x,y chromaticity diagram. A three dimensional, approximately uniform, color space is produced by plotting the quantities L^*, u^*, v^* in rectangular coordinates. L^*, u^*, v^* are defined by the equations:

$$L^* = \begin{cases} 116\cdot\left(\frac{Y}{Y_n}\right)^{\frac{1}{3}} - 16, & \frac{Y}{Y_n} > 0.008856 \\ 903.3\cdot\left(\frac{Y}{Y_n}\right), & \frac{Y}{Y_n} \le 0.008856 \end{cases} \tag{1.1.3.1}$$

$$u^* = 13\cdot L^*\cdot\left(u'-u'_n\right) \tag{1.1.3.2}$$

$$v^* = 13\cdot L^*\cdot\left(v'-v'_n\right) \tag{1.1.3.3}$$

where Y, u', v', describe the color stimulus considered and Y_n, u'_n, v'_n, describe a specified white object color stimulus.

$$u' = \frac{4X}{X+15Y+3Z} \tag{1.1.3.4}$$

$$v' = \frac{9Y}{X+15Y+3Z} \tag{1.1.3.5}$$

$$u'_n = \frac{4X_n}{X_n+15Y_n+3Z_n} \tag{1.1.3.6}$$

$$v'_n = \frac{9Y_n}{X_n+15Y_n+3Z_n} \tag{1.1.3.7}$$

The color difference between two stimuli can be calculated as an Euclidean distance between the points in the space.

$$\Delta E^*_{uv} = \left[(\Delta L^*)^2 + (\Delta u^*)^2 + (\Delta v^*)^2\right]^{\frac{1}{2}} \tag{1.1.3.8}$$

Correlates of lightness, saturation, chroma, and hue, can be calculated as follows

CIE 1976 Lightness, L^*

$$L^* = \begin{cases} 116\left(\dfrac{Y}{Y_n}\right)^{\frac{1}{3}} - 16, & \dfrac{Y}{Y_n} > 0.008856 \\ 903.3\left(\dfrac{Y}{Y_n}\right), & \dfrac{Y}{Y_n} \le 0.008856 \end{cases} \tag{1.1.3.9}$$

CIE 1976 u,v saturation, s_{uv}

$$s_{uv} = 13\left[\left(u' - u'_n\right)^2 + \left(v' - v'_n\right)^2\right]^{\frac{1}{2}} \tag{1.1.3.10}$$

CIE 1976 u,v chroma, C^*_{uv}

$$C^*_{uv} = \left(u^{*2} + v^{*2}\right)^{\frac{1}{2}} = L^* \cdot s_{uv} \tag{1.1.3.11}$$

CIE 1976 u,v hue-angle, h_{uv}

$$\begin{aligned} h_{uv} &= \arctan\left[\frac{v' - v'_n}{u' - u'_n}\right] \\ &= \arctan\left(\frac{v^*}{u^*}\right) \end{aligned} \tag{1.1.3.12}$$

CIE 1976 u,v hue-difference, ΔH^*_{ab}

$$\Delta H^*_{uv} = \left[\left(\Delta E^*_{uv}\right)^2 - \left(\Delta L^*\right)^2 - \left(\Delta C^*_{uv}\right)^2\right]^{\frac{1}{2}} \tag{1.1.3.13}$$

Equations used for the experiment.

Knowns for calculation.

$X_{n,ref}$, $Y_{n,ref}$, $Z_{n,ref}$: White reference TSV for the reference field

$X_{n,test}$, $Y_{n,test}$, $Z_{n,test}$: White reference TSV for the test field

X_{ref}, Y_{ref}, Z_{ref} : TSV of corresponding color for the reference field

Unknowns are X_{test}, Y_{test}, Z_{test}

Condition

$$\begin{bmatrix} L_{test} \\ u^*_{test} \\ v^*_{test} \end{bmatrix} = \begin{bmatrix} L_{ref} \\ u^*_{ref} \\ v^*_{ref} \end{bmatrix} \tag{1.1.3.14}$$

(1) Calculate Y

From the condition (1.1.3.14), $L_{test} = L_{ref}$,

$$Y_{test} = \frac{Y_{n,test}}{Y_{n,ref}} \cdot Y_{ref} \tag{1.1.3.15}$$

(2) Calculate X and Z

From the condition (1.1.3.14), $u^*_{test} = u^*_{ref}$ and $v^*_{test} = v^*_{ref}$

$$u'_{test} = \frac{4X_{test}}{X_{test} + 15Y_{test} + 3Z_{test}} = u'_{ref} - u'_{n,ref} + u'_{n,test} \tag{1.1.3.16}$$

$$v'_{test} = \frac{9Y_{test}}{X_{test} + 15Y_{test} + 3Z_{test}} = v'_{ref} - v'_{n,ref} + v'_{n,test} \tag{1.1.3.17}$$

By dividing (1.1.3.16) with (1.1.3.17)

$$X_{test} = \frac{9}{4} \cdot Y_{test} \cdot \left(\frac{u'_{ref} - u'_{n,ref} + u'_{n,test}}{v'_{ref} - v'_{n,ref} + v'_{n,test}}\right) \tag{1.1.3.18}$$

where u'_{ref}, $u'_{n,ref}$, $u'_{n,test}$, v'_{ref}, $v'_{n,ref}$, $v'_{n,test}$ are known using (1.1.3.4)-(1.1.3.7).

By solving (1.1.3.17) with knowns

$$Z_{test} = \frac{9Y_{test} - (X_{test} + 15Y_{test}) \cdot (v'_{ref} - v'_{n,ref} + v'_{n,test})}{3 \cdot (v'_{ref} - v'_{n,ref} + v'_{n,test})} \tag{1.1.3.19}$$

1.1.4 LABHNU 1977

The LABHNU space was developed by Klaus Richter (1980). It is similar to CIELUV in that it has an embedded chromaticity diagram and translational chromatic adaptation model. It proposed a cube-root chromaticity diagram (A', B') to take care of CIE corrections for saturated yellow and red colors in CIELAB 1976 color spaces.

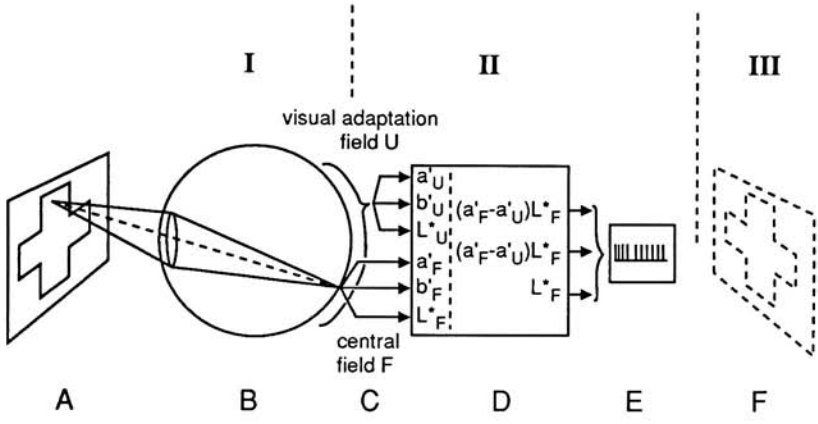

Fig. 1.3 Richter's colorimetric model of the visual process. (I) Stimulus (physics), (II) excitation (physiology), (III) sensation (psychology). (A) Illuminated object(red cross), (B) eye, (c) three signals for central and surround field, (D) transformation, (E) electric spikes, (F) perception of the object(red cross) (Richter, 1980).

From OSA model data and the Munsell system, he concluded LABHNU is a better model than CIELAB and CIELUV. The model uses CIELUV-like chromatic adapation while suggesting that incomplete adaptation can cause deviation from using a_n', b_n' as a visual adaptation field (a_U', b_U').

*note : In LABHNU upper case A and B have the same meaning as a and b .

$$L^* = 116 \cdot \left(\frac{Y}{Y_n}\right)^{1/3} - 16 \qquad (1.1.4.1)$$

$$A^* = 500 \cdot (A' - A'_n) Y^{\frac{1}{3}} \tag{1.1.4.2}$$

$$B^* = 500 \cdot (B' - B'_n) Y^{\frac{1}{3}} \tag{1.1.4.3}$$

where

$$A' = \frac{1}{4} \cdot \left(\frac{x}{y} + \frac{1}{6} \right)^{\frac{1}{3}} \quad RG\text{-chroma} \tag{1.1.4.4}$$

$$B' = \frac{-1}{12} \cdot \left(\frac{z}{y} + \frac{1}{6} \right)^{\frac{1}{3}} \quad JB\text{-chroma} \tag{1.1.4.5}$$

The following color-appearance attributes are defined.

LABHNU 1977 p-Lightness, L^*

$$L^* = 116 \cdot \left(\frac{Y}{Y_n} \right)^{1/3} - 16 \tag{1.1.4.6}$$

LABHNU 1977 (radial) Chroma, C^*_{AB}

$$C^*_{AB} = \left(A^{*2} + B^{*2} \right)^{\frac{1}{2}} \tag{1.1.4.7}$$

or

$$C^*_{AB} = 500 \cdot \left[(A' - A'_n)^2 + (B' - B'_n)^2 \right]^{\frac{1}{2}} Y^{\frac{1}{3}} \tag{1.1.4.8}$$

LABHNU 1977 Saturation, S^*_{AB}

$$S^*_{AB} = \frac{C^*_{AB}}{100 \cdot \left(\frac{Y}{100} \right)^{\frac{1}{3}}} \tag{1.1.4.9}$$

or

$$S^*_{AB} = 5 \cdot (100)^{\frac{1}{3}} \cdot \left[(A' - A'_n)^2 + (B' - B'_n)^2 \right]^{\frac{1}{2}} \tag{1.1.4.10}$$

LABHNU 1977 hue, h^*_{AB}

$$h^*_{AB} = \arctan\left(\frac{B^*}{A^*}\right) \tag{1.1.4.11}$$

LABHNU 1977 blackness, N^*_{AB}

achromatic colors

$$N^*_{AB} = 100 - L^* \tag{1.1.4.12}$$

chromatic colors

$$N^*_{AB} = 100 - L^* + k_{NL} \cdot L^* \cdot \left[\left(A' - A'_n\right)^2 + \left(B' - B'_n\right)^2\right]^{\frac{1}{2}} \tag{1.1.4.13}$$

where

$$k_{NL} = 11.6 = 2.5(100)^{\frac{1}{3}} \tag{1.1.4.14}$$

or

$$N^*_{AB} = 100 - L^* + \frac{1}{2} S^*_{AB} L^* \tag{1.1.4.15}$$

since

$$S^*_{AB} \cong \frac{C^*_{AB}}{L^*} \tag{1.1.4.16}$$

$$N^*_{AB} \cong 100 - L^* - \frac{1}{2} C^*_{AB} \tag{1.1.4.17}$$

LABHNU 1977 brilliance, I^*_{AB}

$$I^*_{AB} = 100 - N^*_{AB} \tag{1.1.4.18}$$

LABHNU 1977 deepness, D^*_{AB}

$$D^*_{AB} = 100 - L^* + \frac{1}{2} C^*_{AB} \tag{1.1.4.19}$$

Equations used for the experiment.

Knowns for calculation.

$X_{n,ref}$, $Y_{n,ref}$, $Z_{n,ref}$: White reference TSV for the reference field

$X_{n,test}$, $Y_{n,test}$, $Z_{n,test}$: White reference TSV for the test field

X_{ref}, Y_{ref}, Z_{ref} : TSV of corresponding color for the reference field

Unknowns are X_{test}, Y_{test}, Z_{test}

Condition

$$\begin{bmatrix} L_{test} \\ A^*_{test} \\ B^*_{test} \end{bmatrix} = \begin{bmatrix} L_{ref} \\ A^*_{ref} \\ B^*_{ref} \end{bmatrix} \tag{1.1.4.20}$$

(1) Calculate Y

From the condition (1.1.4.20), $L_{test} = L_{ref}$,

$$Y_{test} = \frac{Y_{n,test}}{Y_{n,ref}} \cdot Y_{ref} \tag{1.1.4.21}$$

(2) Calculate X and Z

From the condition (1.1.4.20), $A^*_{test} = A^*_{ref}$ and $B^*_{test} = B^*_{ref}$

$$A'_{test} = \frac{1}{4} \cdot \left(\frac{x_{test}}{y_{test}} + \frac{1}{6} \right)^{\frac{1}{3}} = \left(\frac{Y_{ref}}{Y_{test}} \right)^{\frac{1}{3}} (A'_{ref} - A'_{n,ref}) + A'_{n,test} \tag{1.1.4.22}$$

$$B'_{test} = \frac{-1}{12} \cdot \left(\frac{z_{test}}{y_{test}} + \frac{1}{6} \right)^{\frac{1}{3}} = \left(\frac{Y_{ref}}{Y_{test}} \right)^{\frac{1}{3}} (B'_{ref} - B'_{n,ref}) + B'_{n,test} \tag{1.1.4.23}$$

Solve for X_{test} and Y_{test} by substituting $\frac{x_{test}}{y_{test}}$ and $\frac{z_{test}}{y_{test}}$ with $\frac{X_{test}}{Y_{test}}$ and $\frac{Z_{test}}{Y_{test}}$

$$X_{test} = Y_{test} \left(\left(4 \left(\left(\frac{Y_{ref}}{Y_{test}} \right)^{\frac{1}{3}} (A'_{ref} - A'_{n,ref}) + A'_{n,test} \right) \right)^3 - \frac{1}{6} \right) \tag{1.1.4.24}$$

$$Z_{test} = Y_{test} \left(\left(-12 \left(\left(\frac{Y_{ref}}{Y_{test}} \right)^{\frac{1}{3}} (B'_{ref} - B'_{n,ref}) + B'_{n,test} \right) \right)^3 - \frac{1}{6} \right) \tag{1.1.4.25}$$

where A'_{ref}, $A'_{n,ref}$, $A'_{n,test}$, B'_{ref}, $B'_{n,ref}$, $B'_{n,test}$ are known using (1.1.4.4)-(1.1.4.5).

1.1.5 Reilly-Tannenbaum

The Reilly-Tannenbaum model was created at DuPont during the 1970's as a color difference metric. It has been used as a part of their color matching system for automotive colorant formulation and control. It has features of both CIELAB (opponency and cube root) and CIELUV (translational chromatic adaptation model) and has a transformation from CIE tristimulus values to cone fundamentals optimized from color-difference data (Fig. 1.3). It's worth noting that Reilly was one of the key developers of CIELAB; these equations reflect his influence.

Stimuli can be described with L, a, and b.

$$L = 25 \cdot G^{1/3} - 16 \tag{1.1.5.1}$$

$$a = a' - (\frac{Y}{100})^{1/3} a_n \tag{1.1.5.2}$$

$$b = b' - (\frac{Y}{100})^{1/3} b_n \tag{1.1.5.3}$$

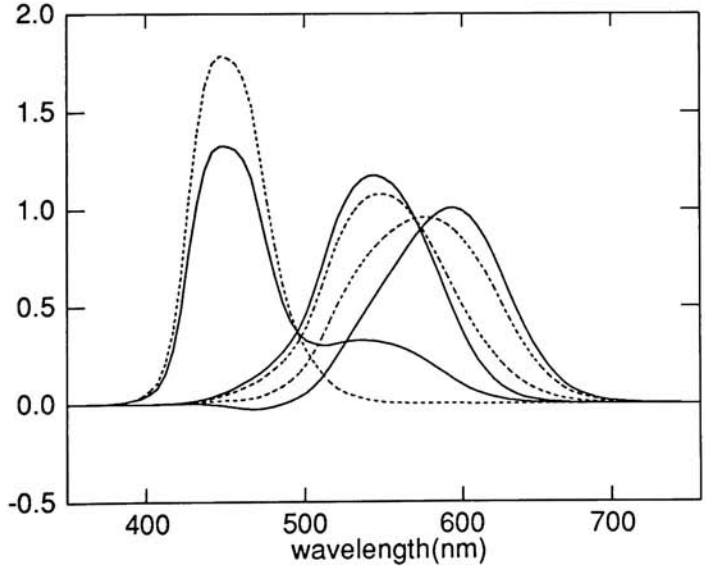

Fig. 1.4 Reilly-Tannenbaum Color Matching Functions (CMF) (solid lines) vs. Stiles-Estévez-Hunt-Pointer Cone Response functions (broken lines).

where

$$a' = 500[(\frac{R}{100})^{1/3} - (\frac{G}{100})^{1/3}] \quad (1.1.5.4)$$

$$b' = 200[(\frac{G}{100})^{1/3} - (\frac{B}{100})^{1/3}] \quad (1.1.5.5)$$

where

$$R = R'(\frac{100}{G_n}) \quad (1.1.5.6)$$

$$G = G'(\frac{100}{G_n}) \quad (1.1.5.7)$$

$$B = B'(\frac{100}{G_n}) \quad (1.1.5.8)$$

$$R' = 0.7584X + 0.2980Y - 0.1564Z \quad (1.1.5.9)$$

$$G' = -0.4632X + 1.3677Y + 0.0955Z \quad (1.1.5.10)$$

$$B' = -0.1220X + 0.3605Y + 0.7615Z \quad (1.1.5.11)$$

Equations (1.1.5.9)-(1.1.5.11) represent a transformation of XYZ to RGB using empirical primaries.

Equations used for the experiment.

Knowns for calculation.

$X_{n,ref}$, $Y_{n,ref}$, $Z_{n,ref}$: White reference TSV for the reference field

$X_{n,test}$, $Y_{n,test}$, $Z_{n,test}$: White reference TSV for the test field

X_{ref}, Y_{ref}, Z_{ref} : TSV of corresponding color for the reference field

Unknowns are X_{test}, Y_{test}, Z_{test}

Condition

$$\begin{bmatrix} L_{test} \\ a_{test} \\ b_{test} \end{bmatrix} = \begin{bmatrix} L_{ref} \\ a_{ref} \\ b_{ref} \end{bmatrix} \quad (1.1.5.12)$$

Equation (1.1.5.12) requires solving an equation of the form: $a \cdot X_{unknown} - b \cdot X_{unknown}^{\frac{1}{3}} + c = 0$. This results in very complex formula. As an

alternative a successive-approximation iterative technique (Newton-Raphson method) was used.

First, calculate appearance attributes for the reference field. With a fixed TSV in the test field, appearance attributes for the test field are calculated. Test field TSV is changed according to the differentials. Appearance attributes for the test field are calculated for the changed TSV. Repeat the change of TSV and calculation of appearance attributes until the given tolerance is achieved.

(1) Calculate the appearance attributes for the reference field.

$$\begin{bmatrix} R'_{ref} \\ G'_{ref} \\ B'_{ref} \end{bmatrix} = M_{\text{Reilly-Tannenbaum}} \cdot \begin{bmatrix} X_{ref} \\ Y_{ref} \\ Z_{ref} \end{bmatrix} \tag{1.1.5.13}$$

$$\begin{aligned} R_{ref} &= R'_{ref} \cdot (\frac{100}{G_{n,ref}}) \\ G_{ref} &= G'_{ref} \cdot (\frac{100}{G_{n,ref}}) \\ B_{ref} &= B'_{ref} \cdot (\frac{100}{G_{n,ref}}) \end{aligned} \tag{1.1.5.14}$$

$$a'_{ref} = 500[(\frac{R_{ref}}{100})^{1/3} - (\frac{G_{ref}}{100})^{1/3}] \tag{1.1.5.15}$$

$$b'_{ref} = 200[(\frac{G_{ref}}{100})^{1/3} - (\frac{B_{ref}}{100})^{1/3}] \tag{1.1.5.16}$$

$$L_{ref} = 25 \cdot G_{ref}^{1/3} - 16 \tag{1.1.5.17}$$

$$a_{ref} = a'_{ref} - (\frac{Y_{ref}}{100})^{1/3} a_{n,ref} \tag{1.1.5.18}$$

$$b_{ref} = b'_{ref} - (\frac{Y_{ref}}{100})^{1/3} b_{n,ref} \tag{1.1.5.19}$$

(2) Repeat calculation of appearance attributes (equations (1.1.5.13)-(1.1.5.19)) for the test field until the differences ($\Delta L = L_{ref} - L_{test}$, $\Delta a = a_{ref} - a_{test}$, $\Delta b = b_{ref} - b_{test}$) of attributes are within the specified tolerance (<0.15). A better estimation of TSV while iterating can be achieved using differential methods. The TSV which yielded attributes within the specified tolerance is the estimated TSV for the test field.

1.1.6 Hunt

Hunt's model (Hunt, 1987, 1990, 1991) is diagrammed in Fig. 1.5.

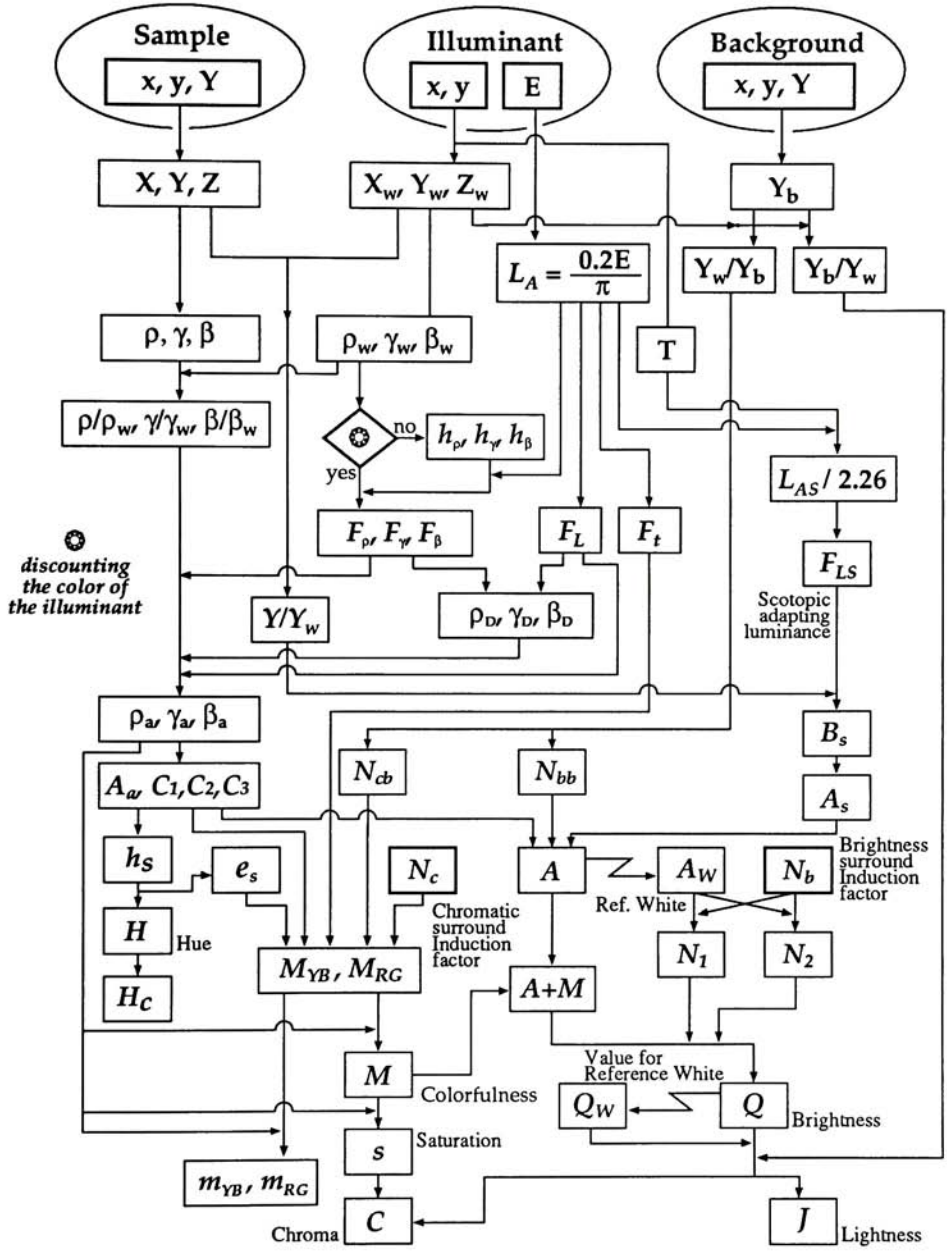

Fig. 1.5 Hunt color appearance model diagram (Modified from Nayatani, 1990)

It incorporates many parameters necessary for cross-media color reproduction. However, it is not invertible and in order to use it for color WYSIWYG, a successive-approximation iterative technique (Newton-Rapson method was used for the experiment) or a multidimensional interpolation technique (Hung, 1993) is required.

Hunt's model is somewhat based on physiology. He divided the overall process into components, and modeled each successively .

1.1.6.1 Cone excitation

The first step for the Hunt model is converting 1931 tristimulus values to ρ, γ, β tristimulus values that represent the excitation of the three cone types. The spectral sensitivitiy of the cone can be obtained by using the following transformation of the color-matching function.

$$\begin{aligned} \rho &= 0.38971X + 0.68898Y - 0.07868Z \\ \gamma &= -0.22981X + 1.18340Y + 0.04641Z \\ \beta &= 1.00000Z \end{aligned} \tag{1.1.6.1}$$

Its inverse is

$$\begin{aligned} X &= 1.91019\rho - 1.11214\gamma + 0.20195\beta \\ Y &= 0.37095\rho + 0.62905\gamma \\ Z &= 1.00000\beta \end{aligned} \tag{1.1.6.2}$$

This conversion also applies to the illuminant which appears as X_w, Y_w, Z_w to ρ_w, γ_w, β_w in Fig. 1.5. The first use of the conversion of XYZ to cone spectral sensitivities was shown in 1982. Since then the set of matrices has been chnaged (1985, 1987).

1.1.6.2 Cone Response Functions

The cone response functions are hyperbolic functions. The values have a maximum of 41 and minimum of 1. The central part is approximately a square root relationship, while the +1 term represents the noise of the system.

$$f_n(\rho)+1 = 40[\rho^{0.73} / (\rho^{0.73}+2)]+1 \quad (1.1.6.3)$$

$$f_n(\gamma)+1 = 40[\gamma^{0.73} / (\gamma^{0.73}+2)]+1 \quad (1.1.6.4)$$

$$f_n(\beta)+1 = 40[\beta^{0.73} / (\beta^{0.73}+2)]+1 \quad (1.1.6.5)$$

Equation 1.1.6.3 is plotted in Fig. 1.6.

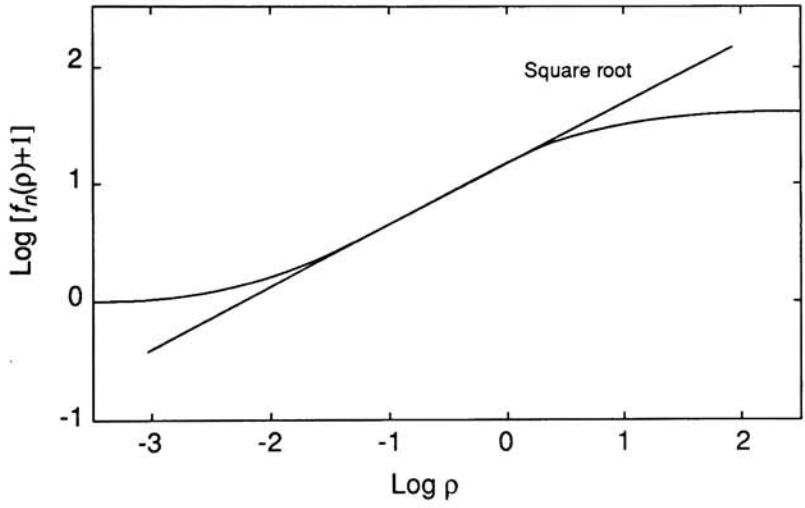

Fig. 1.6 Cone Response function of Hunt appearance model

1.1.6.3 Adaptation

Adaptation consists of a chromatic adaptation factor, F_ρ, F_γ, F_β, a luminance adaptation factor, F_L, a von Kries type of allowance, ρ/ρ_w, γ/γ_w, β/β_w, Helson-Judd effect factors, ρ_D, γ_D, β_D, and cone bleach factors, B_ρ, B_γ,

B_β. The luminance adaptation factor, chromatic adaptation factors and components of von Kries type allowance occur at an early stage in the retina, while the Helson-Judd effect happens extremely fast at a later stage .

$$\rho_a = B_\rho[f_n(F_L F_\rho \rho / \rho_W) + \rho_D] + 1 \tag{1.1.6.6}$$

$$\gamma_a = B_\gamma[f_n(F_L F_\gamma \gamma / \gamma_W) + \gamma_D] + 1 \tag{1.1.6.7}$$

$$\beta_a = B_\beta[f_n(F_L F_\beta \beta / \beta_W) + \beta_D] + 1 \tag{1.1.6.8}$$

This step is shown as ρ, γ, β to ρ_a, γ_a, β_a in Fig. 1.5.

1.1.6.4 Criteria for Achromacy and for Constant Hue

Based on physiological evidence that three different cone types are compared by neurons, color difference signals are introduced. C_1, C_2, C_3 representing Color-difference signals.

$$C_1 = \rho_a - \gamma_a \tag{1.1.6.9}$$

$$C_2 = \gamma_a - \beta_a \tag{1.1.6.10}$$

$$C_3 = \beta_a - \rho_a \tag{1.1.6.11}$$

Achromatic colors are those which are devoid of hue such as white, greys, and black. Therefore the criterion for the achromacy is $\rho_a = \gamma_a = \beta_a$. This results in $C_1 = C_2 = C_3 = 0$, and one can expect that colourfulness increases as C_1, C_2 and C_3 increase.

1.1.6.5 Cone Bleach Factors

At very high level of illumination a cone reduces it's response. It is defined as follows:

$$B_\rho = 10^7 / [10^7 + 5L_A(\rho_W / 100)] \quad (1.1.6.12)$$

$$B_\gamma = 10^7 / [10^7 + 5L_A(\gamma_W / 100)] \quad (1.1.6.13)$$

$$B_\beta = 10^7 / [10^7 + 5L_A(\beta_W / 100)] \quad (1.1.6.14)$$

where L_A is the luminance of the adapting field. In typical viewing conditions, luminance of the reference white is about five times that of the adapting field (assumes the world integrates to a gray of 0.2 luminance factor). Therefore $5L_A$ can be regarded as luminance of the reference white. When the cone pigments are bleached, their spectral absorptions can become narrower, and as a result metameric color matches can break down.

1.1.6.6 Luminance-Level Adaptation Factor, F_L

This factor provides allowance for the level of illumination. It is defined as:

$$F_L = 0.2k^4(5L_A) + 0.1(1-k^4)^2(5L_A)^{1/3} \qquad k = 1/(5L_A + 1) \quad (1.1.6.15)$$

At photopic levels F_L is proportional to the cube root of $5L_A$, and at scotopic levels F_L is proportional to $5L_A$. L_A represents the luminance of the adapting field.

$$F_L \propto \begin{cases} \text{Phtotopic levels} & (5L_A)^{1/3} \\ \text{Scotopic levels} & (5L_A) \end{cases} \quad (1.1.6.16)$$

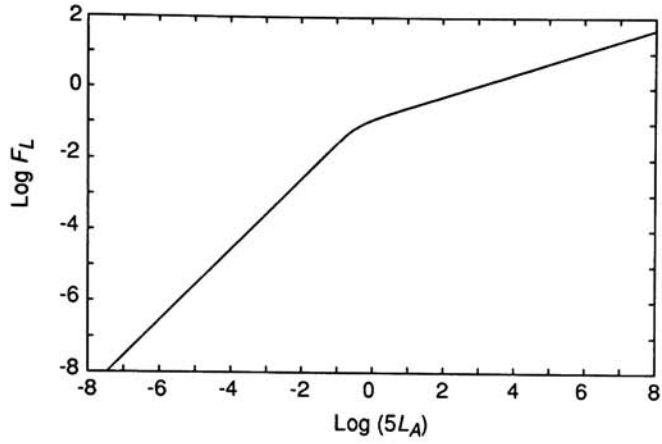

Fig. 1.7 Luminance level adaptation factor.

1.1.6.7 Color differences vs. other factors

If $5L_A$ is the luminance of the reference white, and the sample has the same chromaticity as the reference white, then $5L_A\rho/\rho_W$ is equal to the luminance of the sample. The open circles in the Fig. 1.8 represent colors having the same value of ρ/ρ_W as for the reference white, and the filled circles for a color having ρ/ρ_W equal to 0.03162 time that of the reference white (1.5 less on the log scale). The part between open and filled circle represents the range of colors between white and a black. The position of the adapting field is shown by the plus(+) sign. The range of colors increases as luminance level increases up to certain level. Lower maxima of curves 6, 7 and 8 in the Fig. 1.8 are caused by the cone bleach factors($B_\rho, B_\gamma, B_\beta$).

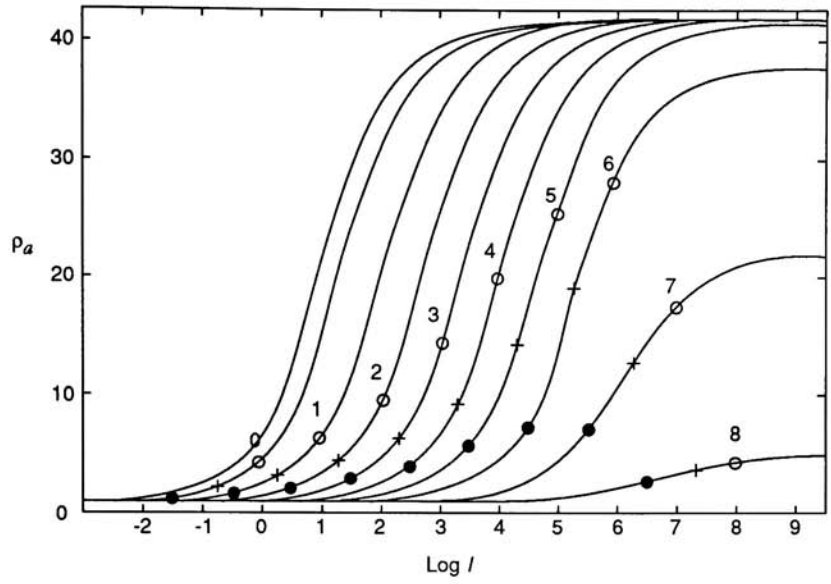

Fig. 1.8 Response funtion for the ρ cones.

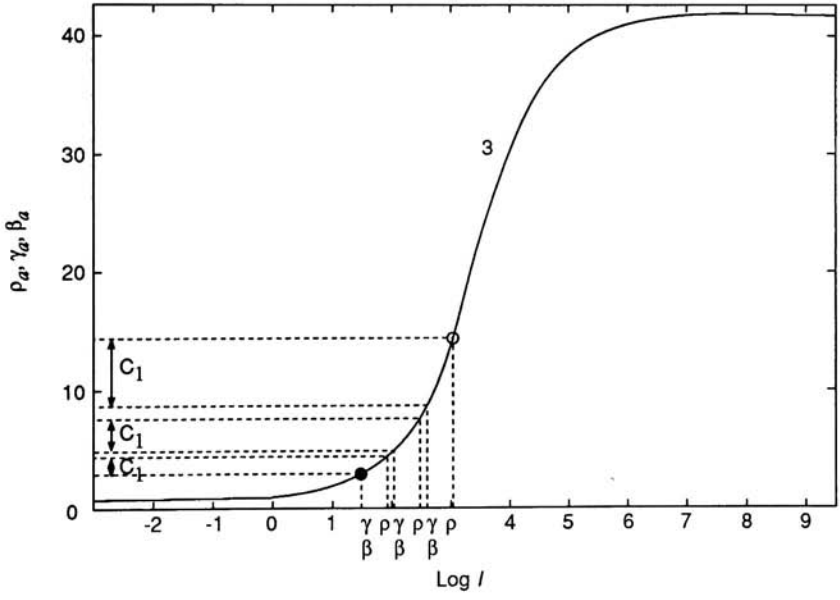

Fig. 1.9 Representations of three stimuli having the same chromaticity but three different luminance factors.

From the shape of the adpatation curve, it is predicted that for colors of a given chromaticity (red as an example in the Fig. 1.8), as the luminance factor is decreased, the colorfulness will usually decrease.

As the luminance of the adapting field decreases, the curves move to the left, indicating increasing sensitivity. But the increase of sensitivity is insufficient to provide full compensation. Therefore the positions of white, the adapting field and black gradually move down to the regions of lower slope. This results in reduction in the differences in response between whites, adapting fields, and blacks. For colors, this results in reduced colorfulness and discrimination.

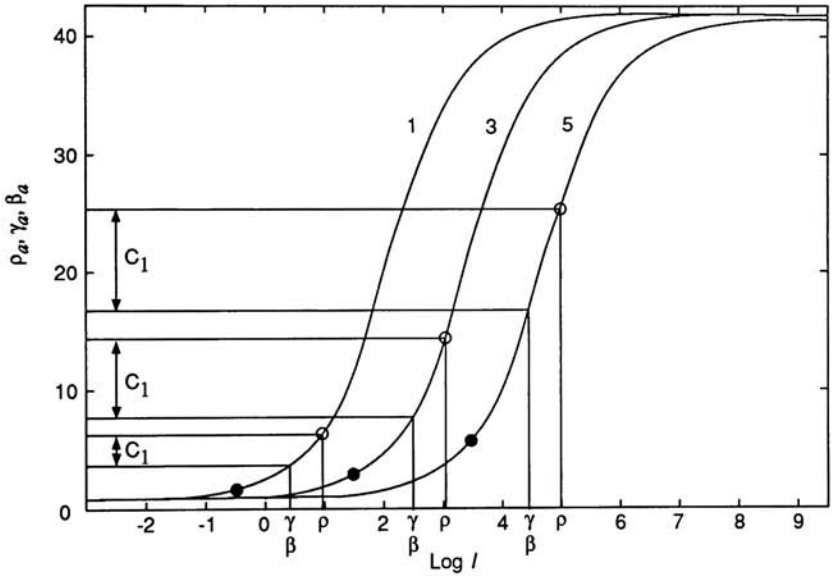

Fig. 1.10 Representations of a color of the same chromaticity and luminance factor in the three different leveles of adapting luminance.

1.1.6.8 Chromatic Adaptation Factors

Adaptation to lights of different colors becomes less and less complete as the purity of the color of the light increases, and more and more complete as the luminance increases. This leads to change of extent of the adaptation.

To take into account the *discounting the color of the illuminant* effect, F_ρ, F_γ, F_β have to be set to unity (yes at decision ❂ in the Fig. 1.5).

$$F_\rho = (1 + L_A^{1/3} + h_\rho) / (1 + L_A^{1/3} + 1/h_\rho) \quad (1.1.6.17)$$

$$F_\gamma = (1 + L_A^{1/3} + h_\gamma) / (1 + L_A^{1/3} + 1/h_\gamma) \quad (1.1.6.18)$$

$$F_\beta = (1 + L_A^{1/3} + h_\beta) / (1 + L_A^{1/3} + 1/h_\beta) \quad (1.1.6.19)$$

where

$$h_\rho = 3\rho_W / (\rho_W + \gamma_W + \beta_W) \quad (1.1.6.20)$$

$$h_\gamma = 3\gamma_W / (\rho_W + \gamma_W + \beta_W) \quad (1.1.6.21)$$

$$h_\beta = 3\beta_W / (\rho_W + \gamma_W + \beta_W) \quad (1.1.6.22)$$

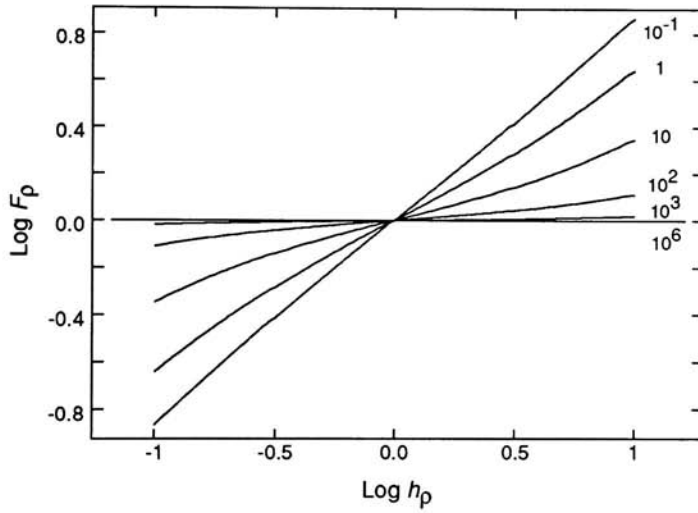

Fig. 1.11 Chromatic adaptation factor.

1.1.6.9 Helson-Judd Effect Factors

When the chromaticity of the illuminant is substantially different from that of the equi-energy stimulus, S_E, white colors tend to appear to be tinged with the hue of the illuminant, and very dark greys with the

complementary hue (Helson-Judd effect). The Helson-Judd effect parameters are defined as:

$$\rho_D = f_n[(Y_b / Y_W)F_L F_\gamma] - f_n[(Y_b / Y_W)F_L F_\rho] \quad (1.1.6.23)$$

$$\gamma_D = 0 \quad (1.1.6.24)$$

$$\beta_D = f_n[(Y_b / Y_W)F_L F_\gamma] - f_n[(Y_b / Y_W)F_L F_\beta] \quad (1.1.6.25)$$

1.1.6.10 Modified Reference White

When simultaneous contrast occurs, the proximal field, which is the immediate environment, causes the appearance of the color element considered to move towards the color that is opposite in hue, saturation, and lightness to the color of the proximal field. But if the the annular subtense of the color element considered becomes less than about a third of a degree, assimulation occurs instead of simultaneous contrast.

$$\rho'_W = \frac{\rho_W[(1-p)r + (1+p)/r]^{1/2}}{[(1+p)r + (1-p)/r]^{1/2}} \quad (1.1.6.26)$$

$$\gamma'_W = \frac{\gamma_W[(1-p)g + (1+p)/g]^{1/2}}{[(1+p)g + (1-p)/g]^{1/2}} \quad (1.1.6.27)$$

$$\beta'_W = \frac{\beta_W[(1-p)b + (1+p)/b]^{1/2}}{[(1+p)b + (1-p)/b]^{1/2}} \quad (1.1.6.28)$$

where

$$r = (\rho_p / \rho_b) \quad (1.1.6.29)$$

$$g = (\gamma_p / \gamma_b) \quad (1.1.6.30)$$

$$b = (\beta_p / \beta_b) \quad (1.1.6.31)$$

where

ρ_p, γ_p and β_p: ρ, γ and β signals for the proximal field.

ρ_b, γ_b and β_b: ρ, γ and β signals for the background.

1.1.6.11 Unique Hues

Hunt defines four unique hues such as red, green, yellow and blue by defining a ratio of two color differences.

Unique red	$C_1=C_2$	(1.1.6.32)
Unique green	$C_1=C_3$	(1.1.6.33)
Unique yellow	$C_1=C_2/11$	(1.1.6.34)
Unique blue	$C_1=C_2/4$	(1.1.6.35)

Because $C_1+C_2+C_3=0$, if one of these ratios is constant, the other will also be constant, and it is unnecessary to specify in addition. Fig. 1.12 shows the comparsion of unique hues of the Hunt model and the Natural Color System.

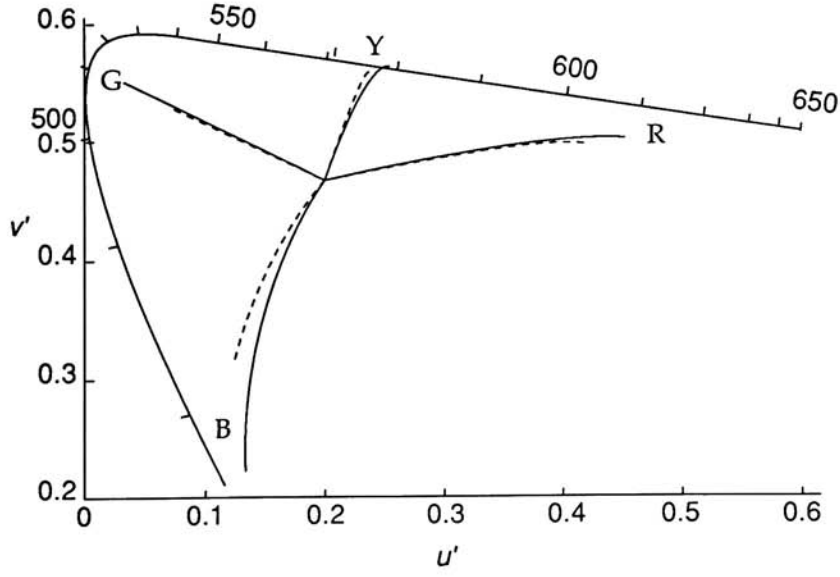

Fig. 1.12 Unique hue loci predicted by the model(solid lines) compared with those of the NCS(dotted lines), for Standard Illuminant C.

1.1.6.12 Hue Angle, h_s

The hue angle coefficient is measure of hue. It describes color by how much an angle deviates from the unique hues. A measure of the yellowness or blueness of both reddish and greenish color is average of two differences: $\frac{1}{2}(C_2\text{-}C_3) = \frac{1}{2}(C_2\text{-}C_1\text{+}C_1\text{-}C_3)$. The redness or greenness measure is different for the yellowish $C_1-(C_2/11)$, and bluish $C_1-(C_2/4)$. Since the yellow hue is more sharply apparent than the unique blue hue, one for the yellowish is used instead of taking their average.

$$h_s = \arctan\left(\frac{\frac{1}{2}(C_2-C_3)/4.5}{C_1-(C_2/11)}\right) \qquad (1.1.6.36)$$

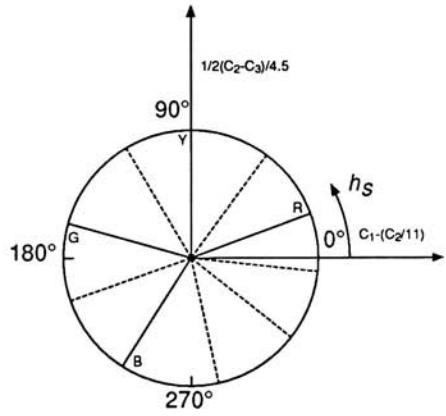

Fig. 1.13 Hue angle, h_s.

1.1.6.13 Eccentricity factor, e_s

This factor is introduced to allow for the asymmetry with which the visual system treats red and green colors, and for the asymmetry with which it treats blue and yellow colors. The values of e_s were deduced from the

eccentricity of illuminant points in loci of constant but very low saturation (Hunt, 1985).

TABLE 1.1 e_1 and h_1

	Red	Yellow	Green	Blue
h_s	20.14	90.00	164.25	237.53
e_s	0.8	0.7	1.0	1.2

$$e_s = e_1 + (e_2 - e_1)(h_s - h_1)/(h_2 - h_1) \qquad (1.1.6.37)$$

e_1 and h_1 are the values of e_s and h_s, respectively, for the unique hue having the nearest lower value of h_s; and e_2 and h_2 are the values of e_s and h_s, respectively, for the unique hue having the nearest higher value of h_s.

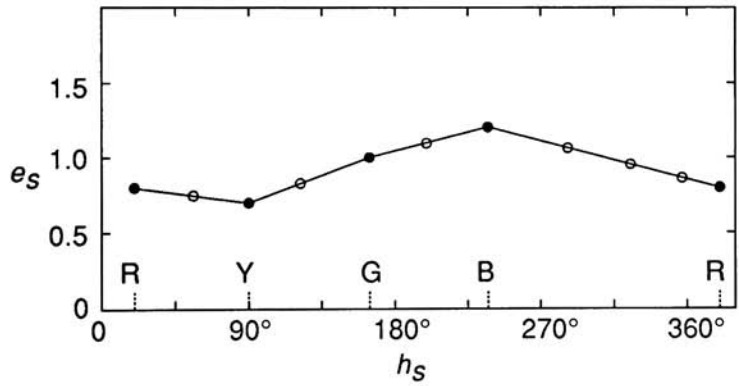

Fig. 1.14 Eccentricity factor, e_s.

1.1.6.14 Hue quadrature, H, and Hue composition, H_C

Hue quadrature expresses color in terms of the proportions of the unique hues. It is a transformation of a hue angle to a quadrant of which axes

are unique hues. The four quadrants do not represent equal differences in hue.

$$H = H_1 + \frac{100[(h_s - h_1)/e_1]}{[(h_s - h_1)/e_1 + (h_2 - h_s)/e_2]} \qquad (1.1.6.38)$$

H_1 is 0, 100, 200, or 300, according to whether red, yellow, green, or blue respectively, is the hue having the nearest lower value of h_s.

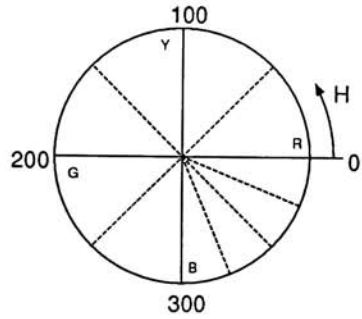

Fig. 1.15 Hue quadrature, H.

Hue can be expressed as number and hue composition, H_C, in terms of the percentages of the component hues. If H is 262, H_C can be expressed as 62B 38G.

1.1.6.15 Correlates of Colourfulness, M, and Saturation, s

Colorfulness, M, is the measure of which hue is how dominant. It is described as yellowness-blueness, M_{YB}, and redness-greeness, M_{RG}.

$$M_{YB} = 100[\frac{1}{2}(C_2 - C_3)/4.5][e_s(10/13)N_c N_{cb} F_t] \qquad (1.1.6.39)$$

$$M_{RG} = 100[C_1 - (C_2/11)][e_s(10/13)N_c N_{cb}] \qquad (1.1.6.40)$$

Correlates of colourfulness, M, and saturation, s, are given by

$$M = (M_{YB}^{\ 2} + M_{RG}^{\ 2})^{1/2} \tag{1.1.6.41}$$

$$s = 50M / (\rho_a + \gamma_a + \beta_a) \tag{1.1.6.42}$$

$$M_{93} = F_L^{0.15} C_{93} \tag{1.1.6.43}$$

Colorfulness consists of several components and those are listed as follows:

1. Eccentricity factor, e_s.

2. A factor of 10/13 to allow for cross-channel noise in the system

3. A chromatic surround induction factor, N_c, is used which makes allowance for the fact that dark or dim surrounds to colours can reduce their colourfulness.

TABLE 1.2 Brightness(N_b) and chromatic(N_c) induction factor.

	N_b	N_c
Small areas in uniform light backgrounds and surrounds	300	1.0
Normal scenes	75	1.0
Television and VDU displays in dim surrounds	25	0.95
Projected photographs in dark surrounds	10	0.9
Arrays of adjacent colours in dark surrounds	5	0.75
CRT's in dim surrounds		1.0
Large transparencies on viewers		0.7
Projected slides		0.7

4. A low-luminance tritanopia factor, F_t, is included in the yellowness-blueness signal, to allow for the fact that, as the illumination level falls, yellowness-blueness discrimination deteriorates earlier than redness-greenness discrimination.

$$F_t = L_A / (L_A + 0.1) \qquad (1.1.6.44)$$

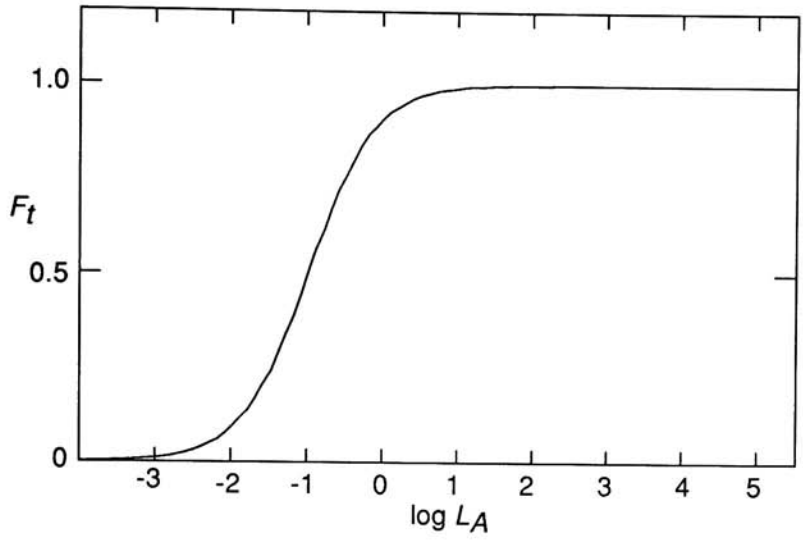

Fig. 1.16 Low luminance tritanopia factor, F_t.

5. A chromatic background induction factor, N_{cb}, is included to allow for the fact that, compared with their appearance when seen against a grey background, the colourfulness of colors tends to be reduced for light backgrounds, and increased for dark backgrounds.

$$N_{cb} = 0.725(Y_W / Y_b)^{0.2} \qquad (1.1.6.45)$$

1.1.6.16 Rod Response

The rod response function is same as for cone, except the scotopic luminance-level adaptation factor, F_{LS}, is used instead of the luminance-level adaptation factor:

$$F_{LS} = 3800 j^2 5L_{AS} / 2.26 + 0.2(1 - j^2)^4 (5L_{AS} / 2.26)^{1/6} \qquad (1.1.6.46)$$

where

$$j = 0.00001 / (5L_{AS} / 2.26 + 0.00001) \tag{1.1.6.47}$$

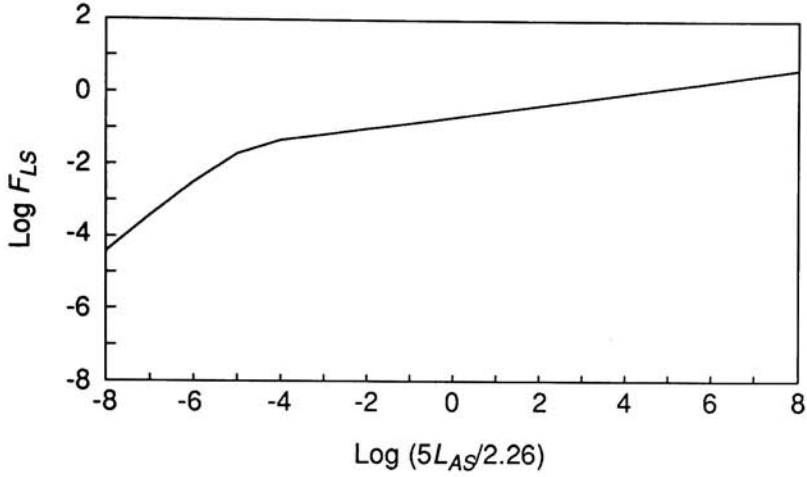

Fig. 1.17 Scotopic luminance level adaptation factor.

The scotopic adapting luminance, L_{AS}, could be unknown and it is not that important to know accurately. The correlated color temperature, T, is used if the adapting field has a chromaticity not too far from that of the Plankian locus. At T=5600, $L_{AS} / 2.26$ for the equi-energy stimulus, S_E, is equal to L_A. Because of it, $L_{AS} / 2.26$ is used instead of L_{AS}.

$$L_{AS} / 2.26 = L_A (T / 4000 - 0.4)^{1/3} \tag{1.1.6.48}$$

To set an upper limit of the rod response, B_S, at high levels of adaptation, the rod bleach factor is introduced.

$$B_S = \frac{0.5}{1 + 0.3 \cdot \left[\left(\frac{5 \cdot L_{AS}}{2.26} \right) \left(\frac{S}{S_W} \right) \right]^{0.3}} + \frac{0.5}{1 + 5 \cdot \left[\frac{5 \cdot L_{AS}}{2.26} \right]} \tag{1.1.6.49}$$

The rod response after adaptation is as follows.

$$A_S = B_S \cdot 3.05 \cdot [f_n(F_{LS} \cdot S / S_W)] + 0.3 \qquad (1.1.6.50)$$

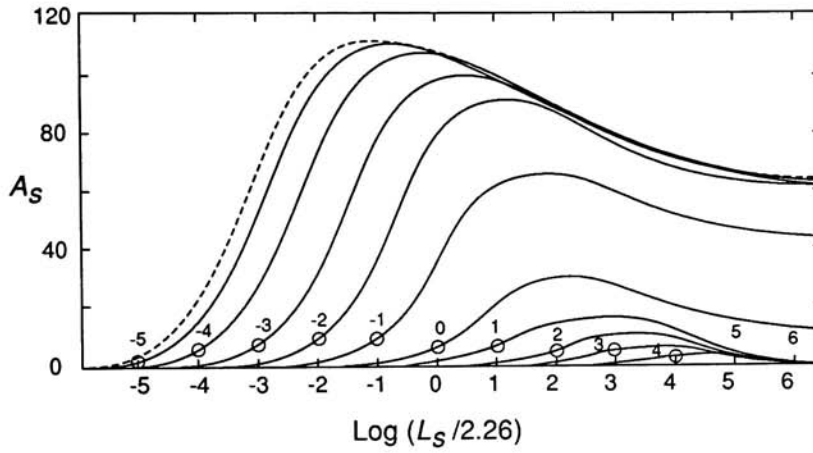

Fig. 1.18 Response function for the rods.

1.1.6.17 Achromatic Response, *A*

The photopic part of the achromatic signal is

$$A_a = 2\rho_a + \gamma_a + (1/20)\beta_a - 3.05 + 1 \qquad (1.1.6.51)$$

The total achromatic signal is

$$A = N_{bb}[A_a - 1 + A_S - 0.3 + (1^2 + 0.3^2)^{1/2}] \qquad (1.1.6.52)$$

N_{bb} is a factor to allow for the brightness induction of the background.

$$N_{bb} = 0.725(Y_W / Y_b)^{0.2} \qquad (1.1.6.53)$$

1.1.6.18 Relative Yellowness-Blueness, m_{YB}, and Relative Redness-Greeness, m_{RG}

$$m_{YB} = M_{YB}(\rho_a + \gamma_a + \beta_a) \tag{1.1.6.54}$$

$$m_{RG} = M_{RG}(\rho_a + \gamma_a + \beta_a) \tag{1.1.6.55}$$

1.1.6.19 Correlates of Brightness, Q

The brightness response is mainly from the achromatic signal, but in consideration of the Helmholtz-Kohlrausch effect, which is the increase in brightness with increasing purity for colors of constant luminance, a color difference signal is added.

$$Q = \{7[A + (M/100)]\}^{0.6} N_1 - N_2 \tag{1.1.6.56}$$

where

$$N_1 = (7A_W)^{0.5} / (5.33N_b^{0.13}) \tag{1.1.6.57}$$

$$N_2 = 7A_W N_b^{0.362} / 200 \tag{1.1.6.58}$$

where A_W is total achromatic signal for the reference white.

1.1.6.20 Correlates of Lightness

Lightness is brightness judged relative to that of the reference white.

$$J = 100(Q / Q_W)^z \tag{1.1.6.59}$$

where

$$z = 1 + (Y_b / Y_W)^{1/2} \tag{1.1.6.60}$$

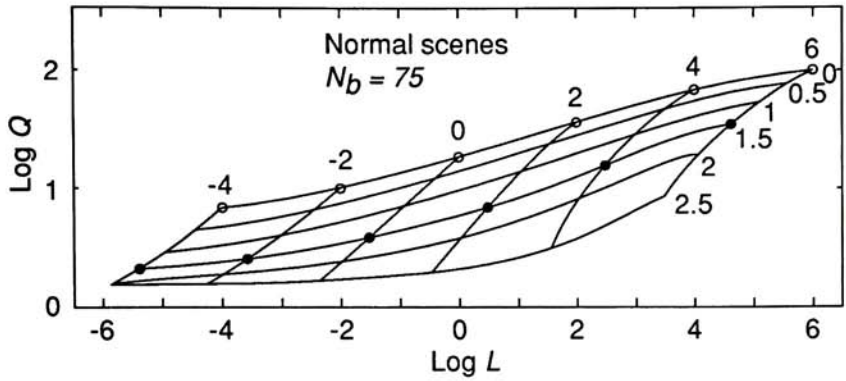

Fig. 1.19 Brightness-luminance relationships.

1.1.6.21 Correlates of Chroma

The correlate of chroma, C, includes a luminance factor, Y_b, of the background and Y_W of the reference white.

$$C = 4s^{0.69}(Q / Q_W)^{Y_b/Y_W}(1.31 - 0.31^{Y_b/Y_W}) \quad (1.1.6.61)$$

$$C_{93} = 2.44s^{0.69}(Q / Q_W)^{Y_b/Y_W}(1.64 - 0.29^{Y_b/Y_W}) \quad (1.1.6.62)$$

* note by Hunt : C and C_{93} are similar for grey backgrounds of Y_b / Y_w equal to about 0.2 but C_{93} is better for white and black background

1.1.6.22 Correlates of Whiteness-Blackness

Nayatani introduced the concept of a whiteness-blackness (1987). Hunt adopted it in his model.

$$Q_{WB} = 20(Q^{0.7} - Q_b^{0.7}) \quad (1.1.6.63)$$

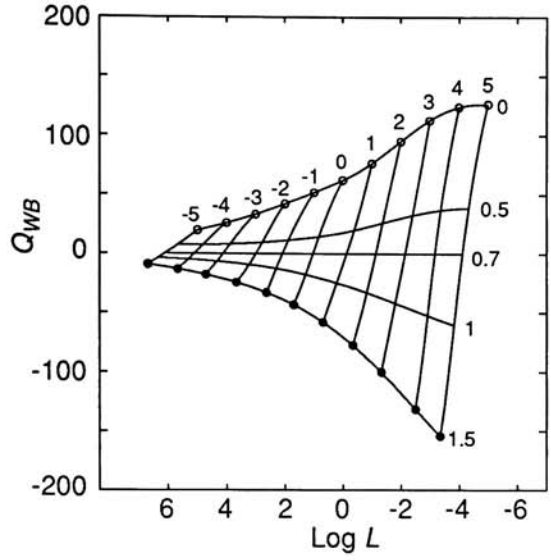

Fig. 1.20 Whiteness-blackness, Q_{WB}.

The Fig. 1.19 shows that the illumination level increases, the whiteness of the whites increases and the blackness of the blacks decreases (Steven's effect). For example, projected slide are viewed with dark surround and require a contrast ratio more than 3.0 (1000:1), while viewing hard copy in a viewing booth requires contrast ratio less than 2.0 (100:1).

Equations used for the experiment.

Knowns for calculation.

M_{E-H-P} : Estévez-Hunt-Pointer Primaries

$X_{n,ref}$, $Y_{n,ref}$, $Z_{n,ref}$: White reference TSV for the reference field

$X_{n,test}$, $Y_{n,test}$, $Z_{n,test}$: White reference TSV for the test field

X_{ref}, Y_{ref}, Z_{ref} : TSV of corresponding color for the reference field

Surround information

Y_b : Background luminace

Y_w : Reference white luminace

N_b : Brightness induction factor

N_c : Chromatic induction factor

Unknowns are X_{test}, Y_{test}, Z_{test}

Pre-calculation

The following terms are calculated for both reference and test fields: Subscripts (*ref, test*) are omitted.

(1) *Cone excitations of reference white* : ρ_w, γ_w, β_w

$$\begin{bmatrix} \rho_w \\ \gamma_w \\ \beta_w \end{bmatrix} = M_{E-H-P} \bullet \begin{bmatrix} X_n \\ Y_n \\ Z_n \end{bmatrix} \tag{1.1.6.64}$$

(2) *Luminance of adapting field* : L_A

$$L_A = 0.2 \cdot L_w \tag{1.1.6.65}$$

where L_w is luminance of reference white

(3) *Scotopic adapting Luminance* : L_{AS}

$$L_{AS} = 2.26 \cdot L_A \cdot (T / 4000 - 0.4)^{1/3} \tag{1.1.6.66}$$

where T is correlated color temperature

(4) *Brightness induction factor* : N_{cb}

$$N_{cb} = 0.725(Y_W / Y_b)^{0.2} \tag{1.1.6.45}$$

(5) *Chromatic induction of background factor* : N_{bb}

$$N_{bb} = 0.725(Y_W / Y_b)^{0.2} \tag{1.1.6.53}$$

(6) *Luminance-Level adaptation factor* : F_L

$$F_L = 0.2 \cdot k^4 \cdot (5 \cdot L_A) + 0.1 \cdot (1 - k^4)^2 (5 \cdot L_A)^{1/3}$$
$$k = 1/(5 \cdot L_A + 1) \qquad (1.1.6.15)$$

where $5 \cdot L_A$ is same as L_w (1.1.6.64) in this experiment.

(7) *Chromatic adaptation factor* : F_ρ, F_γ, F_β

$$F_\rho = F_\gamma = F_\beta = 1.0 \qquad (1.1.6.67)$$

* Because hardcopy was used, full discounting of the color of the illuminant was assumed.

(8) *Helson-Judd Effect factor* : ρ_D, γ_D, β_D

$$\rho_D = 0$$
$$\gamma_D = 0 \quad \text{for discounting} \qquad (1.1.6.23\text{-}1.1.6.25)$$
$$\beta_D = 0$$

(9) *Cone Bleach factor* : B_ρ, B_γ, B_β

$$B_\rho = 10^7 / [10^7 + 5 \cdot L_A \cdot (\rho_w / 100)]$$
$$B_\gamma = 10^7 / [10^7 + 5 \cdot L_A \cdot (\gamma_w / 100)] \qquad (1.1.6.12\text{-}1.1.6.14)$$
$$B_\beta = 10^7 / [10^7 + 5 \cdot L_A \cdot (\beta_w / 100)]$$

(10) *Adaptation factors of reference white* ρ_a, γ_a, β_a .

$$\rho_{a,w} = B_\rho \cdot [f_n(F_L \cdot F_\rho) + \rho_D] + 1$$
$$\gamma_{a,w} = B_\gamma \cdot [f_n(F_L \cdot F_\gamma) + \gamma_D] + 1 \qquad (1.1.6.68)$$
$$\beta_{a,w} = B_\beta \cdot [f_n(F_L \cdot F_\beta) + \beta_D] + 1$$

(11) *Color difference signals of reference white* $C_{1,w}$, $C_{2,w}$, $C_{3,w}$

$$\begin{aligned} C_{1,w} &= \rho_{a,w} - \gamma_{a,w} \\ C_{2,w} &= \gamma_{a,w} - \beta_{a,w} \\ C_{3,w} &= \beta_{a,w} - \rho_{a,w} \end{aligned} \tag{1.1.6.69}$$

(12) *Hue Angle of reference white* h_s

$$h_{s,w} = \arctan\left(\frac{\frac{1}{2}(C_{2,w} - C_{3,w}) / 4.5}{C_{1,w} - (C_{2,w} / 11)}\right) \tag{1.1.6.70}$$

(13) *Eccentricity factor of reference white,* e_s

$$e_{s,w}\begin{cases} 1.2 - 0.4 \cdot \dfrac{(h_{s,w} + 122.47)}{142.61}, & 0^\circ \le h_{s,w} < 20.14^\circ \\ 0.8 - 0.1 \cdot \dfrac{(h_{s,w} - 20.14)}{69.86}, & 20.14^\circ \le h_{s,w} < 90^\circ \\ 0.7 + 0.3 \cdot \dfrac{(h_{s,w} - 90.0)}{74.25}, & 90^\circ \le h_{s,w} < 164.25^\circ \\ 1.0 + 0.2 \cdot \dfrac{(h_{s,w} - 164.25)}{73.28}, & 164.25^\circ \le h_{s,w} < 237.53^\circ \\ 1.2 - 0.4 \cdot \dfrac{(h_{s,w} - 237.53)}{142.61}, & 237.53^\circ \le h_{s,w} < 360^\circ \end{cases} \tag{1.1.6.71}$$

(14) *Low-luminance tritanopia factor* F_t

$$F_t = L_A / (L_A + 0.1) \tag{1.1.6.44}$$

(15) *Colorfulness* M,

$$M_{YB,w} = 100 \cdot [\frac{1}{2}(C_{2,w} - C_{3,w}) / 4.5] \cdot [e_{s,w} \cdot (10/13) \cdot N_{c,w} \cdot N_{cb,w} \cdot F_t] \tag{1.1.6.72}$$

$$M_{RG,w} = 100 \cdot [C_{1,w} - (C_{2,w} / 11)] \cdot [e_{s,w} \cdot (10/13) \cdot N_{c,w} \cdot N_{cb,w}]$$

$$M_w = ({M_{YB,w}}^2 + {M_{RG,w}}^2)^{1/2} \tag{1.1.6.73}$$

(16) *Rod Response* F_{LS},

$$F_{LS} = 3800 \cdot j^2 \cdot 5 \cdot L_{AS} / 2.26 + 0.2 \cdot (1 - j^2)^4 \cdot (5 \cdot L_{AS} / 2.26)^{1/6} \qquad (1.1.6.46)$$

where

$$j = 0.00001 / (5 \cdot L_{AS} / 2.26 + 0.00001) \qquad (1.1.6.47)$$

Scotopic adapting Luminance, L_{AS} is acquired from (1.1.6.66).

(17) *Rod Bleach Factor* B_S,

$$B_{S,w} = \frac{0.5}{1 + 0.3 \cdot \left[\left(\frac{5 \cdot L_{AS}}{2.26}\right)\right]^{0.3}} + \frac{0.5}{1 + 5 \cdot \left[\frac{5 \cdot L_{AS}}{2.26}\right]} \qquad (1.1.6.74)$$

$\left(\frac{S}{S_W}\right)$ for the white reference becomes 1.0 in (1.1.6.49).

(18) *Rod Response after adaptation,* A_s

$$A_{S,w} = B_{S,w} \cdot 3.05 \cdot [f_n(F_{LS})] + 0.3 \qquad (1.1.6.75)$$

(19) *Total Achromatic Signal of white reference,* A_w

$$A_w = N_{bb} \cdot [A_{a,w} - 1 + A_{S,w} - 0.3 + (1^2 + 0.3^2)^{1/2}] \qquad (1.1.6.76)$$

(20) N_1 and N_2 factors for calculating Brightness

$$N_1 = (7 \cdot A_W)^{0.5} / (5.33 \cdot N_b{}^{0.13})$$
$$N_2 = 7 \cdot A_W \cdot N_b{}^{0.362} / 200 \qquad (1.1.6.57\text{-}1.1.6.58)$$

(21) *Brightness of white reference,* Q_w

$$Q_w = \{7 \cdot [A_w + (M_w / 100)]\}^{0.6} \cdot N_1 - N_2 \qquad (1.1.6.77)$$

where A_w is *Total Achromatic Signal* (1.1.6.76) and M_w is *Colorfulness* (1.1.6.73) of reference white.

(22) z factor for calculating Lightness

$$z = 1 + (Y_b / Y_W)^{1/2} \tag{1.1.6.60}$$

Main-calculation

(1) Calculate ρ, γ, β

$$\begin{bmatrix} \rho \\ \gamma \\ \beta \end{bmatrix} = M_{E-H-P} \cdot \begin{bmatrix} X \\ Y \\ Z \end{bmatrix} \tag{1.1.6.78}$$

(2) Calculate ρ_a, γ_a, β_a

$$\begin{aligned} \rho_a &= B_\rho \cdot [f_n(F_L \cdot F_\rho \cdot \rho / \rho_W) + \rho_D] + 1 \\ \gamma_a &= B_\gamma \cdot [f_n(F_L \cdot F_\gamma \cdot \gamma / \gamma_W) + \gamma_D] + 1 \\ \beta_a &= B_\beta \cdot [f_n(F_L \cdot F_\beta \cdot \beta / \beta_W) + \beta_D] + 1 \end{aligned} \tag{1.1.6.6-1.1.6.8}$$

F_L : Pre-calculation (6)

F_ρ, F_γ, F_β : Pre-calculation (7)

ρ_W, γ_W, β_W : Pre-calculation (1)

ρ_D, γ_D, β_D : Pre-calculation (8)

(3) Calculate C_1, C_2, C_3

$$\begin{aligned} C_1 &= \rho_a - \gamma_a \\ C_2 &= \gamma_a - \beta_a \\ C_3 &= \beta_a - \rho_a \end{aligned} \tag{1.1.6.9-1.1.6.11}$$

(4) Calculate *Hue Angle*, h_s

$$h_s = \arctan(\frac{\frac{1}{2}(C_2 - C_3)/4.5}{C_1 - (C_2/11)}) \tag{1.1.6.36}$$

(5) Calculate *Eccentricity factor*, e_s

$$e_s \begin{cases} 1.2 - 0.4 \cdot \dfrac{(h_s + 122.47)}{142.61}, & 0^\circ \le h_s < 20.14^\circ \\ 0.8 - 0.1 \cdot \dfrac{(h_s - 20.14)}{69.86}, & 20.14^\circ \le h_s < 90^\circ \\ 0.7 + 0.3 \cdot \dfrac{(h_s - 90.0)}{74.25}, & 90^\circ \le h_s < 164.25^\circ \\ 1.0 + 0.2 \cdot \dfrac{(h_s - 164.25)}{73.28}, & 164.25^\circ \le h_s < 237.53^\circ \\ 1.2 - 0.4 \cdot \dfrac{(h_s - 237.53)}{142.61}, & 237.53^\circ \le h_s < 360^\circ \end{cases} \tag{1.1.6.79}$$

(6) Calculate *Colorfulness*, M, and *Saturation*, s.

$$M_{YB} = 100 \cdot [\frac{1}{2}(C_2 - C_3)/4.5] \cdot [e_s \cdot (10/13) \cdot N_c \cdot N_{cb} \cdot F_t] \tag{1.1.6.39}$$

$$M_{RG} = 100 \cdot [C_1 - (C_2/11)] \cdot [e_s \cdot (10/13) \cdot N_c \cdot N_{cb}] \tag{1.1.6.40}$$

$$M = ({M_{YB}}^2 + {M_{RG}}^2)^{1/2} \tag{1.1.6.41}$$

$$s = 50 \cdot \frac{M}{(\rho_a + \gamma_a + \beta_a)} \tag{1.1.6.42}$$

N_c : Known

N_{cb} : Pre-calculation (4)

(7) Calculate *Brightness*, Q. Calculations of B_s, A_s, A_a, A are required beforehand.

$$B_S = \frac{0.5}{1 + 0.3 \cdot \left[\left(\frac{5 \cdot L_{AS}}{2.26}\right)\left(\frac{S}{S_W}\right)\right]^{0.3}} + \frac{0.5}{1 + 5 \cdot \left[\frac{5 \cdot L_{AS}}{2.26}\right]} \tag{1.1.6.49}$$

$$A_S = B_S \cdot 3.05 \cdot [f_n(F_{LS} \cdot S / S_W)] + 0.3 \tag{1.1.6.50}$$

$$A_a = 2 \cdot \rho_a + \gamma_a + (1/20) \cdot \beta_a - 3.05 + 1 \quad (1.1.6.51)$$

$$A = N_{bb} \cdot [A_a - 1 + A_S - 0.3 + (1^2 + 0.3^2)^{1/2}] \quad (1.1.6.52)$$

$$Q = \{7 \cdot [A + (M/100)]\}^{0.6} \cdot N_1 - N_2 \quad (1.1.6.56)$$

L_{AS} : Pre-calculation (3)

N_{bb} : Pre-calculation (5)

F_{LS} : Pre-calculation (16)

N_1, N_2 : Pre-calculation (20)

(8) Calculate *Lightness*, J.

$$J = 100 \cdot (Q/Q_W)^z \quad (1.1.6.59)$$

Q_w : Pre-calculation (21)

z : Pre-calculation (22)

(9) Calculate *Chroma*, C.

$$C = 4 \cdot s^{0.69} \cdot (Q/Q_W)^{Y_b/Y_W} \cdot (1.31 - 0.31^{Y_b/Y_W}) \quad (1.1.6.61)$$

Q_w : Pre-calculation (21)

Using the precalculation and main calculation for the reference field, calculate appearance attributes, J, C. h_s. for the reference field. Repeat calculation of appearance attributes using precalculation and main calculation for the test field until the differences (ΔE of CIELAB equivalent can be calculated by changing J, C. h_s in polar coordinates to Cartesian coordinates) of attributes are within the specified tolerance (<0.15). A better estimation of TSV while iterating can be achieved using differential methods. The TSV which yielded attributes within the specified tolerance was the estimated TSV for the test field.

1.1.7 Nayatani

Nayatani's color appearance model (Nayatani, 1981, 1982, 1986, 1987, 1987, 1988, 1988, 1989, 1990, 1991, Takahama, 1984) is diagrammed in Fig. 1.21.

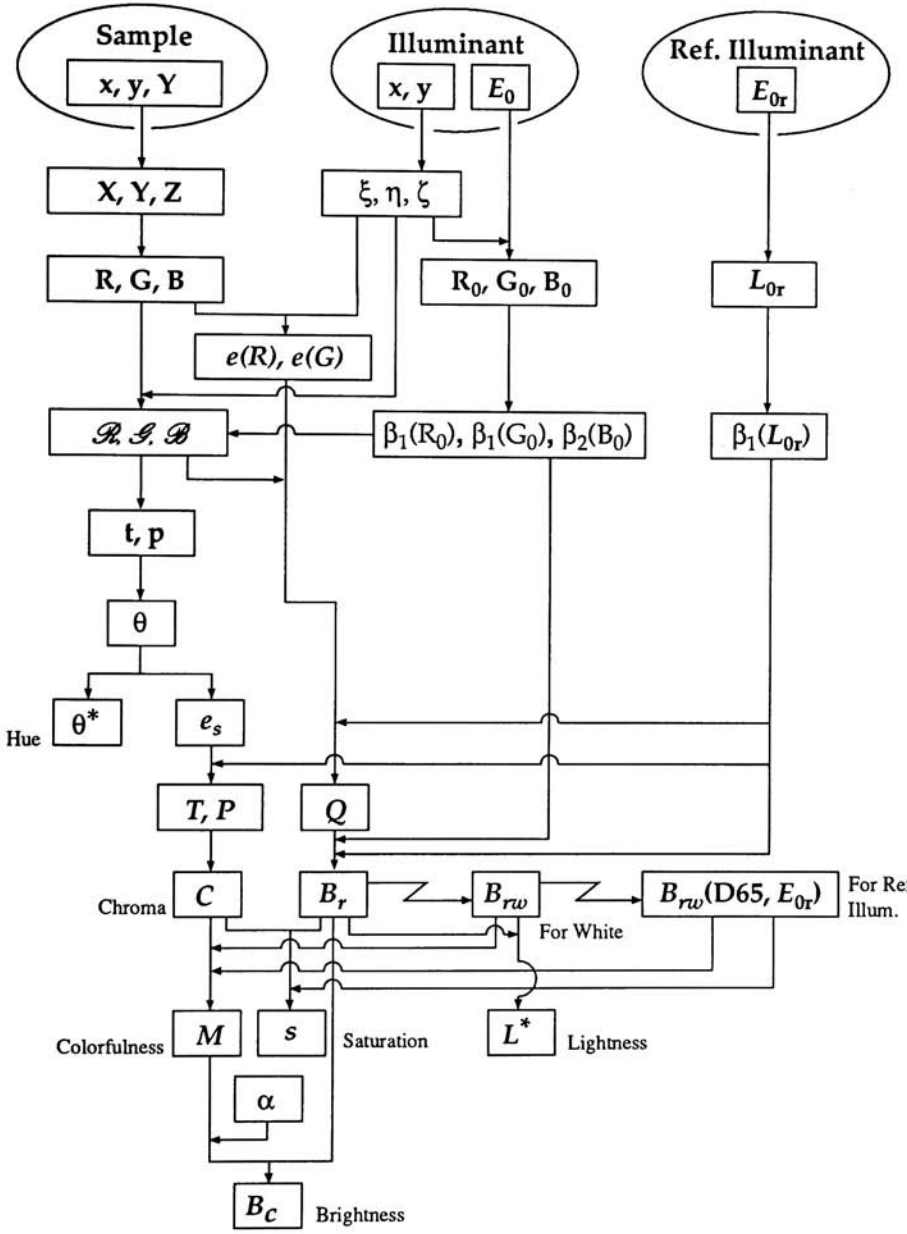

Fig. 1.21 Nayatani color appearance model diagram (Modified from Nayatani, 1990)

Although there are many similarities to Hunt's model, the non-linear compression stages are quite different and Nayatani's model is defined only for object colors, possibly limiting its use in color WYSIWYG. An advantage of this model over Hunt's model is its relative ease in inversion.

The situation studied by Nayatani is shown in Figure 1.22. The test field consists of a nonselective background and a test sample on it. The test field is uniformly illuminated by a given illuminant at a given illuminace. A medium-gray surface of luminance factor 0.2 is used as the background. The reference field has the same gray background as the test field.

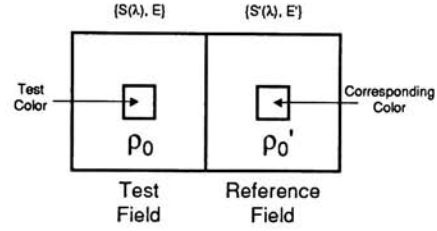

Fig. 1.22 The situation studied by the Nayatani model (Nayatani, 1981)

The adaptation process of the model consists of two steps. The first step is a modified von Kries transformation. The second step is a nonlinear transformation corresponding to a compression of response of each transmission mechanism from receptor to brain. The original outline of the model is shown in Fig. 1.23.

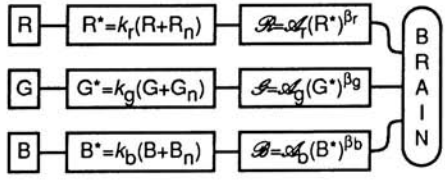

Fig. 1.23 The outline of the Nayatani model (Nayatani, 1981)

A detailed diagram of the model is shown in the Fig. 1.24.

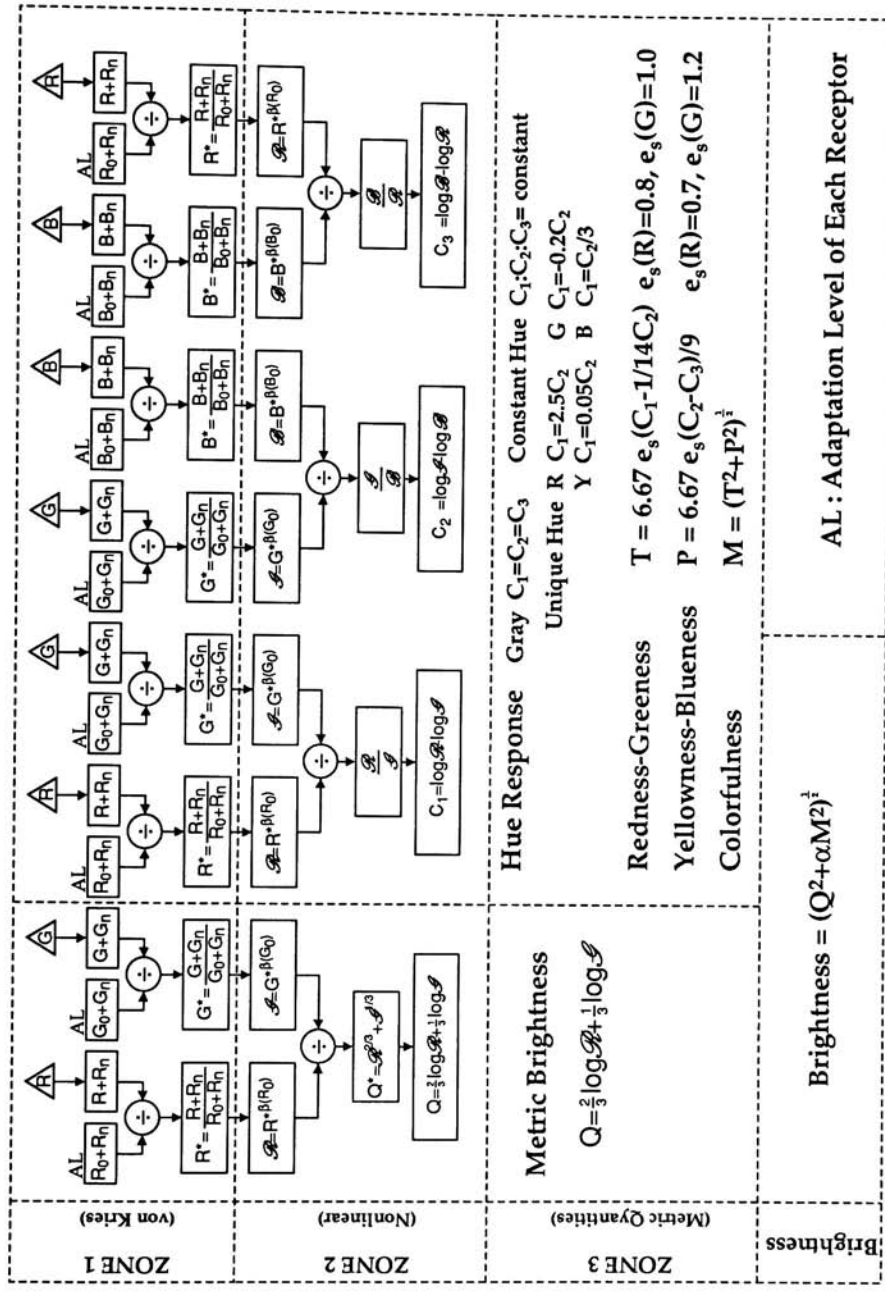

Fig. 1.24 Schematic diagram of the Nayatani color appearance model (Nayatani, 1986)

1.1.7.1 Estévez-Hunt-Pointer Primaries

The Pitt primaries were used prior to 1987 for the Nayatani model (Nayatani, 1981). Hunt and Pointer (1985) used the new primaries which are intended to predict well the spectral responses of cones from the CIE 1931 matching functions. The target cone responses were derived by Estèvez from the 2° color matching functions by Stiles and color-deficiency data. Nayatani adopted this to his model (1987). He concluded that it shows insignificant differences in the predictions of color appearance.

The absolute tristimulus values, R, G, B, of the test sample in a fundamental-primary system uses E-H-P primaries (Nayatani, 1987).

$$R = 0.40024X + 0.70760Y - 0.08081Z \tag{1.1.7.1}$$

$$G = -0.22630X + 1.16532Y + 0.04570Z \tag{1.1.7.2}$$

$$B = 0.91822Z \tag{1.1.7.3}$$

There is minor difference between Nayatani's and Hunt's E-H-P primaries. Hunt's is normalized, Nayatani's is not. For the experiment, Nayatani's original E-H-P primaries were used to process Nayatani's model.

The quantities ξ, η, ζ, define the test illuminant.

$$\begin{bmatrix} \xi \\ \eta \\ \zeta \end{bmatrix} = M \cdot \begin{bmatrix} x/y \\ 1 \\ z/y \end{bmatrix} \tag{1.1.7.4}$$

The matrix M is calculated from E-H-P primaries (Nayatani, 1987).

$$\xi = (0.48105x + 0.78841y - 0.08081)/y \tag{1.1.7.5}$$

$$\eta = (-0.27200x + 1.11962y + 0.04570)/y \tag{1.1.7.6}$$

$$\zeta = 0.91822(1 - x - y)/y \tag{1.1.7.7}$$

R_0, G_0 and B_0 represent the effective adapting level of the three receptors assumining a Lambertian 0.2 luminance factor background.

$$\begin{bmatrix} R_0 \\ G_0 \\ B_0 \end{bmatrix} = \frac{0.2E_0}{\pi} \begin{bmatrix} \xi \\ \eta \\ \zeta \end{bmatrix} \tag{1.1.7.8}$$

1.1.7.2 Nonlinear characteristics of each of the three receptors

The exponents of the nonlinear process for the three response mechanisms are $\beta_1(R_0)$, $\beta_1(G_0)$, $\beta_2(B_0)$ (Nayatani, 1987).

$$\beta_1(R_0) = \frac{6.469 + 6.362R_0^{0.4495}}{6.469 + R_0^{0.4495}} \tag{1.1.7.9}$$

$$\beta_1(G_0) = \frac{6.469 + 6.362G_0^{0.4495}}{6.469 + G_0^{0.4495}} \tag{1.1.7.10}$$

$$\beta_2(B_0) = 0.7844\frac{8.414 + 8.091B_0^{0.5128}}{8.414 + B_0^{0.5128}} \tag{1.1.7.11}$$

Equation 1.1.7.9, 1.1.7.10 and 1.1.7.11 are shown in Fig. 1.25.

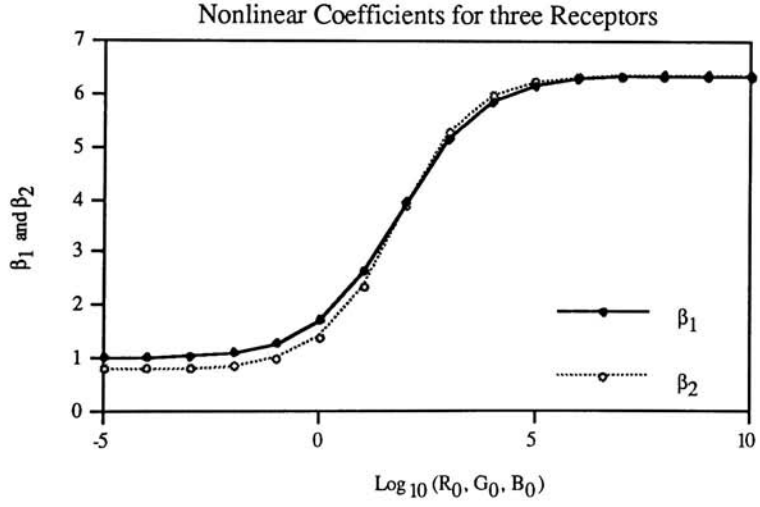

Fig. 1.25 Nonlinear Characteristics of receptors

Nayatani's response mechanisms of three receptors are similar to Hunt's cone response function. Both are S shaped which implies that there are maximum and minimum stimuli limitations.

1.1.7.3 The normalizing constant of the normalizing illuminance, $\beta_1(L_{0r})$

The calculation of achromatic brightness, B_r, uses a normalizing constant of the reference illuminant, $\beta_1(L_{0r})$. The formula is the same as the nonlinear characteristics of the three receptors.

$$\beta_1(L_{0r}) = \frac{6.469 + 6.362 L_{0r}^{0.4495}}{6.469 + L_{0r}^{0.4495}} \tag{1.1.7.12}$$

where

$$L_{0r} = 0.2 E_{0r} / \pi \tag{1.1.7.13}$$

1.1.7.4 Tri-chromatic responses

Tri-chromatic responses which are similar to Hunt's cone responses, $\mathscr{R}$, $\mathscr{G}$ and $\mathscr{B}$ have nonlinear relationships to R, G and B.

$$\mathscr{R} = \mathscr{A}\left[\frac{R+1}{Y_0\xi+1}\right]^{\beta_1(R_0)} \tag{1.1.7.14}$$

$$\mathscr{G} = \mathscr{A}\left[\frac{G+1}{Y_0\eta+1}\right]^{\beta_1(G_0)} \tag{1.1.7.15}$$

$$\mathscr{B} = \mathscr{A}\left[\frac{B+1}{Y_0\zeta+1}\right]^{\beta_2(B_0)} \tag{1.1.7.16}$$

The $\mathscr{A}$ is defined in equation 1.1.7.20.

1.1.7.5 Unnormalized Opponent-color responses

The quanities q, t and p correspond to unnormalized responses of whiteness-blackness, redness-greenness, and yellowness-blueness.

$$q = \frac{2}{3}\log\mathscr{R} + \frac{1}{3}\log\mathscr{G} \tag{1.1.7.17}$$

$$t = \log\mathscr{R} - \frac{12}{11}\log\mathscr{G} + \frac{1}{11}\log\mathscr{B} \tag{1.1.7.18}$$

$$p = \frac{1}{9}\log\mathscr{R} + \frac{1}{9}\log\mathscr{G} - \frac{2}{9}\log\mathscr{B} \tag{1.1.7.19}$$

And it's expanded forms are

$$q = \frac{2}{3}\beta_1(R_0)\log\frac{R+1}{Y_0\xi+1} + \frac{1}{3}\beta_1(G_0)\log\frac{G+1}{Y_0\eta+1} + \log\mathscr{A} \tag{1.1.7.20}$$

$$t = \beta_1(R_0)\log\frac{R+1}{Y_0\xi+1} - \frac{12}{11}\beta_1(G_0)\log\frac{G+1}{Y_0\eta+1} + \frac{1}{11}\beta_2(B_0)\log\frac{B+1}{Y_0\zeta+1} \tag{1.1.7.21}$$

$$p = \frac{1}{9}\beta_1(R_0)\log\frac{R+1}{Y_0\xi+1} + \frac{1}{9}\beta_1(G_0)\log\frac{G+1}{Y_0\eta+1} - \frac{2}{9}\beta_2(B_0)\log\frac{B+1}{Y_0\zeta+1} \tag{1.1.7.22}$$

The parameter $\mathscr{A}$ is found only for q not in t and p. As Nayatani stated (1990), the model does not take into consideration other than a gray background with Y_0=20 relative to PRD (Perfect Reflecting Diffuser) where Y=100.

1.1.7.6 Condition of grayness constancy

The condition of grayness constancy (whiteness = blackness) requires q=0 for the achromatic sample with Y_0=20.

$$\frac{2}{3}\beta_1(R_0)\log\frac{20\xi+1}{Y_0\xi+1} + \frac{1}{3}\beta_1(G_0)\log\frac{20\xi+1}{Y_0\xi+1} + \log\mathscr{A} = 0 \tag{1.1.7.23}$$

$\mathscr{A}$ is obtained by solving the equation 1.1.7.19.

$$\mathscr{A} = \left[\frac{Y_0\xi+1}{20\xi+1}\right]^{\frac{2}{3}\beta_1(R_0)} \cdot \left[\frac{Y_0\eta+1}{20\eta+1}\right]^{\frac{1}{3}\beta_1(G_0)} \tag{1.1.7.24}$$

1.1.7.7 $e_s(\theta)$

The parameter e_s is an eccentricity factor, the same as those used by Hunt (section 1.1.6.13). Each angle represents NCS unique colors.

$$e_s(R) = 0.8, \quad \theta_R = 20.14^\circ \tag{1.1.7.25}$$

$$e_s(Y) = 0.7, \quad \theta_Y = 90.00^\circ \tag{1.1.7.26}$$

$$e_s(G) = 1.0, \quad \theta_G = 164.25^\circ \tag{1.1.7.27}$$

$$e_s(B) = 1.2, \quad \theta_B = 231.00^\circ \tag{1.1.7.28}$$

$$e_s(\theta)\begin{cases} \left[(\theta+360-\theta_B)e_s(R)+(\theta_R-\theta)e_s(B)\right]/\phi_{RB}, & 0^\circ \le \theta < \theta_R \\ \left[(\theta-\theta_R)e_s(Y)+(\theta_Y-\theta)e_s(R)\right]/\phi_{YR}, & \theta_R \le \theta < \theta_Y \\ \left[(\theta-\theta_Y)e_s(G)+(\theta_G-\theta)e_s(Y)\right]/\phi_{GY}, & \theta_Y \le \theta < \theta_G \\ \left[(\theta-\theta_G)e_s(B)+(\theta_B-\theta)e_s(G)\right]/\phi_{BG}, & \theta_G \le \theta < \theta_B \\ \left[(\theta-\theta_B)e_s(R)+(\theta_R+360-\theta)e_s(B)\right]/\phi_{RB}, & \theta_B \le \theta < 360^\circ \end{cases} \tag{1.1.7.29}$$

where

$$\phi_{RB} = 149.14^\circ \tag{1.1.7.30}$$

$$\phi_{YR} = 69.86^\circ \tag{1.1.7.31}$$

$$\phi_{GY} = 74.25^\circ \tag{1.1.7.32}$$

$$\phi_{BG} = 66.75^\circ \tag{1.1.7.33}$$

1.1.7.8 Appearance attributes

Whiteness-blackness, Q

$$Q = \frac{41.69}{\beta_1(L_{or})}\left(\frac{2}{3}\beta_1(R_0)e(R)\log\frac{R+1}{20\xi+1} + \frac{1}{3}\beta_1(G_0)e(G)\log\frac{G+1}{20\eta+1}\right) \tag{1.1.7.34}$$

where

$$e(R)\begin{cases} 1.758, & R \ge 20\xi \\ 1, & R < 20\xi \end{cases} \tag{1.1.7.35}$$

$$e(G)\begin{cases} 1.758, & G \ge 20\eta \\ 1, & G < 20\eta \end{cases} \tag{1.1.7.36}$$

Redness-Greenness, T

$$T = \frac{488.93}{\beta_1(L_{or})} e_s(\theta) \left(\beta_1(R_0) \log \frac{R+1}{Y_0 \xi + 1} - \frac{12}{11} \beta_1(G_0) \log \frac{G+1}{Y_0 \eta + 1} + \frac{1}{11} \beta_2(B_0) \log \frac{B+1}{Y_0 \zeta + 1} \right) \quad (1.1.7.37)$$

Yellowness-Blueness, P

$$P = \frac{488.93}{\beta_1(L_{or})} e_s(\theta) \left(\frac{1}{9} \beta_1(R_0) \log \frac{R+1}{Y_0 \xi + 1} + \frac{1}{9} \beta_1(G_0) \log \frac{G+1}{Y_0 \eta + 1} - \frac{2}{9} \beta_2(B_0) \log \frac{B+1}{Y_0 \zeta + 1} \right) \quad (1.1.7.38)$$

Achromatic Brightness, B_r

$$B_r = \frac{41.69}{\beta_1(L_{or})} \left(\frac{2}{3} \beta_1(R_0) e(R) \log \frac{R+1}{20\xi + 1} + \frac{1}{3} \beta_1(G_0) e(G) \log \frac{G+1}{20\eta + 1} \right) + \frac{50}{\beta_1(L_{or})} \left(\frac{2}{3} \beta_1(R_0) + \frac{1}{3} \beta_1(G_0) \right) \quad (1.1.7.39)$$

*Note :

B_{rw}: Achromatic Brightness for white.

$B_{rw}(D_{65}, E_{or})$: Achromatic Brightness for reference illuminant.

Lightness, L^*

$$L^* = \frac{41.69}{\beta_1(L_{or})} \beta_1(L_o) e(Y) \log \frac{Y+1}{21} + 50 \quad (1.1.7.40)$$

where

$$e(Y) \begin{cases} 1.758, & Y \geq 20 \\ 1, & Y < 20 \end{cases} \quad (1.1.7.41)$$

Colorfulness, M

$$M = (T^2 + P^2)^{1/2} \frac{B_{rw}}{B_{rw}(D_{65}, E_{or})} = C \frac{B_{rw}}{B_{rw}(D_{65}, E_{or})} \quad (1.1.7.42)$$

$$M_{RG} = T \frac{B_{rw}}{B_{rw}(D_{65}, E_{or})} \quad (1.1.7.43)$$

$$M_{YB} = P \frac{B_{rw}}{B_{rw}(D_{65}, E_{or})} \quad (1.1.7.44)$$

Chroma, C

$$C = (T^2 + P^2)^{1/2} \tag{1.1.7.45}$$

Hue Angle, θ

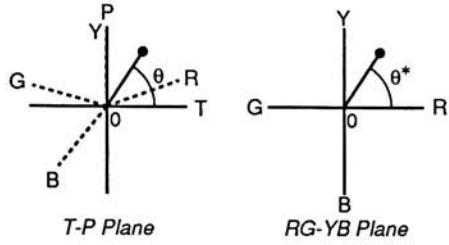

Fig. 1.26 Metric hue angle in P-T plane and RG-YB plane.

$$\theta = \tan^{-1}(P/T) \tag{1.1.7.46}$$

$$\text{if } \theta_\eta \text{ is } \theta_Y \le \theta_\eta \le \theta_G$$
$$\frac{\theta_G - \theta_\eta}{\theta_\eta - \theta_Y} = \frac{e_s(G)}{e_s(Y)} \tag{1.1.7.47}$$

TABLE 1.3 Metric Hue Angle

Hue	θ	θ*
R	20.14°	0°
YR	57.40°	45°
Y	90.00°	90°
GY	120.57°	135°
G	164.25°	180°
BG	194.59°	225°
B	231.00°	270°
PB	280.71°	292.5°
P	320.48°	315°
RP	353.02°	337.5°

Saturation, s

$$s = \frac{M}{\left(\frac{B_r}{B_{rw}(D_{65}, E_{or})}\right)} = C\,\frac{B_{rw}}{B_r} \tag{1.1.7.48}$$

$$s_{R-G} = \frac{M_{R-G}}{\left(\frac{B_r}{B_{rw}(D_{65}, E_{or})}\right)} = T\,\frac{B_{rw}}{B_r} \tag{1.1.7.49}$$

$$s_{Y-B} = \frac{M_{Y-B}}{\left(\frac{B_r}{B_{rw}(D_{65}, E_{or})}\right)} = P\,\frac{B_{rw}}{B_r} \tag{1.1.7.50}$$

Brightness, B_c

$$B_c = \left(B_r{}^2 + \alpha M^2\right)^{1/2} = B_r\left(1 + \frac{\alpha}{\left[B_{rw}(D_{65}, E_{or})\right]^2}\left\{\frac{B_{rw}}{B_r}\right\}\left(T^2 + P^2\right)\right)^{1/2} \tag{1.1.7.51}$$

Note : α in Fig. A-2 (Nayatani, 1988).

$$\alpha = \frac{B_{r,reference}^2 - B_{r,test}^2}{M_{reference}^2 - M_{test}^2} \tag{1.1.7.52}$$

Equations used for the experiment.

Knowns for calculation.

M_{E-H-P} : Estévez-Hunt-Pointer Primaries

$X_{n,ref}$, $Y_{n,ref}$, $Z_{n,ref}$: White reference TSV for the reference field

$X_{n,test}$, $Y_{n,test}$, $Z_{n,test}$: White reference TSV for the test field

X_{ref}, Y_{ref}, Z_{ref} : TSV of corresponding color for the reference field

E_{0r} : Normalizing illuminance in lux (1000 lux)

Unknowns are X_{test}, Y_{test}, Z_{test}

Pre-calculation

(1) Calculate the chromaticity values for the illuminants.

$$x_{ref} = \frac{X_{n,ref}}{X_{n,ref} + Y_{n,ref} + Z_{n,ref}} \quad x_{test} = \frac{X_{n,test}}{X_{n,test} + Y_{n,test} + Z_{n,test}}$$
$$y_{ref} = \frac{Y_{n,ref}}{X_{n,ref} + Y_{n,ref} + Z_{n,ref}} \quad y_{test} = \frac{Y_{n,test}}{X_{n,test} + Y_{n,test} + Z_{n,test}} \tag{1.1.7.53}$$

(2) Calculate ξ, η, ζ for both fields.

$$\begin{bmatrix} \xi_{ref} \\ \eta_{ref} \\ \zeta_{ref} \end{bmatrix} = M_{E-H-P} \cdot \begin{bmatrix} x_{ref} / y_{ref} \\ 1 \\ z_{ref} / y_{ref} \end{bmatrix} \quad \begin{bmatrix} \xi_{test} \\ \eta_{test} \\ \zeta_{test} \end{bmatrix} = M_{E-H-P} \cdot \begin{bmatrix} x_{test} / y_{test} \\ 1 \\ z_{test} / y_{test} \end{bmatrix} \tag{1.1.7.54}$$

(3) Calculate ξ, η, ζ for both fields.

$$\begin{bmatrix} R_{0,ref} \\ G_{0,ref} \\ B_{0,ref} \end{bmatrix} = \frac{0.2E_{0,ref}}{\pi} \begin{bmatrix} \xi_{ref} \\ \eta_{ref} \\ \zeta_{ref} \end{bmatrix} \quad \begin{bmatrix} R_{0,test} \\ G_{0,test} \\ B_{0,test} \end{bmatrix} = \frac{0.2E_{0,test}}{\pi} \begin{bmatrix} \xi_{test} \\ \eta_{test} \\ \zeta_{test} \end{bmatrix} \tag{1.1.7.55}$$

(4) Calculate $\beta_1(R_0)$, $\beta_1(G_0)$, $\beta_2(B_0)$ for both fields.

$$\beta_1(R_{0,ref})_{ref} = \frac{6.469 + 6.362R_{0,ref}^{0.4495}}{6.469 + R_{0,ref}^{0.4495}}$$
$$\beta_1(G_{0,ref})_{ref} = \frac{6.469 + 6.362G_{0,ref}^{0.4495}}{6.469 + G_{0,ref}^{0.4495}}$$
$$\beta_2(B_{0,ref})_{ref} = 0.7844\frac{8.414 + 8.091B_{0,ref}^{0.5128}}{8.414 + B_{0,ref}^{0.5128}}$$
$$\beta_1(R_{0,test})_{test} = \frac{6.469 + 6.362R_{0,test}^{0.4495}}{6.469 + R_{0,test}^{0.4495}}$$
$$\beta_1(G_{0,test})_{test} = \frac{6.469 + 6.362G_{0,test}^{0.4495}}{6.469 + G_{0,test}^{0.4495}} \tag{1.1.7.56}$$
$$\beta_2(B_{0,test})_{test} = 0.7844\frac{8.414 + 8.091B_{0,test}^{0.5128}}{8.414 + B_{0,test}^{0.5128}}$$

(5) Calculate $\beta_1(L_{0r})$for reference field using equation (1.1.7.12)-(1.1.7.13).

$$L_{0r} = 0.2E_{0r} / \pi \tag{1.1.7.57}$$

$$\beta_1(L_{0r}) = \frac{6.469 + 6.362L_{0r}^{0.4495}}{6.469 + L_{0r}^{0.4495}} \tag{1.1.7.58}$$

Main-calculation

(1) Calculate R, G, B for reference field.

$$\begin{bmatrix} R_{ref} \\ G_{ref} \\ B_{ref} \end{bmatrix} = M_{E-H-P} \bullet \begin{bmatrix} X_{ref} \\ Y_{ref} \\ Z_{ref} \end{bmatrix} \tag{1.1.7.59}$$

(2) Calculate $e(R)$ and $e(G)$ using equation (1.1.7.35)-(1.1.7.36).

(3) Calculate Whiteness-Blackness, Q for reference field using equation (1.1.7.34).

(4) Calculate $\frac{T}{e_s(\theta)}$ and $\frac{P}{e_s(\theta)}$ (Redness-Greeness and Yellowness-Blueness without $e_s(\theta)$) for reference field using equation (1.1.7.37)-(1.1.7.38).

(5) Calculate Hue Angle, θ for reference field using equation (1.1.7.46).

(6) Calculate Hue Angle, $e_s(\theta)$ for reference field using equation (1.1.7.29).

(7) Calculate Redness-Greeness, T and Yellowness-Blueness, P for reference field by multipling $e_s(\theta)$ (*step 6*) to $\frac{T}{e_s(\theta)}$ and $\frac{P}{e_s(\theta)}$ (*step 4*).

(8) Calculate q, t, p for the test field considering $Q_{test} = Q_{ref}$, $T_{test} = T_{ref}$, and $P_{test} = P_{ref}$.

$$\begin{aligned} q_{test} &= 3 \cdot Q \cdot \beta_1(L_{or,ref})_{ref} / 41.69 \\ &\quad - \left(2 \cdot \beta_1(R_{0,test})_{test} \cdot e(R) \cdot \log \frac{Y_0 \cdot \xi_{test} + 1}{20 \cdot \xi_{test} + 1} \right. \\ &\quad \left. + \beta_1(G_{0,test})_{test} \cdot e(G) \cdot \log \frac{Y_0 \cdot \eta_{test} + 1}{20 \cdot \eta_{test} + 1} \right) \\ t_{test} &= \frac{11 \cdot T_{ref} \cdot \beta_1(L_{or,ref})_{ref}}{488.93 \cdot e_s(\theta)} \\ p_{test} &= \frac{9 \cdot P_{ref} \cdot \beta_1(L_{or,ref})_{ref}}{488.93 \cdot e_s(\theta)} \end{aligned} \tag{1.1.7.60}$$

where $e_s(\theta) \equiv e_s(\theta_{ref}) = e_s(\theta_{test})$.

(9) Calculate K_R, K_G, K_B

$$\begin{aligned} K_R &= \frac{23 \cdot q_{test} + (2 \cdot t_{test} + p_{test}) \cdot e(G)}{23 \cdot [2 \cdot e(R) + e(G)]} \\ K_G &= \frac{23 \cdot q_{test} - 2 \cdot (2 \cdot t_{test} + p_{test}) \cdot e(R)}{23 \cdot [2 \cdot e(R) + e(G)]} \\ K_G &= \frac{23 \cdot q_{test} - [2 \cdot e(R) - e(G)] \cdot t_{test} - [24 \cdot e(R) + 11 \cdot e(G)] \cdot p_{test}}{23 \cdot [2 \cdot e(R) + e(G)]} \end{aligned} \tag{1.1.7.61}$$

where $e(R) \equiv e(R_{ref}) = e(R_{test})$ *and* $e(G) \equiv e(G_{ref}) = e(G_{test})$.

(10) Calculate R_{test}, G_{test}, B_{test}

$$
\begin{aligned}
R_{test} &= 10^{\frac{K_R}{\beta_1 (R_{0,test})_{test}}} \cdot (Y_0 \cdot \xi_{test} + 1) - 1 \\
G_{test} &= 10^{\frac{K_G}{\beta_1 (G_{0,test})_{test}}} \cdot (Y_0 \cdot \eta_{test} + 1) - 1 \\
B_{test} &= 10^{\frac{K_B}{\beta_1 (B_{0,test})_{test}}} \cdot (Y_0 \cdot \zeta_{test} + 1) - 1
\end{aligned}
\tag{1.1.7.62}
$$

(11) Calculate X_{test}, Y_{test}, Z_{test}

$$
\begin{bmatrix} X_{test} \\ Y_{test} \\ Z_{test} \end{bmatrix} = M_{E-H-P}^{-1} \bullet \begin{bmatrix} R_{test} \\ G_{test} \\ B_{test} \end{bmatrix}
\tag{1.1.7.63}
$$

1.1.8 RLAB

The RLAB model developed by Fairchild and Berns (Fairchild and Berns, 1993) can be thought of as a simplification of the Hunt model; it incorporates viewing condition parameters and is mathematically efficient and invertible, all necessary requirements for color WYSIWYG. It is based on Fairchild's model of chromatic adaptation, uses CIELAB for perceptual metrics, and takes into account differences in surround relative luminance.

1.1.8.1 Changes to fundamental tristimulus values

The first step of the model is a transformation from CIE tristimulus values (X, Y, Z) to fundamental tristimulus values (L, M, S) using the Estévez-Hunt-Pointer transformation (Hunt, 1985, Estevez, 1979, Nayatani, 1987).

$$L = 0.4002X + 0.7076Y - 0.0808Z \quad (1.1.8.1)$$

$$M = -0.2263X + 1.1653Y + 0.0457Z \quad (1.1.8.2)$$

$$S = 0.9182Z \quad (1.1.8.3)$$

The equations 1.1.8.1, 1.1.8.2 and 1.1.8.3 can be represented in matrix form as in equation 1.1.8.4 and 1.1.8.5.

$$\begin{bmatrix} L \\ M \\ S \end{bmatrix} = M \begin{bmatrix} X \\ Y \\ Z \end{bmatrix} \quad (1.1.8.4)$$

where

$$M = \begin{bmatrix} 0.4002 & 0.7076 & -0.0808 \\ -0.2263 & 1.1653 & 0.0457 \\ 0.0 & 0.0 & 0.9182 \end{bmatrix} \quad (1.1.8.5)$$

1.1.8.2 Modified form of the von Kries chromatic adaptation transform with incomplete chromatic adaptation

A von Kries model is modified to take account of the actual degree of chromatic adaptation by making the multiplicative scaling factors functions of the adapting conditions.

$$L_a = p_L \frac{L}{L_n} \quad (1.1.8.6)$$

$$M_a = p_M \frac{M}{M_n} \quad (1.1.8.7)$$

$$S_a = p_S \frac{S}{S_n} \quad (1.1.8.8)$$

L_a, M_a, and S_a represent the cone signals after adaptation, L, M, and S are the cone excitations, L_n, M_n, and S_n are the maximum excitations generally used in the von Kries model, and p_L, p_M, and p_S are parameters representing the degree of chromatic adaptation of each mechnism. The values of the degree of adaptation parameters are functions of the chromaticity and

luminance of the adapting source. These parameters will differ from unity for sources for which adaptation is incomplete (Fairchild 1991).

To take into account incomplete chromatic adaptation, the degree of adaptation for each mechanism is expressed as a function of the proportion of excitation of that mechanism and luminance. The proportion of excitation is defined by fundamental chromaticity coordinates rather than tristimulus values. RLAB equations for this originate with Hunt. The modified chromaticities are defined as:

$$l_E = \frac{3\frac{L_N}{L_E}}{\frac{L_N}{L_E}+\frac{M_N}{M_E}+\frac{S_N}{S_E}} \tag{1.1.8.9}$$

$$m_E = \frac{3\frac{M_N}{M_E}}{\frac{L_N}{L_E}+\frac{M_N}{M_E}+\frac{S_N}{S_E}} \tag{1.1.8.10}$$

$$s_E = \frac{3\frac{S_N}{S_E}}{\frac{L_N}{L_E}+\frac{M_N}{M_E}+\frac{S_N}{S_E}} \tag{1.1.8.11}$$

where L_N, M_N, and S_N are the fundamental tristimulus values of the adapting source or background and L_E, M_E, and S_E are the fundamental tristimulus values of an equal energy source. Including a dependency on luminance whereby adaptation becomes more complete as luminance is increased the degree of adaptation functions become:

$$p_L = \frac{(1+Y_N{}^{1/3}+l_E)}{(1+Y_N{}^{1/3}+\frac{1}{l_E})} \tag{1.1.8.12}$$

$$p_M = \frac{(1+Y_N{}^{1/3}+m_E)}{(1+Y_N{}^{1/3}+\frac{1}{m_E})} \tag{1.1.8.13}$$

$$p_S = \frac{(1 + Y_N^{1/3} + s_E)}{(1 + Y_N^{1/3} + \frac{1}{s_E})} \tag{1.1.8.14}$$

where p_L, p_M, and p_S are the degrees of adaptation, l_E, m_E, and s_E are the modified fundamental chromaticity coordinates of the adapting stimulus, and Y_N is the luminance of the adapting stimulus in units of cd/m^2.

Equations 1.1.8.6-1.1.8.14 can be expressed in matrix form (equation 1.1.8.18) by forming matrix A using equations 1.1.8.15-1.1.8.17.

$$a_L = \frac{p_L}{L_n} \tag{1.1.8.15}$$

$$a_M = \frac{p_M}{M_n} \tag{1.1.8.16}$$

$$a_S = \frac{p_S}{S_n} \tag{1.1.8.17}$$

$$A = \begin{bmatrix} a_L & 0.0 & 0.0 \\ 0.0 & a_M & 0.0 \\ 0.0 & 0.0 & a_S \end{bmatrix} \tag{1.1.8.18}$$

$$\begin{bmatrix} L' \\ M' \\ S' \end{bmatrix} = A \begin{bmatrix} L \\ M \\ S \end{bmatrix} \tag{1.1.8.19}$$

1.1.8.3 Luminance-dependent interaction between the three cone types

The last step of the transformation is to allow luminance dependent interaction between the three cone types.

$$C = \begin{bmatrix} 1 & c & c \\ c & 1 & c \\ c & c & 1 \end{bmatrix} \tag{1.1.8.20}$$

The c term was derived from the *linkage model* of Takahama *et al* (Takahama, 1977).

$$c = 0.219 - 0.0784 \log_{10}(Y_N) \tag{1.1.8.21}$$

$$\begin{bmatrix} L_a \\ M_a \\ S_a \end{bmatrix} = C \begin{bmatrix} L' \\ M' \\ S' \end{bmatrix} \tag{1.1.8.22}$$

1.1.8.4 The model in matrix form

The L_a, M_a, and S_a of test and reference field can be expressed as

$$\begin{bmatrix} L_a \\ M_a \\ S_a \end{bmatrix} = C_{ref} \cdot A_{ref} \cdot M \cdot \begin{bmatrix} X_{ref} \\ Y_{ref} \\ Z_{ref} \end{bmatrix} \tag{1.1.8.23}$$

$$\begin{bmatrix} L_a \\ M_a \\ S_a \end{bmatrix} = C_{test} \cdot A_{test} \cdot M \cdot \begin{bmatrix} X_{test} \\ Y_{test} \\ Z_{test} \end{bmatrix} \tag{1.1.8.24}$$

from equations 1.1.8.4, 1.1.8.19 and 1.1.8.22. By equating 1.1.8.23 and 1.1.8.24, the entire model can be expressed as a single matrix equation.

$$\begin{bmatrix} X_{test} \\ Y_{test} \\ Z_{test} \end{bmatrix} = M^{-1} \cdot A_{test}^{-1} \cdot C_{test}^{-1} \cdot C_{ref} \cdot A_{ref} \cdot M \cdot \begin{bmatrix} X_{ref} \\ Y_{ref} \\ Z_{ref} \end{bmatrix} \tag{1.1.8.25}$$

Equations used for the experiment.

Knowns for calculation.

M_{E-H-P} : Estévez-Hunt-Pointer Primaries

$X_{n,ref}$, $Y_{n,ref}$, $Z_{n,ref}$: White reference TSV for the reference field

$X_{n,test}$, $Y_{n,test}$, $Z_{n,test}$: White reference TSV for the test field

X_{ref}, Y_{ref}, Z_{ref} : TSV of corresponding color for the reference field

$Y_{N,ref}$: Luminance of the reference field in units of cd/m^2

$Y_{N,test}$: Luminance of the test field in units of cd/m^2

Unknowns are X_{test}, Y_{test}, Z_{test}

Pre-calculation

(1) Calculate fundamental tristimulus values L_n, M_n, S_n

$$\begin{bmatrix} L_{n,ref} \\ M_{n,ref} \\ S_{n,ref} \end{bmatrix} = M_{E-H-P} \cdot \begin{bmatrix} X_{n,ref} \\ Y_{n,ref} \\ Z_{n,ref} \end{bmatrix} \quad \begin{bmatrix} L_{n,test} \\ M_{n,test} \\ S_{n,test} \end{bmatrix} = M_{E-H-P} \cdot \begin{bmatrix} X_{n,test} \\ Y_{n,test} \\ Z_{n,test} \end{bmatrix} \tag{1.1.8.26}$$

(2) Calculate chromatic adaptation matrix A

Since hardcopy is used in both fields, complete adaptation is assumed.

$$\begin{aligned} a_{L,ref} &= \frac{1}{L_{n,ref}} \quad a_{L,test} = \frac{1}{L_{n,test}} \\ a_{M,ref} &= \frac{1}{M_{n,ref}} \quad a_{M,test} = \frac{1}{M_{n,test}} \\ a_{S,ref} &= \frac{1}{S_{n,ref}} \quad a_{S,test} = \frac{1}{S_{n,test}} \end{aligned} \tag{1.1.8.27}$$

$$A_{ref} = \begin{bmatrix} a_{L,ref} & 0.0 & 0.0 \\ 0.0 & a_{M,ref} & 0.0 \\ 0.0 & 0.0 & a_{S,ref} \end{bmatrix} \quad A_{test} = \begin{bmatrix} a_{L,test} & 0.0 & 0.0 \\ 0.0 & a_{M,test} & 0.0 \\ 0.0 & 0.0 & a_{S,test} \end{bmatrix} \tag{1.1.8.28}$$

(3) Luminance-dependent interaction matrix C

Luminances were 214 cd/m^2 for the reference field, 71, 214 and 624 cd/m^2 for the test fields.

$$\begin{aligned} c_{ref} &= 0.219 - 0.0784 \log_{10}(214) = 0.03630 \\ c_{test} &= 0.219 - 0.0784 \log_{10}\left(\begin{bmatrix} 71 \\ 214 \\ 624 \end{bmatrix}\right) = 0.03630 \end{aligned} \tag{1.1.8.29}$$

$$C_{ref}=\begin{bmatrix}1 & c_{ref} & c_{ref}\\ c_{ref} & 1 & c_{ref}\\ c_{ref} & c_{ref} & 1\end{bmatrix}\quad C_{test}=\begin{bmatrix}1 & c_{test} & c_{test}\\ c_{test} & 1 & c_{test}\\ c_{test} & c_{test} & 1\end{bmatrix} \tag{1.1.8.30}$$

(4) In single matrix form

From the equation (1.1.8.25), the matrix portion can be simplified.

$$\mathscr{M}_{\mathrm{RLAB}}=M_{E-H-P}^{-1}\cdot A_{test}^{-1}\cdot C_{test}^{-1}\cdot C_{ref}\cdot A_{ref}\cdot M_{E-H-P} \tag{1.1.8.31}$$

Main-calculation

$$\begin{bmatrix}X_{test}\\ Y_{test}\\ Z_{test}\end{bmatrix}=\mathscr{M}_{\mathrm{RLAB}}\bullet\begin{bmatrix}X_{test}\\ Y_{test}\\ Z_{test}\end{bmatrix} \tag{1.1.8.32}$$

1.2 Viewing Method

There are a number of viewing techniques that are applicable to testing color appearance models: memory matching, haploscopic, and successive haploscopic techniques (Wright, 1981).

1.2.1 Memory Method - Direct Scaling

This technique is suited to studying color appearance under the steady-state-adaptation situation using solid color patches. It requires memorizing perceptual attributes such as the Munsell or NCS designations. Since this experiment uses pictorial scenes, the technique could not be validated for this purpose. It would be too difficult for an observer to memorize a reference image, wait until adapted in full and then make a judgment.

1.2.2 Haploscopic Viewing Method

An observer views the test field in one eye and judges it against a reference field viewed in the other eye. The precision of haploscopic matching is higher than memory method but lower than that of matches made when viewing the two fields in the same eye, while the validity of the technique depends on the assumption that adaptation of one eye does not affect the sensitivity of the other eye. This is almost certainly not strictly true, although the effect on the other eye is quite small, especially in relation to the major changes in sensitivity in the directly adapted eye.

1.2.3 Successive Haploscopic Viewing Method

One eye is exposed to a given adapting stimulus while the second eye is occluded. When the second eye is exposed to the second adapting stimulus,

the first eye is occluded. The observer never views the two different adapting situations simultaneously, but rather views them in succession. This method leaves the state of adaptation undefined.

1.2.4 Successive-*Ganzfeld* Haploscopic Viewing Method

Because of the limitation in the memory , haploscopic and successive haploscopic viewing methods, a new technique was developed. This technique allows direct comparisons and matches to be made across different adapting conditions. The technique eliminates binocular rivalry and confusion of cognitive chromatic-adaptation mechanisms since only a single stimulus is perceived at any given time. The main advantage of the successive-*Ganzfeld* haploscopic viewing technique is that the state of the sensory chromatic-adaptation mechamisms is well-defined and constant for each eye while binocular rivalry and problems with cognitive mechanisms are eliminated. Greater detail can be found in Fairchild, Pirrotta and Kim (1993).

2. EXPERIMENTAL

2.1 Apparatus

Hardware for the experiment consist of the viewing booth and the successive-Ganzfeld haploscopic device.

2.1.1 Viewing Booth

The housings for the light bulbs were acquired from old Diano Lite light boxes. The viewing booth was constructed using plywood. The layout of the viewing booth was carefully designed so the two light housings could fit well. The partition in the center was inserted so that either field or light source does not interfere each other.

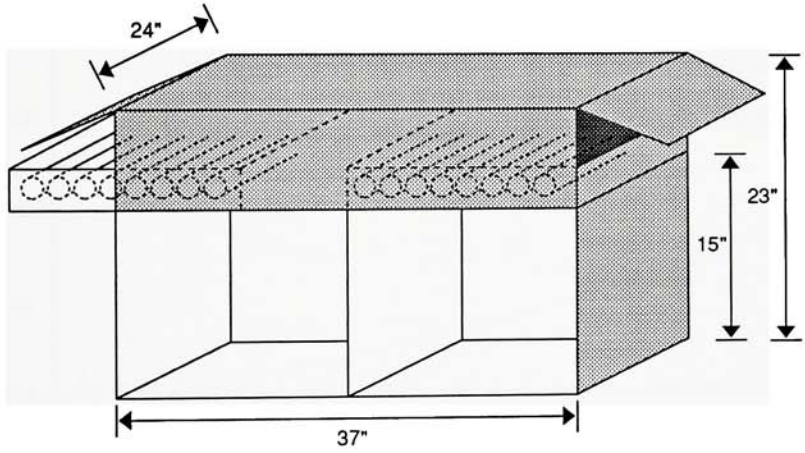

Fig. 2.1 Viewing Booth. The right viewing field is illuminated with simulated source A and the left field, simulated D65. Switches allow control of each bulb in order to vary luminance.

The interior was painted with an approximately spectrally non-selective gray paint with a luminance factor of 0.2. Diffusing panels were inserted underneath each set of light sources to improve the uniformity of the illumination.

2.1.2 Illumination

The right side of the booth (reference field) had tungsten bulbs closely simulating CIE illuminant A at 214 cd/m². The left side (test field) had high color rendering fluorescent tubes with chromaticities near D65. The daylight test field had three luminance level settings which were equivalent, 1/3 and 3 times the luminance level of the reference illuminant A field (71, 214 and 642 cd/m²). The test field setting were named as D65-M, D65-L and D65-H for convenience. The spectral power distributions are shown in Fig. 2.2 (spectral data is in Appendix C).

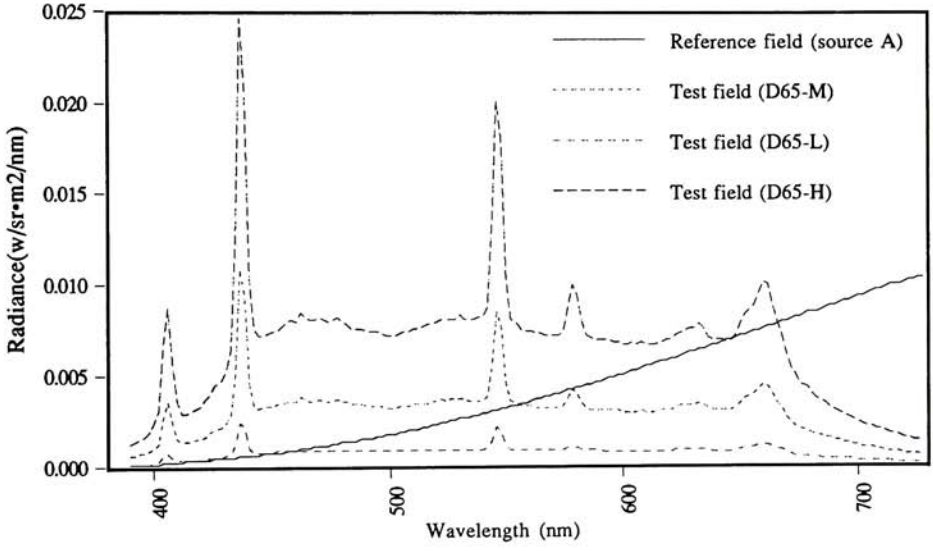

Fig. 2.2. Spectral power distribution plots of the sources

The measurement of luminances of the booth was made with a Photo Research PR703 by measuring a piece of Halon as a white reference as it is viewed from the viewing device. Three luminance levels of the test field were achieved by manipulating an electrical power transformer, individual switches for each bulb and a screen (no color, used to attenuate the light)

underneath the bulbs. Detailed information such as TSV, luminance and correlated color temperature on booth settings are shown in TABLE 2.1.

TABLE 2.1 Illuminants used in the experiment.

	X	Y	Z	Luminance (cd/m^2)	Correlated Color Temperature
Reference Illuminant (simulated Source A)	115.20	100.00	25.06	214	2488
Test Illuminant (Simulated D65-M)	94.73	100.00	102.89	71	6170
Test Illuminant (Simulated D65-L)	94.92	100.00	96.85	214	5816
Test Illuminant (Simulated D65-H)	94.44	100.00	101.58	642	6119

2.1.3 Successive-*Ganzfeld* Haploscopic Devices

To achieve successive viewing, a shutter mechanism with diffusers made from frosted Mylar™ was devised as shown in Fig. 2.3 (Fairchild, Pirrotta, Kim, 1993). The observer could control via a foot pedal whether the *Ganzfeld* blocked the test or reference field. The purpose of this alternating

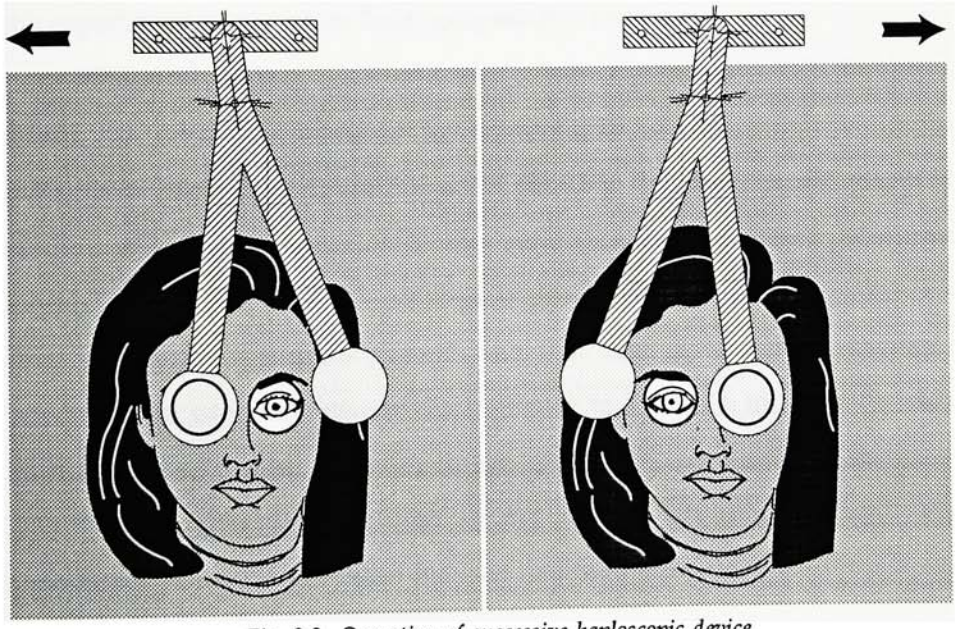

Fig. 2.3 Operation of successive haploscopic device

viewing was to maintain each eye's state of chromatic adaptation while preventing the simultaneous viewing of images. A detailed diagram (Fig. F-1) of the device is shown in Appendix F.

2.2 Sample Preparation

Four images were acquired from ISO SCID (Standard Color Image Data)[1] set: "fruit basket," "orchid," "musicians," and "candles." The four-color CMYK 8 bit 2048 by 2560 pixel images were transformed into 3 color CMY 8 bit 1024 by 1280 pixel images using lookup tables based on CIELAB matching of the DuPont 4Cast™ dye-diffusion thermal-transfer printer.

The reason for the four (CMYK) to three (CMY) color conversion is to avoid difficulty of 3 (XYZ) to 4 (CMYK) channels conversion which can result in multiple solutions, which adds one more variable to the experiment. The three color printed images were good enough to be used in the experiment (the experiment does not include acceptability test).

When calculating corresponding colors, a significant shift in the color gamut can result for some of the appearance models resulting in many unprintable colors (*e.g.*, LABHNU and CIELUV). To avoid gamut mapping as another experimental variable, the reference images were compressed linearly in CIELAB until all the models predicted corresponding colors that were within the printer's gamut (see Fig. 2.4). (Because of this gamut reduction, the exclusion of the black printer in the XYZ to CMY conversion did not adversely affect the color image quality.) Four sets of the compressed CMY 8 bit images were defined as the original reference images. Visual inspection assured proper color balance and tone rendition.

---

[1] It will be available in CD-ROM from ISO as ISO 12640, developed by ISO/TC130/WG2.

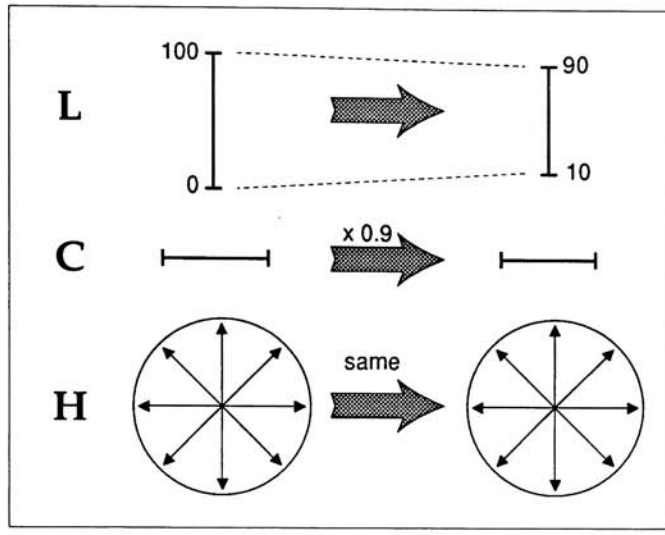

Fig. 2.4 Gamut compression of original images. Pixel information was transformed into LCH and L and C were used to calculate new color coordinates.

The XYZ values for the 125 5x5x5 target patches that were used to build lookup tables were calculated with each of the illuminant and spectral reflectance factors measured with a BYK-Gardner color-view™. For example, four sets of XYZ values were calculated, one with simulated source A for the reference field and three others with D65-M, D65-L and D65-H for the test fields.

To simplify the process of running many images through two successive tetrahedral interpolation lookup tables, CMY to XYZ for the reference condition and XYZ to CMY for each of three test conditions, $CMY_{reference}$ to CMY_{test} lookup tables were built each with 33x33x33 entries based on the method of Hung (1992) (Calibration result in Appendix B).

Once corresponding images were computed, image pairs were printed for each pairwise combination of the eight appearance models corresponding to 28 pairs in random order. This was repeated for each test field condition. A different random order was used for each test condition.

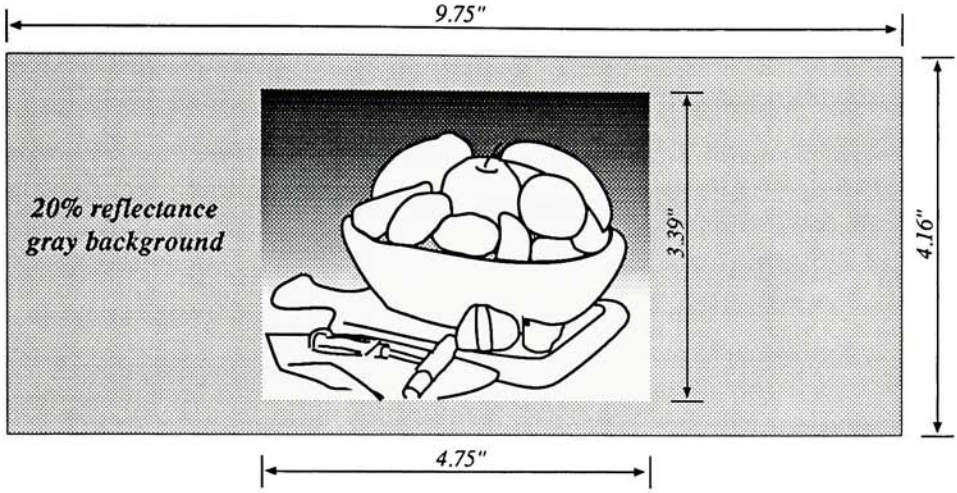

Fig. 2.5 Sample layout of reference field image .

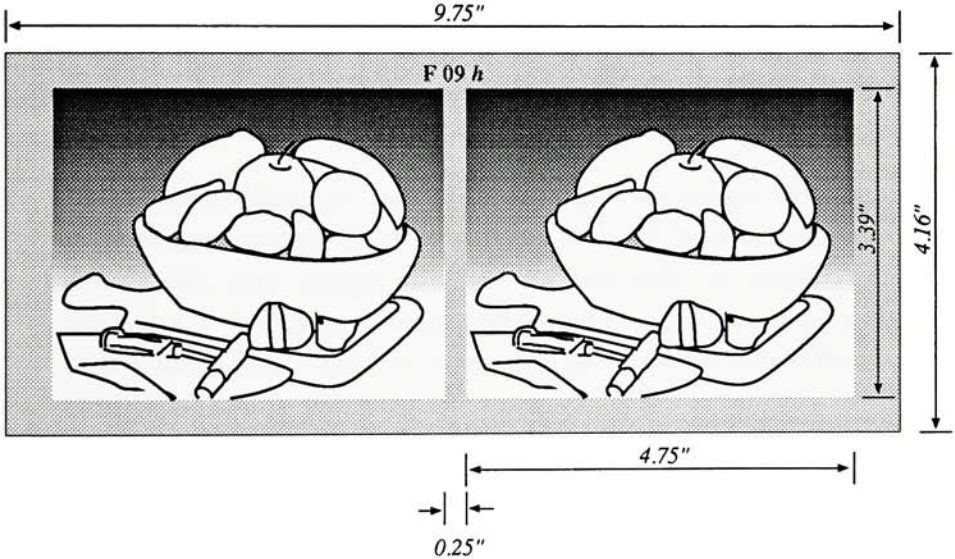

Fig. 2.6 Sample layout of test field image .

The layout of the reference field image is shown in Fig. 2.5. The size of image was determined considering viewing angle and distance from viewing device. The image is surrounded with 20% reflectance neutral. The CMY

value for the neutral can be found using XYZ to CMY conversion method using the 20% of reference white XYZ values.

The layout of the test field image is shown in Fig. 2.6. The size of the image itself is the same as reference image. Each image represents an appearance model. Each plate was numbered to identify the pair (paired randomly).

2.3 Psychophysics

Thirty color-normal observers with varying imaging experience took part in the experiment. Observers were instructed to select one of the images from the test pair that most closely matched the reference image. The following instructions were provided at the start of each experimental session:

> "In this experiment, you will be comparing two images at a time. A reference image is on the right side of booths(source A simulated), test images are on the left side of booths(D65 simulated). A reference image and tested images can not be seen at the same time. One of them will be blocked with diffuser. Using foot switch you can toggle between the booths. You must choose from tested images by saying 'left' or 'right' which appears closest to reference image. If they appear the same, you must still make a choice. If you can't decide, just guess. Many pairs of images will appear identical, please do not let this frustrate you. You should make overall judgements and not compare very small image areas. There are three sessions. Each session has 4 scenes and 28 pairs of images per scene."

Three separate observering sessions were used corresponding to the three test field conditions (D65-M, D65-L and D65-H). A total of 336 observations resulted per observer.

Observer data were collected and summed on tally sheets as in TABLE 2.2. Each cell represents preference of one model (column) over another model (row). For example, the column 3 and row 4 cell which has 30 means that CIELAB was preferred 30 times out of 30 over CIELUV.

TABLE 2.2 Count tally sheet

	VK	CIELAB	CIELUV	HNULAB	RT	Hunt	Nayatani	RLAB
VK	*	16	0	0	3	15	10	13
CIELAB	14	*	0	0	1	14	13	15
CIELUV	30	30	*	28	30	30	30	30
HNULAB	30	30	2	*	16	30	25	30
RT	27	29	0	14	*	30	23	28
Hunt	15	16	0	0	0	*	8	15
Nayatani	20	17	0	5	7	22	*	21
RLAB	17	15	0	0	2	15	9	*

*Abbreviation note: VK-von Kries, RT-Reilly Tannenbaum.

Each cell was divided by the total number of judgments to calculate proportions (TABLE 2.3). Using Thurstone's law of comparative judgments (Gescheider, 1985, Appendix G), Z-scores were calculated (TABLE 2.4). The column sum results in an interval scale where the larger the number, the more accurate a model was in predicting appearance matches. The scale values are in units of standard deviations ($1/\sqrt{2} = 0.7071$ represents 1 standard deviation). Differences between models greater than 1.39 are statistically significant at a 95% confidence interval.

TABLE 2.3 Normalized matrix

	VK	CIELAB	CIELUV	HNULAB	RT	Hunt	Nayatani	RLAB
VK	*	0.53	0.00	0.00	0.10	0.50	0.33	0.43
CIELAB	0.47	*	0.00	0.00	0.03	0.47	0.43	0.50
CIELUV	1.00	1.00	*	0.93	1.00	1.00	1.00	1.00
HNULAB	1.00	1.00	0.07	*	0.53	1.00	0.83	1.00
RT	0.90	0.97	0.00	0.47	*	1.00	0.77	0.93
Hunt	0.50	0.53	0.00	0.00	0.00	*	0.27	0.50
Nayatani	0.67	0.57	0.00	0.17	0.23	0.73	*	0.70
RLAB	0.57	0.50	0.00	0.00	0.07	0.50	0.30	*

☞ If normalized values are greater than 0.99 or smaller than 0.01, z-scores are clipped to 2.33 or -2.33.

TABLE 2.4 z-score matrix

	VK	CIELAB	CIELUV	HNULAB	RT	Hunt	Nayatani	RLAB
VK	*	0.08	-2.33	-2.33	-1.28	0.00	-0.44	-0.18
CIELAB	-0.10	*	-2.33	-2.33	-1.88	-0.10	-0.18	0.00
CIELUV	2.33	2.33	*	1.48	2.33	2.33	2.33	2.33
HNULAB	2.33	2.33	-1.56	*	0.08	2.33	0.95	2.33
RT	1.28	1.75	-2.33	-0.10	*	2.33	0.71	1.48
Hunt	0.00	0.08	-2.33	-2.33	-2.33	*	-0.64	0.00
Nayatani	0.41	0.15	-2.33	-0.99	-0.74	0.61	*	0.52
RLAB	0.15	0.00	-2.33	-2.33	-1.56	0.00	-0.52	*
SUM	6.40	6.72	-15.54	-8.93	-5.38	7.50	2.21	6.48

3. RESULTS AND DISCUSSION

The z scores along with their 96% confidence limits (±2 σ, standard deviation) for each image and the four images combined (total) are shown in Fig 3.1 - 3.19. Each model is shown along the ordinate in order of the combined scale value (z-score).

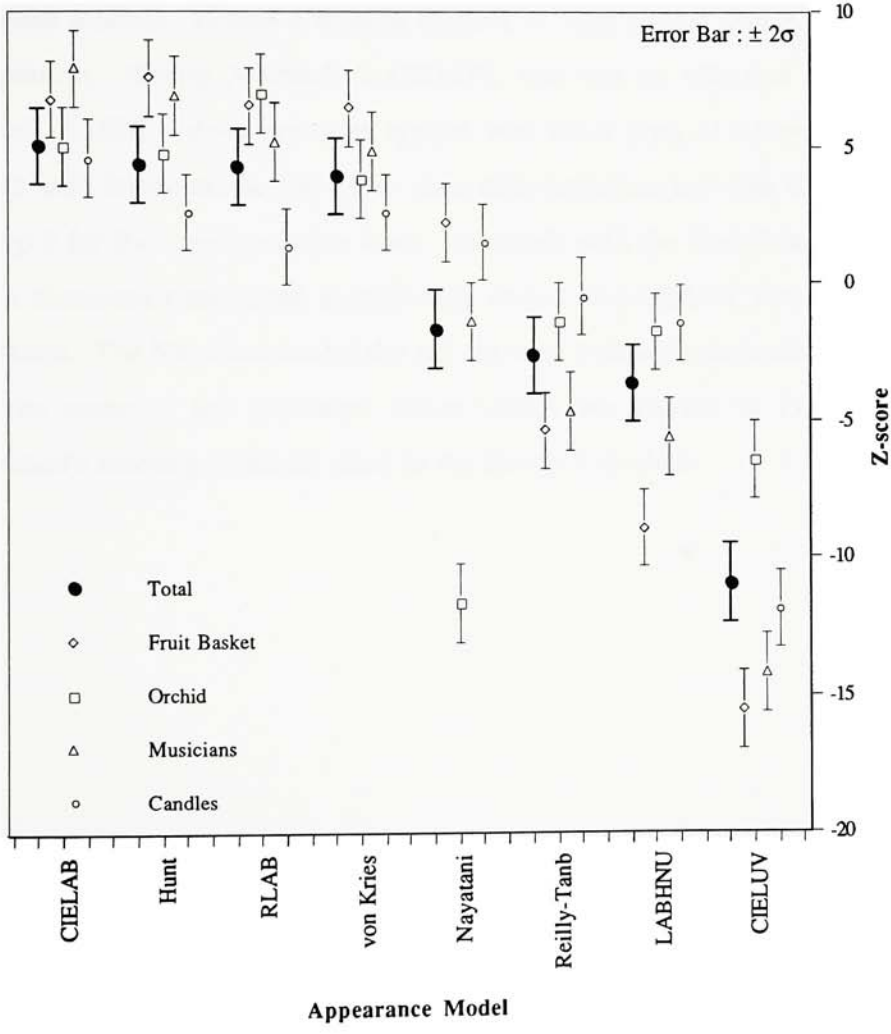

Fig. 3.1. Z-score plot at the same luminance level

Results for the *same luminance level* are shown in Fig. 3.1-3.6. The results show that there are three groups. Group 1, which is CIELAB, Hunt, RLAB and von Kries, shows no significant difference in result with *total* between models. Group 1 models are all based on von Kries type of adaptation and sample targets are similar (Hunt and RLAB at the *same luminance level* are the same as von Kries). Group 2, which are Nayatani, Reilly-Tannenbaum and LABHNU, shows statistically no significant difference in result with *total* between models. Group 2 models include at least partial von Kries type of adaptation. Group 3, which is CIELUV, was not an effective appearance model. CIELUV does not uses typical von Kries type of adaptation. The result with image *candle* shows no clear differentiation between Group 1 and Group 2 for the *same luminance level*. The result with the *Orchid* image, which has a dominant dark tinted background, shows that CIELUV was better than Nayatani. The Nayatani model did not do very well with dark colors. Except for the some of the saturated colors which are shown in *Fruit Basket*, Nayatani's model performed close to the Group 1 models.

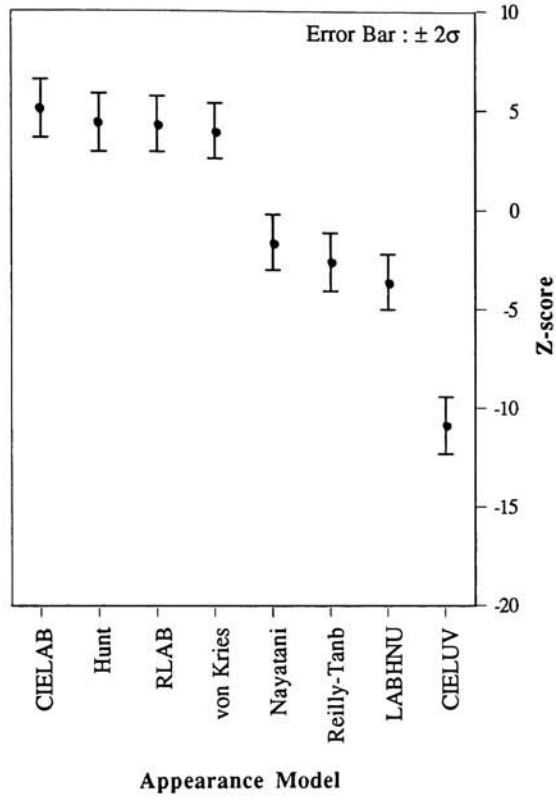

Fig. 3.2. Z-score plot of *Total* at the same luminance level

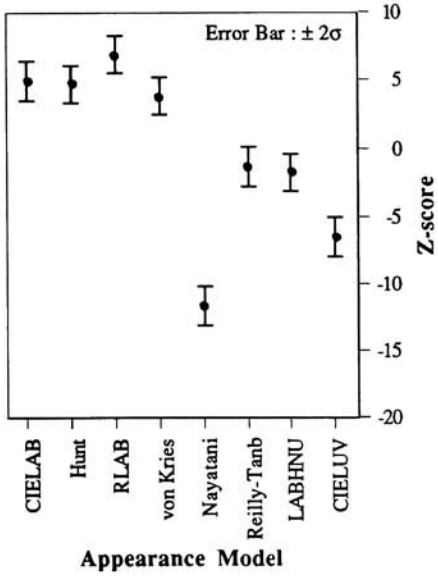

Fig. 3.3. Z-score plot of *Orchid* at the same luminance level

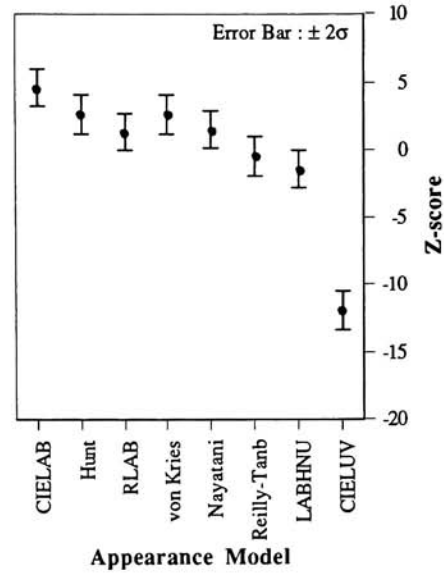

Fig. 3.4. Z-score plot of *Candles* at the same luminance level

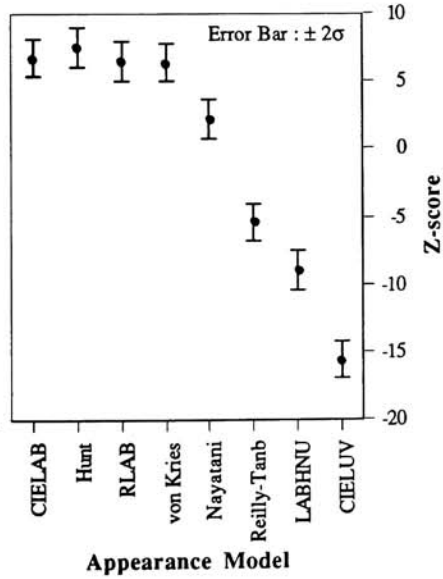

Fig. 3.5. Z-score plot of *Fruit Basket* at the same luminance level

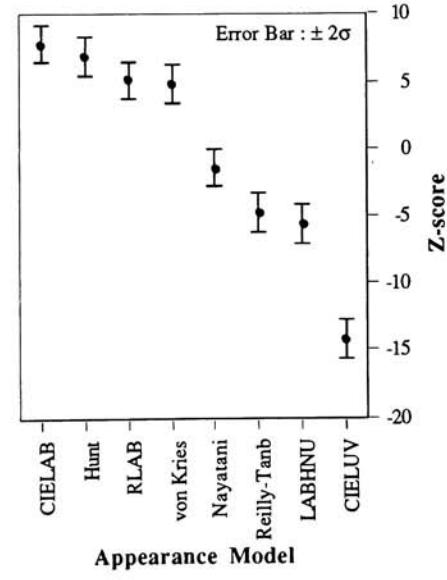

Fig. 3.6. Z-score plot of *Musicians* at the same luminance level

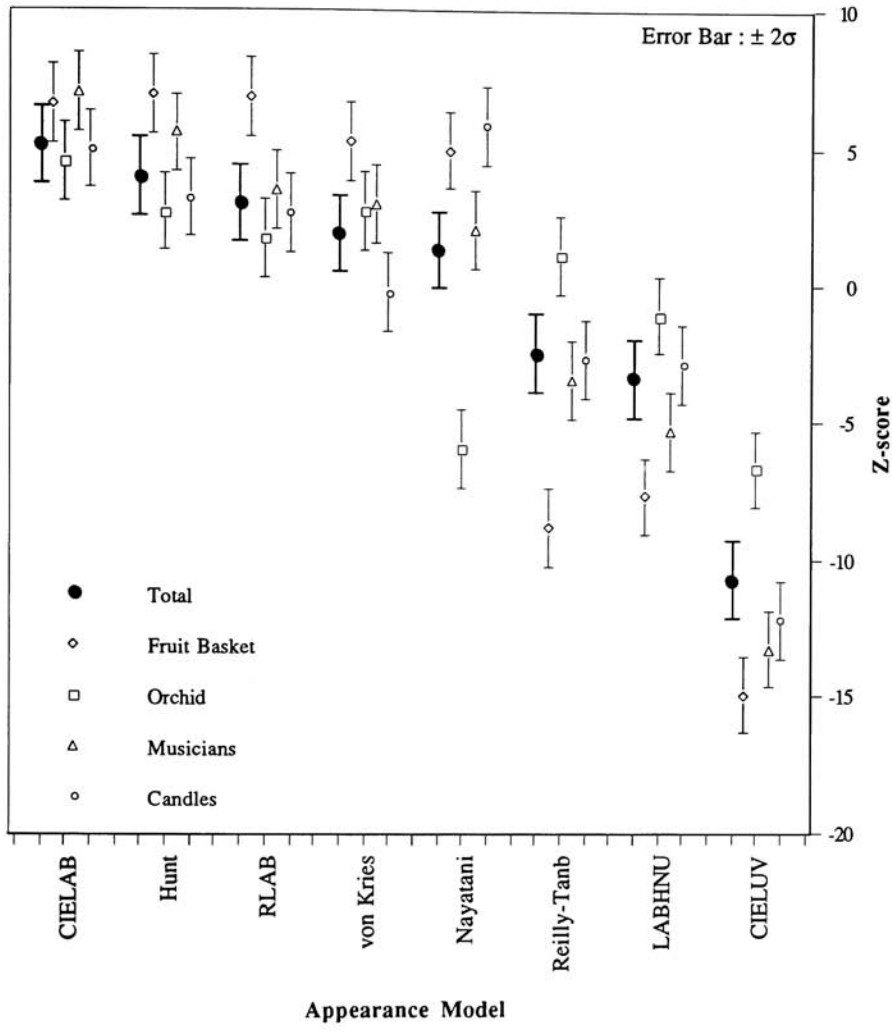

Fig. 3.7. Z-score plot at the 1/3 luminance level

Result for the *1/3 luminance level* are shown in Fig. 3.7-3.12. The result shows that there are three groups. Group 1, which is CIELAB, Hunt, RLAB, von Kries and Nayatani, shows no statistically significant difference in result with *total* between models. Group 1 models are all based on von Kries type of adaptation. Hunt Nayatani, and RLAB take into account luminance level

changes. Result shows that at the *1/3 luminance level* the luminance dependency model is not working very well. Note that for a reduced luminance level the Nayatani model is in Group 1. It's luminance level consideration is the major reason. Group 2, which are Reilly-Tannenbaum and LABHNU, shows statistically no significant difference in result with *total* between models. Group 3 which is the worst one among the models is CIELUV. Dark color problems with Nayatani's model were repeated for the *1/3 luminance level.*

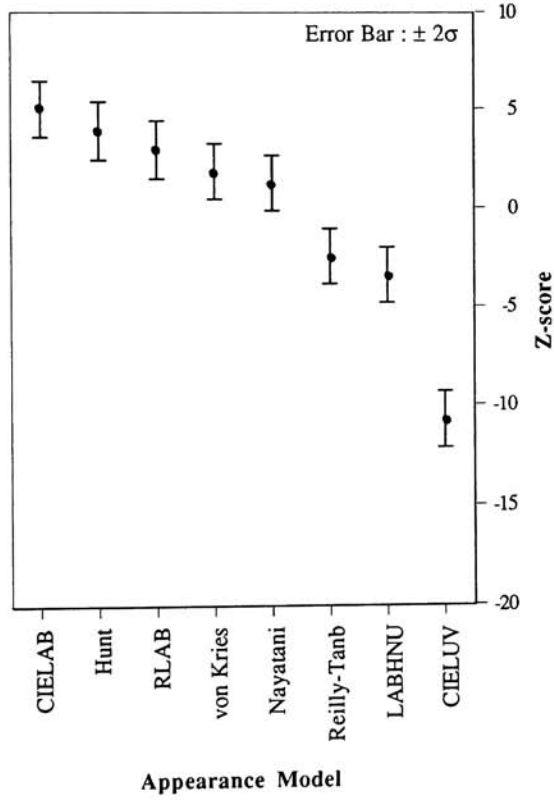

Fig. 3.8. Z-score plot of *Total* at the 1/3 luminance level

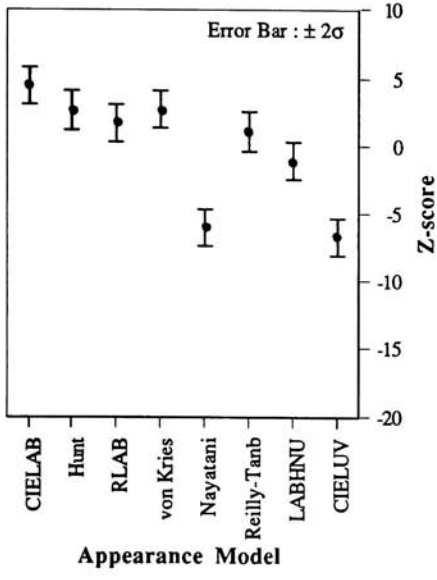

Fig. 3.9. Z-score plot of *Orchid* at the 1/3 luminance level

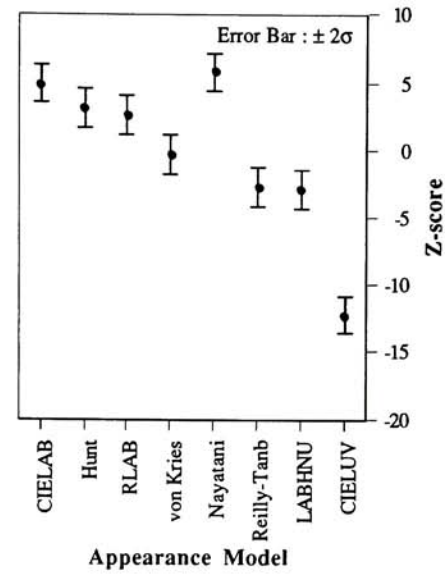

Fig. 3.10. Z-score plot of *Candles* at the 1/3 luminance level

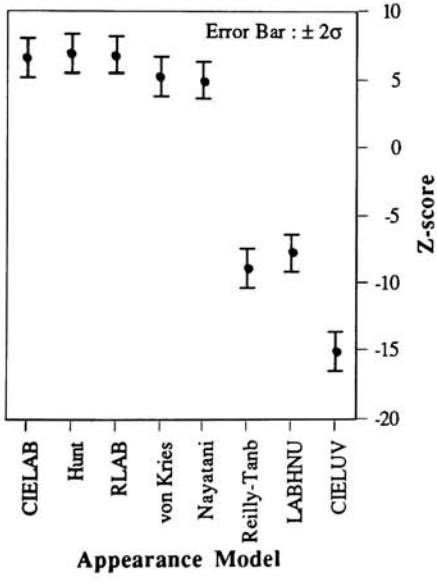

Fig. 3.11. Z-score plot of *Fruit Basket* at the 1/3 luminance level

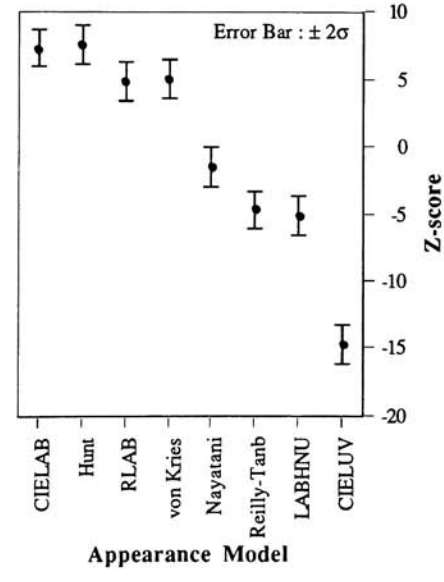

Fig. 3.12. Z-score plot of *Musicians* at the 1/3 luminance level

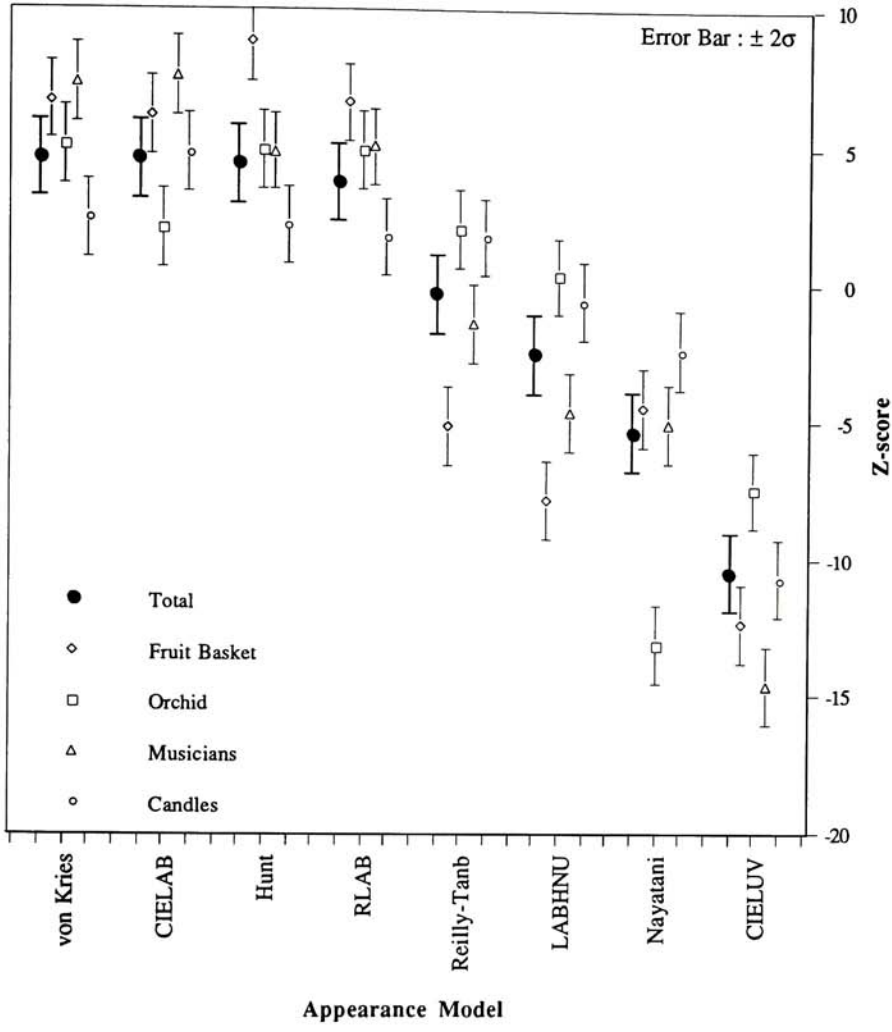

Fig. 3.13. Z-score plot at the 3 times luminance level

Results for the *3 times luminance level* are shown in Fig. 3.13-3.18. There are again three groups. Group 1, which is CIELAB, Hunt, RLAB and von Kries, shows no significant difference in result with *total* between models. Group 1 models are all based on von Kries type of adaptation. Group 2, which are Reilly-Tannenbaum, LABHNU and Nayatani, are positioned between group 1

and group 3. There is a statistically significance difference between Reilly-Tannenbaum and Nayatani. Nayatani's model includes a luminance dependency. Group 3, which is CIELUV, was not an effective appearance model. Nayatani's luminance dependency made results of this model worse than the *same luminance* and *1/3 luminance levels*. It is obvious that Nayatani's luminance dependency does not properly predict the effect of changes in luminance under the same conditions.

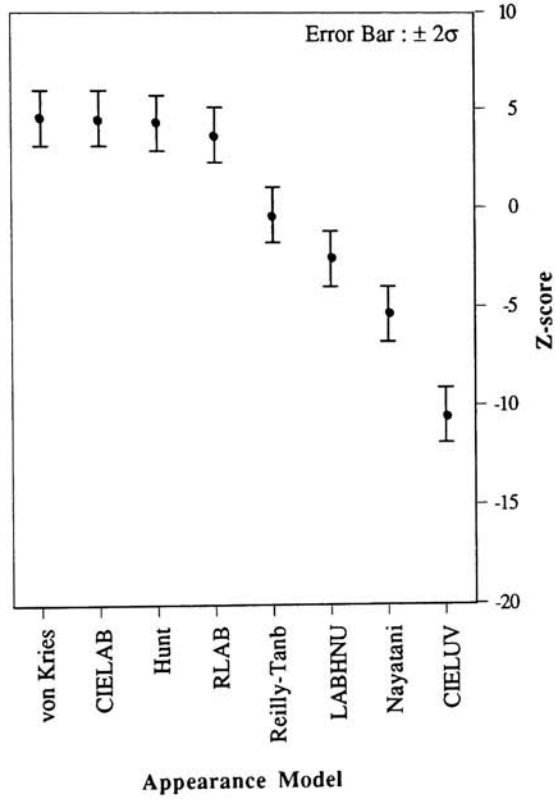

Fig. 3.14. Z-score plot of *Total* at the 3 times luminance level

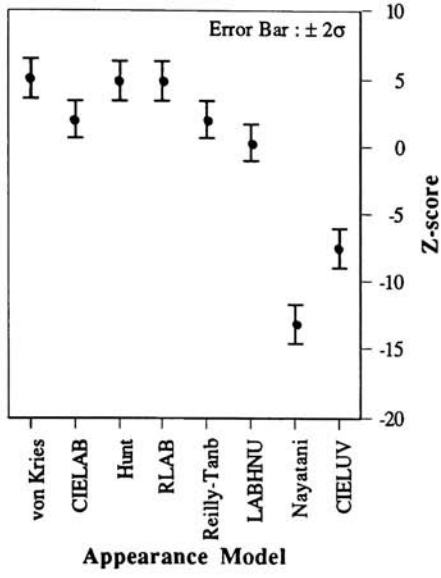

Fig. 3.15. Z-score plot of *Orchid* at the 3 times luminance level

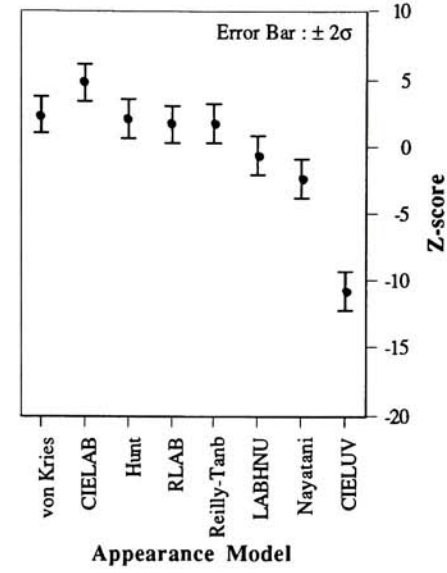

Fig. 3.16. Z-score plot of *Candles* at the 3 times luminance level

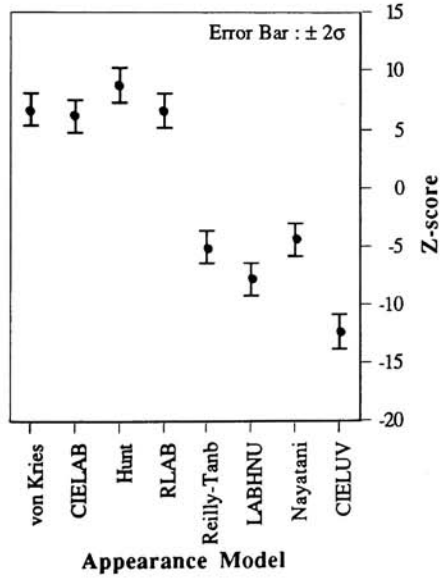

Fig. 3.17. Z-score plot of *Fruit Basket* at the 3 times luminance level

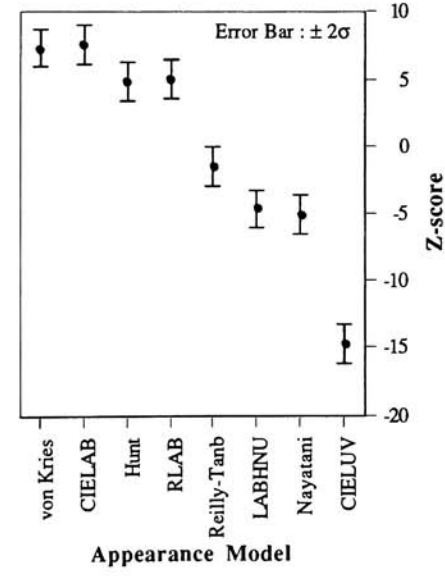

Fig. 3.18. Z-score plot of *Musicians* at the 3 times luminance level

The model order changed slightly with differences in adapting luminance level of the test field; these differences, however, were not statistically significant. This was a somewhat surprising result. The models of von Kries, CIELAB, CIELUV, Reilly-Tannenbaum, and Richter are all luminance invariant while the remaining models take into account adapting luminance. This suggests that for these experimental conditions, luminance did not affect observer judgments of hue, lightness, and chroma. This result may not persist for different experimental conditions or when viewing single stimuli rather than images.

The models which showed poorer performance also showed strong image dependence. This was particularly notable for the Nayatani model results. Image "orchid" always yielded very poor performance because of its predominant dark-bluish background. The Nayatani model predicts a large change in hue and lightness of the background to take into account the Helson-Judd[1] and Steven's effects.[2] The effects were not observed causing the large discrepancy between the observed and predicted results. The LABHNU model provides another image-dependent example where the image "fruit basket" always had the poorest performance; in this case the hues of the high-chroma fruit colors were incorrectly predicted.

The average for all four images and three test field conditions is shown in Fig. 3.19. The appearance models could be divided into three statistical categories. The first category consisted of von Kries, CIELAB, Hunt, and RLAB; these models produced images that most closely matched the reference images. The differences between these models were not statistically significant. The second category consisted of LABHNU, Reilly-Tannenbaum,

---

[1] see 1.1.6.9
[2] see 1.1.6.22

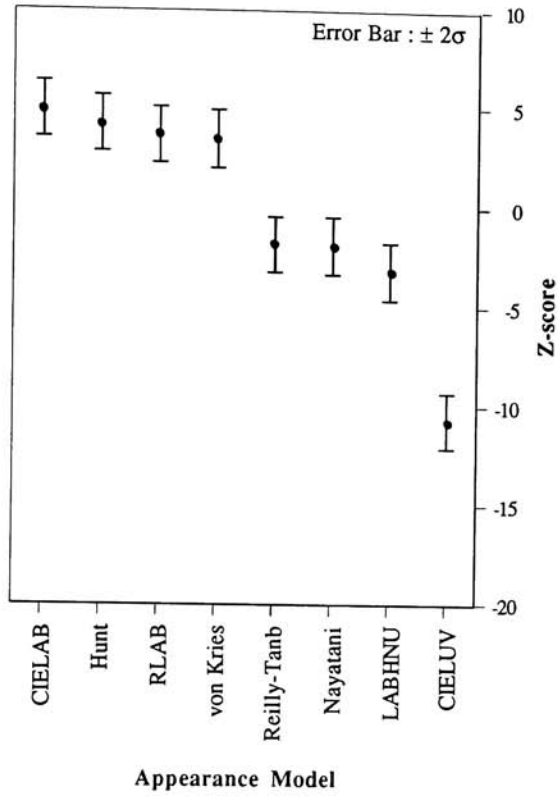

Fig. 3.19 Plot of z-scores for average of all three luminance levels.

and Nayatani which produced significantly poorer results. The third category consisted of CIELUV producing the worst results. For these viewing conditions, von Kries-based appearance models, with the exception of Nayatani, were the most effective models in yielding color appearance matches. The Nayatani model could be improved to the level of performance of the other von Kries-type models by reducing the Helson-Judd and Steven's effects. Both effects adversely altered the tone reproduction by changing the gray balance (light grays became yellowish and dark grays became bluish) and reducing contrast. Changes in tone reproduction and gray balance are very noticeable in images.

4. CONCLUSION

The color appearance models of von Kries, CIELAB, Hunt, and RLAB, which are based on von Kries type adaptation, were the most effective models in predicting color appearance matches under the conditions studied: successive-Ganzfeld haploscopic viewing, fluorescent-daylight and tungsten sources, and pictorial stimuli.

Luminance dependent models such as Hunt and RLAB did not perform better than von Kries or CIELAB with varying luminance levels. Nayatani's model did not perform as well as the other von Kries type models, but it's luminance dependency became effective when the luminance level was reduced. This was not true for the *tripled luminance level.* CIELUV, which does not have an effective adaptation term, (subtraction rather than division like von Kries) performed most poorly among the models. Clearly, the proportionality rule of the von Kries model was capable of predicting most of the effect of changing illuminants as described in this thesis.

LABHNU, which is similar to CIELUV but uses X and Z terms instead of chromaticity (x, y) to determine hue, performed better than CIELUV. This implies that the use of chromaticity values is not as effective as using TSVs.

It is interesting to note that the simplest models, CIELAB, von Kries, and RLAB were as least as effective as the much more complicated Hunt, and Nayatani models. WYSIWYG color transformations may thus be practical for (using colorimetry based) some hardcopy systems.

This psychophysical experiment, however, generated interval scales of matching effectiveness, not scales of acceptability. The issue of acceptability, so important in a practical system, is not addressed. Further testing is required under typical WYSIWYG conditions (in order to determine

acceptability). From the author's subjective point of view, the color appearance models of von Kries, CIELAB, Hunt, and RLAB are performing as barely acceptable. Since there is no absolute reference, judgment is only possible by comparison. With development of better models, the subjective acceptablity can be changed easily.

5. REFERENCES

1. C. J. Bartleson and E. J. Breneman, Brightness perception in complex fields, J. Opt. Soc. Am. 57, 953-957 (1967).

2. C. J. Bartleson, Comparison of chromatic-adaptation transforms, *Color Res. Appl.* **3**, 129-136 (1978).

3. C. J. Bartleson, A review of chromatic adaptation, in *AIC Proceedings, Color 77, Troy, NY, 1977*, edited by F. W. Billmeyer, Jr. and G. Wyszecki, Adam Hilger, Bristol, 1978, pp. 63-96.

4. C. J. Bartleson, Predicting corresponding colors with changes in adaptation, *Color Res. Appl.* **4**, 143-155 (1979).

5. C. J. Bartleson, On chromatic adaptation and persistence, *Color Res. Appl.*, **6**, 153-160 (1981).

6. W. L. Brewer, Fundamental response functions and binocular color matching, *J. Opt. Soc. Am.* **44**, 207-212 (1954).

7. E. J. Breneman, Corresponding chromaticities for different states of adaptation to complex visual fields, *J. Opt. Soc. Am. A*, **4**, 1115-1129 (1987).

8. Commission Internationale de l'Eclairage (CIE), *Colorimetry Publication CIE No 15.2*, Central Bureau of the CIE, Paris, 1978.

9. O. Estevez, On the fundamental data base of normal and dichromatic colour vision, Ph.D. Thesis, University of Amsterdam, 1979.

10. M. D. Fairchild, Chromatic adaptation and color appearance, Ph.D. Dissertation, University of Rochester, (1990).

11. M. D. Fairchild, Formulation and testing of an incomplete-chromatic-adaptation model, *Color Res. Appl.* **16**, 243-250 (1991).

12. M. D. Fairchild and R. S. Berns, Image Color-Appearance Specification Through Extension of CIELAB, *Color Res. Appl.* **18**, 178-190 (1993).

13. M. D. Fairchild, E. Pirrotta, T. Kim, Successive-Ganzfield Haploscopic Viewing Technique for Color-Appearance Research, *Color Res. Appl.* in press, 1994.

14. M. D. Fairchild and E. Pirrotta, Predicting the lightness of chromatic object colors using CIELAB, *Color Res. Appl.* **16**, 385-393 (1991).

15. G. A. Gescheider, *Psychophysics Method, Theory, and Application*, Lawrence Erlbaum Associates, 1985, pp264.

16. P. Hung, Tetrahedral division technique applied to colorimetric calibration for imaging media, *IS&T Final Program and Advance Printing of Paper Summaries*, 419-422 (1992).

17. P. Hung, Colorimetric calibration in electronic imaging devices using a look-up-table model and interpolations, *J. Electronic Imaging*, **2(1)**, 53-61 (1993).

18. R. W. G. Hunt, The specification of colour appearance. II. Effects of changes in viewing conditions, *Color Res. Appl.* **3**, 109-120 (1977).

19. J. E. Hochberg, W. Triebel, and G. Seaman, Color adaptation under conditions of homogeneous visual stimulation,., (1950).

20. R. W. G. Hunt, The effects of daylight and tungsten light adaptation on color perception, *J. Opt. Soc. Am.* **40**, 362-371 (1950).

21. R. W. G. Hunt, Light and dark adaptation and the perception of color, *J. Opt. Soc. Am.* **42**, 190-199 (1952).

22. R. W. G. Hunt, The perception of color in 1° field for different states of adaptation, *J. Opt. Soc. Am.* **43**, 479-484 (1953).

23. R. W. G. Hunt, The specification of colour appearance. II. Effects of changes in viewing conditions, *Color Res. Appl.* **3**, 109-120 (1977).

24. R. W. G. Hunt, A model of colour vision for predicting colour appearance, *Color Res. Appl.* **7**, 95-112 (1982).

25. R. W. G. Hunt and M. R. Pointer, A colour-appearance transform for the CIE 1931 standard colorimetric observer, *Color Res. Appl.* **10**, 165-179 (1985).

26. R. W. G. Hunt, A model of colour vision for predicting colour appearance in various viewing conditions, *Color Res. Appl.* **12**, 297-314 (1987).

27. R. W. G. Hunt, Hue shifts in unrelated and related colours, *Color Res. Appl.* **14**, 235-239 (1989).

28. R. W. G. Hunt, *Measuring Colour, 2nd Ed.* Chichester, 1990, pp 213-258.

29. R. W. G. Hunt, Revised Colour-Appearance Model for Related and Unrelated Colours, *Color Res. Appl.* **16**, 25-43 (1991).

30. M. Ikeda, C. C. Huang, and S. Ashizawa, Equivaluent lightness of colored objects at illuminances from the scotopic to the photopic level, *Color Res. Appl.* **14**, 198-206 (1989).

31. M. Ikeda and S. Ashizawa, Equivaluent lightness of colored objects of equal Munsell chroma and of equal Munsell value at various illuminances, *Color Res. Appl.* **16**, 72-80 (1991).

32. D. Jameson and L. M. Hurvich, Some quantitative aspects of an opponent-colors theory. III. Changes in brightness, saturation and hue with chromatic adaptation, *J. Opt. Soc. Am.* **46**, 405-415 (1956).

33. D. B. Judd, Hue saturation and lightness of surface colors with chromatic illumination, *J. Opt. Soc. Am.* **30**, 2-32 (1940).

34. D. B. Judd, Appraisal of Land's work on two-primary color projections, *J. Opt. Soc. Am.* **50**, 254-268 (1960).

35. M. R. Luo, A. A. Clarke, P. A. Rhodes, A. Schappo, S. A. R. Scrivener, and C. J. Tait, Quantifying colour appearance. I. LUTCHI Colour-appearance data, *Color Res. Appl.* **16**, 166-180 (1991); Quantifying colour appearance. II. Testing colour models performance using LUTCHI colour-appearance data, *Color Res. Appl.* **16**, 181-197 (1991)

36. D. L. MacAdam, A nonlinear hypothesis for chromatic adaptation, *Vision Res.* **1**, 9-41 (1961).

37. D. L. MacAdam, Chromatic adaptation, *J. Opt. Soc. Am.* **46**, 500-513 (1956).

38. J. J. McCann, S. P. McKee, and T. H. Taylor, Quantitative studies in retinex theory - a comparison between theoretical predictions and observer responses to the "color Mondrian" experiments, *Vision Res.* **16**, 445-458 (1976).

39. Y. Nayatani, K. Takahama, and H. Sobagaki, A nonlinear model of chromatic adaptation, *Color Res. Appl.* **6**, 161-171 (1981).

40. Y. Nayatani, K. Takahama, H. Sobagaki, and J. Hirono, On exponents of a nonlinear model of chromatic adaptation, *Color Res. Appl.* **7**, 34-45 (1982).

41. Y. Nayatani, K. Takahama, and H. Sobagaki, Prediction of color appearance under various adapting conditions, *Color Res. Appl.* **11**, 62-71 (1986).

42. Y. Nayatani, K. Hashimoto, K. Takahama, and H. Sobagaki, Whiteness-blackness and brightness response in a nonlinear color-appearance model, *Color Res. Appl.* **12**, 121-127 (1987).

43. Y. Nayatani, K. Hashimoto, K. Takahama, and H. Sobagaki, A nonlinear color-appearance model using Estévez-Hunt-Pointer primaries, *Color Res. Appl.* **12**, 231-242 (1987).

44. Y. Nayatani, K. Takahama, and H. Sobagaki, Field trials on color appearance of chromatic colors under various light sources, *Color Res. Appl.* **13**, 307-317 (1988).

45. Y. Nayatani, Y. Umemura, K. Hashimoto, K. Takahama, and H. Sobagaki, Analyzing the natural color system's color-order system by using a nonlinear color-appearance model, *Color Res. Appl.* **14**, 69-78 (1989).

46. Y. Nayatani, K. Takahama, and H. Sobagaki, Field trials on color appearance and brightness of chromatic object colors under differenct adapting-illuminance levels, *Color Res. Appl.* **13**, 307-317 (1988).

47. Y. Nayatani, K. Takahama, H. Sobagaki and K. Hashimoto, Color-appearance model and chromatic-adaptation transform, *Color Res. Appl.* **15**, 210-221 (1990).

48. Y. Nayatani, Y. Umemura, H. Sobagaki, K. Takahama, and K. Hashimoto, Lightness perception of chromatic object colors, *Color Res. Appl.* **16**, 15-25 (1991).

49. M. R. Pointer, Color discrimination as a function of observer adaptation, *J. Opt. Soc. Am.* **64**, 750-759 (1974).

50. M. R. Pointer, analysis of colour-appearance grids and chromatic-adaptation transforms, *Color Res. Appl.* **7**, 113-118 (1982).

51. R. W. Pridmore, Model of saturation and brightness: Relations with luminance, *Color Res. Appl.* **15**, 334-357 (1990).

52. K. Richter, Cube-Root Color Spaces and Chromatic Adaptation, *Color Res. Appl.* **1**, 25-43 (1980).

53. A. R. Robertson, The CIE 1976 color-difference formulae, *Color Res. Appl.* **2**, 7-11 (1977).

54. C. L. Sanders and G. Wyszecki, Correlate for lightness in terms of CIE-tristimulus values. Part I, *J. Opt. Soc. Am.* **47**, 398-404 (1957).

55. C. L. Sanders and G. Wyszecki, L/Y rations in terms of CIE-chromaticity coordinates, *J. Opt. Soc. Am.* **48**, 389-392 (1958).

56. H. Sobagaki, T. Yamanaka, K. Takahama and Y. Nayatani, Chromatic-adaptation study by subjective-estimation method, *J. Opt. Soc. Am.* **64**, 743-749 (1974).

57. J. C. Stevens and S. S. Stevens, Brightness functions: Effects of adaptation, *J. Opt. Soc. Am.* **53**, 375-385 (1963).

58. K. Takahama, H. Sobagaki and Y. Nayatani, Analysis of chromatic-adaptation effect by a linkage model, *J. Opt. Soc. Am.* **67**, 651-656 (1977).

59. K. Takahama, H. Sobagaki and Y. Nayatani, Formulation of a nonlinear model of chromatic adaptation for a light-gray background, *Color Res. Appl.* **9**, 106-115 (1984).

60. J. Walraven, Discounting the background-The missing link in the explanation of chromatic induction, *Vision Res.* **16**, 289-295 (1976).

61. W. D. Wright, Why and how chromatic adaptation has been studied, *Color Res. Appl.* **6**, 147-152 (1981).

62. G. Wyszecki and C. L. Sanders, Correlate for lightness in terms of CIE-tristimulus values. Part II, *J. Opt. Soc. Am.* **47**, 840-842 (1957).

63. G. Wyszecki, Correlate for lightness in terms of CIE chromaticity coordinates and luminous reflectance, *J. Opt. Soc. Am.* **57**, 254-257 (1967).

Appendix A DuPont® 4Cast™ Dye Diffusion Thermal Transfer Printer Characteristics

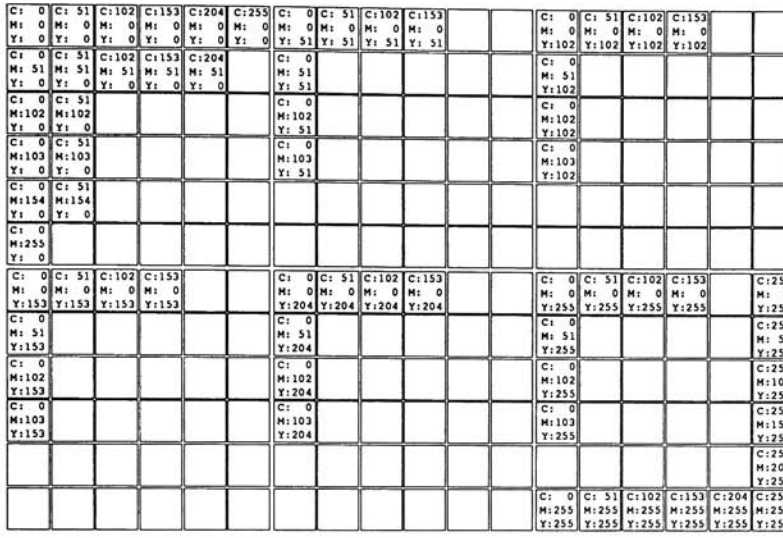

Fig. A-1. Test target for printer calibration and stability test

To see the variability of the printer, three test targets shown in Fig. A-1 consists of 216 color patches each CMY values ranging from 0 to 255 in 6 steps were printed and measured during test image printing using BYK-Gardner color-view™. CIELAB values for D65 and 2° standard observer were calculated from the spectral data. Standard deviations from the three prints were calculated. The TABLE A-1 shows the average, minimum and maximum values of the standard deviations of the 216 patches. With 96% of confidence, one can say that the variability of the printer is ΔE^*_{ab} 1.18 ($\sqrt{(0.32\times2)^2+(0.34\times2)^2+(0.36\times2)^2}$) during the sample generation.

TABLE A-1. DuPont® 4Cast™ dye diffusion thermal transfer printer stability test result

	L*	a*	b*
Average of 216 Standard Deviations	0.32	0.34	0.36
Minimum of 216 Standard Deviations	0.05	0.02	0.02
Maximum of 216 Standard Deviations	0.62	0.83	0.88

Appendix B Printer Calibration using Tetrahedral Interpolation Evaluation

To verify the precision of the CMY to XYZ conversion method (tetrahedral interpolation method) which was built based on 5x5x5 target[1] patches, TSVs were calculated from spectral reflectance data measured with a BYK-Gardner color-view™ using spectral radiance information of specific illuminant. For the CMY to XYZ, D65 was used), 6x6x6 target[2] was generated and measured. Only 8 of 216 6x6x6 target patches have same CMY values of 125 5x5x5 target patches. ΔE^*_{ab} values were calculated from the measured TSVs of 216 6x6x6 target patches and predicted TSVs by the CMY to XYZ conversion method. The result is shown in TABLE B-1 and Fig. B-1. The calibration evaluation result includes printer variability.

TABLE B-1. Statistical result of CMY to XYZ conversion using Tetrahedral LUT method

Mean	Std Dev	Std Err Mean	upper 95% Mean	lower 95% Mean	N
2.5477	1.3524	0.0920	2.7291	2.3664	216

The verification of XYZ to CMY conversion method used a similar technique as in CMY to XYZ conversion verification. XYZ values used were from CMY to XYZ conversion, which could be treated as arbitrary but well distributed throughout the color space. Because of errors during the calculation, 18 of the 216 XYZ values were out of range for the XYZ to CMY

[1] 5x5x5 target means combination of 5 steps of Cyan, 5 steps of Magenta and 5 steps of Yellow, totaling 125 patches . For the 5 stpes, 0, 63, 127, 191 and 255 were used.

[2] 6x6x6 target means combination of 6 steps of Cyan, 6 steps of Magenta and 6 steps of Yellow, totaling 216 patches . For the 6 stpes, 0, 51, 102, 153, 204 and 255 were used.

conversion method and were dropped. The result is shown in TABLE B-2 and Fig. B-2.

TABLE B-2. Statistical result of XYZ to CMY conversion using Tetrahedral LUT method

Mean	Std Dev	Std Err Mean	upper 95% Mean	lower 95% Mean	N
2.5717	1.4402	0.1023	2.7736	2.3699	198

The image transformation process for the experiment shown in Fig. 1.1 involves two LUT conversions which are CMY to XYZ and XYZ to CMY. This process was merged into one LUT to process CMY_{ref} to CMY_{test}. To estimate the error, the CMY to XYZ conversion LUT and XYZ to CMY conversion LUT were merged and 216 6x6x6 target patches were processed. The test result is shown in TABLE B-3 and Fig. B-3. The result shows that the error of the merged LUT is similar to the error of the each individual LUT; the error does not add.

TABLE B-3. Statistical result of merged LUT of CMY to XYZ and XYZ to CMY conversions using Tetrahedral LUT method

Mean	Std Dev	Std Err Mean	upper 95% Mean	lower 95% Mean	N
2.4959	1.0639	0.0724	2.6386	2.3532	216

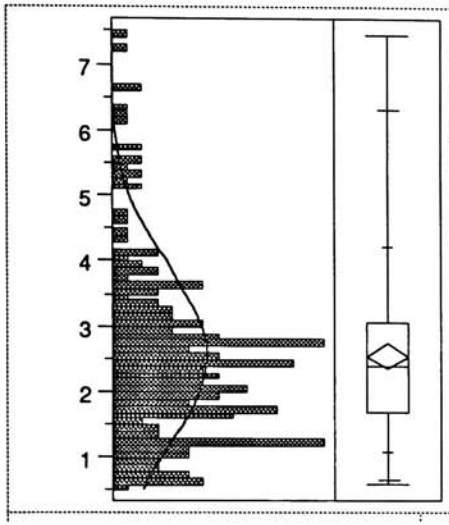

Quantiles

maximum	100.0%	7.4500
	99.5%	7.4364
	97.5%	6.3015
	90.0%	4.2320
quartile	75.0%	3.0700
median	50.0%	2.3850
quartile	25.0%	1.6700
	10.0%	1.0680
	2.5%	0.6685
	0.5%	0.5925
minimum	0.0%	0.5900

Fig. B-1. CIELAB ΔE^*_{ab} distribution of CMY to XYZ conversion using Tetrahedral LUT method (216 patches used)

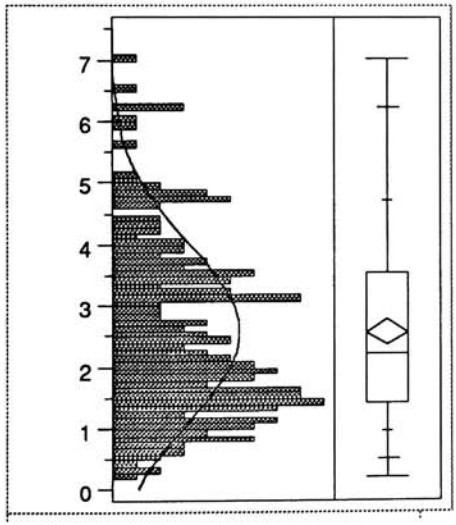

Quantiles

maximum	100.0%	7.0200
	99.5%	7.0200
	97.5%	6.2215
	90.0%	4.7260
quartile	75.0%	3.5375
median	50.0%	2.2200
quartile	25.0%	1.4375
	10.0%	0.9560
	2.5%	0.5072
	0.5%	0.2000
minimum	0.0%	0.2000

Fig. B-2. CIELAB ΔE^*_{ab} distribution of XYZ to CMY conversion using Tetrahedral LUT method (198 patches used)

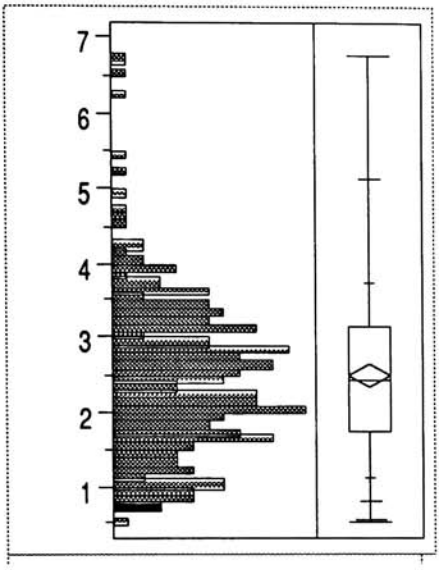

Quantiles

maximum	100.0%	6.7727
	99.5%	6.7496
	97.5%	5.1421
	90.0%	3.7133
quartile	75.0%	3.1334
median	50.0%	2.4333
quartile	25.0%	1.7325
	10.0%	1.1129
	2.5%	0.8070
	0.5%	0.5513
minimum	0.0%	0.5354

Fig. B-3. CIELAB ΔE^*_{ab} distribution of merged LUT of CMY to XYZ and XYZ to CMY conversions using Tetrahedral LUT method (216 patches used)

Appendix C Light Source Data

TABLE C-1. Spectral data of the light sources

wavelength (nm)	source A (w/sr·m^2/nm)	D65-M (w/sr·m^2/nm)	D65-L (w/sr·m^2/nm)	D65-H (w/sr·m^2/nm)
390	1.15E-04	6.31E-04	1.66E-04	1.29E-03
392	1.30E-04	7.22E-04	1.76E-04	1.48E-03
394	1.54E-04	7.66E-04	1.89E-04	1.59E-03
396	1.69E-04	8.14E-04	2.06E-04	1.71E-03
398	1.89E-04	9.14E-04	2.33E-04	1.95E-03
400	2.16E-04	1.07E-03	2.62E-04	2.40E-03
402	2.36E-04	1.30E-03	3.15E-04	3.03E-03
404	2.62E-04	2.72E-03	6.40E-04	6.68E-03
406	2.85E-04	3.61E-03	8.22E-04	8.64E-03
408	3.15E-04	2.41E-03	5.59E-04	5.58E-03
410	3.33E-04	1.57E-03	4.00E-04	3.54E-03
412	3.57E-04	1.41E-03	3.77E-04	3.02E-03
414	3.81E-04	1.41E-03	3.84E-04	2.97E-03
416	4.02E-04	1.46E-03	4.06E-04	3.03E-03
418	4.18E-04	1.53E-03	4.30E-04	3.16E-03
420	4.38E-04	1.63E-03	4.58E-04	3.36E-03
422	4.59E-04	1.75E-03	4.85E-04	3.67E-03
424	4.82E-04	1.90E-03	5.15E-04	4.03E-03
426	5.10E-04	2.08E-03	5.46E-04	4.45E-03
428	5.27E-04	2.21E-03	5.83E-04	4.76E-03
430	5.46E-04	2.40E-03	6.21E-04	5.23E-03
432	5.70E-04	2.80E-03	6.98E-04	6.37E-03
434	5.88E-04	5.18E-03	1.28E-03	1.24E-02
436	6.23E-04	1.08E-02	2.52E-03	2.47E-02
438	6.47E-04	9.26E-03	2.14E-03	2.06E-02
440	6.72E-04	4.59E-03	1.08E-03	1.02E-02
442	6.89E-04	3.40E-03	8.46E-04	7.53E-03
444	7.12E-04	3.25E-03	8.34E-04	7.12E-03
446	7.47E-04	3.29E-03	8.42E-04	7.19E-03
448	7.73E-04	3.34E-03	8.64E-04	7.28E-03
450	8.01E-04	3.39E-03	8.71E-04	7.39E-03
452	8.26E-04	3.42E-03	8.99E-04	7.44E-03
454	8.64E-04	3.49E-03	9.19E-04	7.60E-03
456	8.94E-04	3.59E-03	9.41E-04	7.88E-03
458	9.43E-04	3.65E-03	9.53E-04	8.00E-03
460	9.70E-04	3.59E-03	9.60E-04	7.85E-03
462	1.04E-03	3.79E-03	9.64E-04	8.37E-03
464	1.05E-03	3.69E-03	9.68E-04	8.11E-03
466	1.09E-03	3.66E-03	9.71E-04	8.04E-03

468	1.13E-03	3.66E-03	9.73E-04	8.03E-03
470	1.16E-03	3.67E-03	9.67E-04	8.10E-03
472	1.21E-03	3.66E-03	9.64E-04	8.04E-03
474	1.24E-03	3.60E-03	9.57E-04	7.90E-03
476	1.31E-03	3.66E-03	9.49E-04	8.07E-03
478	1.35E-03	3.67E-03	9.46E-04	8.12E-03
480	1.38E-03	3.57E-03	9.36E-04	7.85E-03
482	1.41E-03	3.54E-03	9.34E-04	7.77E-03
484	1.45E-03	3.46E-03	9.27E-04	7.56E-03
486	1.49E-03	3.42E-03	9.19E-04	7.48E-03
488	1.54E-03	3.43E-03	9.14E-04	7.53E-03
490	1.58E-03	3.37E-03	9.08E-04	7.40E-03
492	1.63E-03	3.37E-03	9.06E-04	7.39E-03
494	1.67E-03	3.35E-03	8.98E-04	7.35E-03
496	1.71E-03	3.31E-03	8.86E-04	7.30E-03
498	1.76E-03	3.28E-03	8.85E-04	7.20E-03
500	1.80E-03	3.26E-03	8.84E-04	7.17E-03
502	1.85E-03	3.27E-03	8.86E-04	7.20E-03
504	1.91E-03	3.31E-03	8.97E-04	7.28E-03
506	1.97E-03	3.34E-03	8.99E-04	7.37E-03
508	2.03E-03	3.38E-03	9.10E-04	7.45E-03
510	2.08E-03	3.42E-03	9.18E-04	7.54E-03
512	2.12E-03	3.42E-03	9.33E-04	7.54E-03
514	2.18E-03	3.46E-03	9.45E-04	7.63E-03
516	2.24E-03	3.51E-03	9.59E-04	7.72E-03
518	2.30E-03	3.55E-03	9.69E-04	7.81E-03
520	2.37E-03	3.62E-03	9.82E-04	7.95E-03
522	2.43E-03	3.67E-03	9.89E-04	8.06E-03
524	2.47E-03	3.65E-03	9.90E-04	8.01E-03
526	2.53E-03	3.67E-03	9.94E-04	8.06E-03
528	2.59E-03	3.67E-03	9.96E-04	8.06E-03
530	2.66E-03	3.71E-03	9.83E-04	8.24E-03
532	2.70E-03	3.67E-03	9.88E-04	8.09E-03
534	2.77E-03	3.66E-03	9.88E-04	8.07E-03
536	2.82E-03	3.66E-03	9.86E-04	8.08E-03
538	2.89E-03	3.66E-03	9.78E-04	8.14E-03
540	2.95E-03	3.66E-03	9.72E-04	8.20E-03
542	3.00E-03	3.79E-03	1.01E-03	8.65E-03
544	3.06E-03	5.54E-03	1.48E-03	1.33E-02
546	3.13E-03	8.38E-03	2.17E-03	2.01E-02
548	3.21E-03	7.64E-03	1.92E-03	1.80E-02
550	3.26E-03	4.59E-03	1.18E-03	1.05E-02
552	3.32E-03	3.56E-03	9.47E-04	8.00E-03
554	3.40E-03	3.46E-03	9.24E-04	7.74E-03
556	3.45E-03	3.38E-03	9.23E-04	7.46E-03
558	3.53E-03	3.35E-03	9.22E-04	7.40E-03
560	3.60E-03	3.33E-03	9.12E-04	7.34E-03
562	3.67E-03	3.28E-03	9.02E-04	7.28E-03
564	3.75E-03	3.28E-03	8.85E-04	7.28E-03

566	3.80E-03	3.23E-03	9.03E-04	7.13E-03
568	3.88E-03	3.22E-03	8.99E-04	7.11E-03
570	3.95E-03	3.22E-03	8.91E-04	7.14E-03
572	4.02E-03	3.22E-03	8.91E-04	7.14E-03
574	4.10E-03	3.31E-03	9.16E-04	7.42E-03
576	4.17E-03	3.73E-03	1.01E-03	8.61E-03
578	4.24E-03	4.23E-03	1.12E-03	9.90E-03
580	4.31E-03	4.04E-03	1.07E-03	9.34E-03
582	4.38E-03	3.48E-03	9.45E-04	7.90E-03
584	4.46E-03	3.19E-03	8.86E-04	7.13E-03
586	4.53E-03	3.15E-03	8.81E-04	7.03E-03
588	4.59E-03	3.12E-03	8.78E-04	6.95E-03
590	4.67E-03	3.10E-03	8.72E-04	6.88E-03
592	4.74E-03	3.08E-03	8.69E-04	6.86E-03
594	4.83E-03	3.08E-03	8.67E-04	6.86E-03
596	4.90E-03	3.06E-03	8.66E-04	6.79E-03
598	4.97E-03	3.05E-03	8.63E-04	6.75E-03
600	5.04E-03	3.02E-03	8.58E-04	6.69E-03
602	5.12E-03	3.02E-03	8.56E-04	6.67E-03
604	5.21E-03	3.02E-03	8.53E-04	6.71E-03
606	5.29E-03	3.02E-03	8.47E-04	6.70E-03
608	5.38E-03	3.03E-03	8.42E-04	6.72E-03
610	5.45E-03	3.02E-03	8.50E-04	6.67E-03
612	5.54E-03	3.02E-03	8.47E-04	6.70E-03
614	5.59E-03	3.01E-03	8.54E-04	6.66E-03
616	5.70E-03	3.04E-03	8.58E-04	6.76E-03
618	5.77E-03	3.07E-03	8.68E-04	6.84E-03
620	5.85E-03	3.11E-03	8.69E-04	6.95E-03
622	5.91E-03	3.21E-03	9.05E-04	7.14E-03
624	5.99E-03	3.29E-03	9.29E-04	7.33E-03
626	6.09E-03	3.31E-03	9.24E-04	7.41E-03
628	6.22E-03	3.38E-03	9.38E-04	7.57E-03
630	6.25E-03	3.39E-03	9.51E-04	7.59E-03
632	6.36E-03	3.46E-03	9.56E-04	7.73E-03
634	6.44E-03	3.36E-03	9.17E-04	7.53E-03
636	6.50E-03	3.17E-03	8.86E-04	7.06E-03
638	6.60E-03	3.10E-03	8.61E-04	6.89E-03
640	6.67E-03	3.10E-03	8.62E-04	6.87E-03
642	6.78E-03	3.13E-03	8.61E-04	6.94E-03
644	6.84E-03	3.08E-03	8.51E-04	6.82E-03
646	6.94E-03	3.11E-03	8.58E-04	6.88E-03
648	7.00E-03	3.21E-03	8.93E-04	7.13E-03
650	7.09E-03	3.51E-03	9.71E-04	7.80E-03
652	7.17E-03	3.74E-03	1.03E-03	8.33E-03
654	7.26E-03	3.84E-03	1.06E-03	8.59E-03
656	7.34E-03	3.93E-03	1.08E-03	8.83E-03
658	7.42E-03	4.22E-03	1.16E-03	9.49E-03
660	7.53E-03	4.49E-03	1.22E-03	1.01E-02
662	7.62E-03	4.40E-03	1.20E-03	9.88E-03

664	7.71E-03	3.92E-03	1.07E-03	8.80E-03
666	7.82E-03	3.51E-03	9.60E-04	7.88E-03
668	7.93E-03	3.22E-03	8.75E-04	7.17E-03
670	7.93E-03	2.76E-03	7.59E-04	6.11E-03
672	8.04E-03	2.47E-03	6.91E-04	5.43E-03
674	8.16E-03	2.25E-03	6.13E-04	4.94E-03
676	8.20E-03	2.04E-03	5.82E-04	4.44E-03
678	8.41E-03	1.98E-03	5.66E-04	4.30E-03
680	8.42E-03	1.86E-03	5.34E-04	4.01E-03
682	8.46E-03	1.73E-03	5.08E-04	3.74E-03
684	8.58E-03	1.68E-03	4.90E-04	3.61E-03
686	8.65E-03	1.59E-03	4.69E-04	3.42E-03
688	8.77E-03	1.53E-03	4.47E-04	3.28E-03
690	8.83E-03	1.45E-03	4.34E-04	3.11E-03
692	8.92E-03	1.39E-03	4.18E-04	3.00E-03
694	9.05E-03	1.33E-03	4.01E-04	2.87E-03
696	9.11E-03	1.26E-03	3.82E-04	2.72E-03
698	9.18E-03	1.20E-03	3.66E-04	2.59E-03
700	9.27E-03	1.14E-03	3.48E-04	2.46E-03
702	9.35E-03	1.08E-03	3.27E-04	2.35E-03
704	9.44E-03	1.03E-03	3.12E-04	2.24E-03
706	9.56E-03	1.00E-03	3.01E-04	2.18E-03
708	9.64E-03	9.67E-04	2.91E-04	2.11E-03
710	9.70E-03	9.21E-04	2.75E-04	2.03E-03
712	9.80E-03	8.55E-04	2.51E-04	1.94E-03
714	9.92E-03	8.42E-04	2.42E-04	1.86E-03
716	9.93E-03	7.97E-04	2.35E-04	1.77E-03
718	1.00E-02	7.53E-04	2.19E-04	1.66E-03
720	1.01E-02	7.23E-04	2.10E-04	1.61E-03
722	1.02E-02	7.03E-04	2.02E-04	1.58E-03
724	1.02E-02	6.59E-04	1.91E-04	1.47E-03
726	1.03E-02	6.31E-04	1.80E-04	1.42E-03
728	1.03E-02	6.09E-04	1.78E-04	1.37E-03
730	1.04E-02	5.84E-04	1.70E-04	1.27E-03

Appendix D Color Measurement Instruments

Photo Research PR-703

A spectroradiometer, it was used to measure light booth illuminance with a piece of Halon as a target. The Photo Research PR-703 outputs spectral information from 390nm to 730nm at 2 nm interval.

Minolta CS-100

A colorimeter, it was used when the illuminance of the booth was changed.

BYK-Gardner color-view™

A spectrophotometer, calibration of the experiment is based on measurement from this instrument.

Appendix E Experimental Result

* Abbreviation.
VK : von Kries
CLAB : CIELAB
CLUV : CIELUV
LABH : LABHNU
RT : Reilly-Tannenbaum
Nay : Nayatani

TABLE E-1. Count Tally sheet at the same luminance level

		VK	CLAB	CLUV	LABH	RT	Hunt	Nay	RLAB
Total	VK		67	9	9	25	69	28	61
	CLAB	53		4	20	12	47	29	58
	CLUV	111	116		112	113	113	101	114
	LABH	111	100	8		62	105	66	107
	RT	95	108	7	58		103	65	97
	Hunt	51	73	7	15	17		27	59
	Nay	92	91	19	54	55	93		89
	RLAB	59	62	6	13	23	61	31	
Fruit Basket	VK		16	0	0	3	15	10	13
	CLAB	14		0	0	1	14	13	15
	CLUV	30	30		28	30	30	30	30
	LABH	30	30	2		16	30	25	30
	RT	27	29	0	14		30	23	28
	Hunt	15	16	0	0	0		8	15
	Nay	20	17	0	5	7	22		21
	RLAB	17	15	0	0	2	15	9	
Orchid	VK		9	5	3	9	23	1	20
	CLAB	21		3	6	3	17	0	15
	CLUV	25	27		25	25	25	14	27
	LABH	27	24	5		10	21	4	28
	RT	21	27	5	20		24	2	23
	Hunt	7	13	5	9	6		0	23
	Nay	29	30	16	26	28	30		30
	RLAB	10	15	3	2	7	7	0	
Musician	VK		20	2	1	4	15	4	16
	CLAB	10		0	4	0	11	3	14
	CLUV	28	30		30	29	30	29	29
	LABH	29	26	0		17	30	21	29
	RT	26	30	1	13		28	20	26
	Hunt	15	19	0	0	2		6	12
	Nay	26	27	1	9	10	24		24
	RLAB	14	16	1	1	4	18	6	
Candles	VK		22	2	5	9	16	13	12
	CLAB	8		1	10	8	5	13	14
	CLUV	28	29		29	29	28	28	28
	LABH	25	20	1		19	24	16	20
	RT	21	22	1	11		21	20	20
	Hunt	14	25	2	6	9		13	9
	Nay	17	17	2	14	10	17		14
	RLAB	18	16	2	10	10	21	16	

TABLE E-2. Normalized matrix at the same luminance level

		VK	CLAB	CLUV	LABH	RT	Hunt	Nay	RLAB
Total	VK		0.56	0.08	0.08	0.21	0.58	0.23	0.51
	CLAB	0.44		0.03	0.17	0.10	0.39	0.24	0.48
	CLUV	0.93	0.97		0.93	0.94	0.94	0.84	0.95
	LABH	0.93	0.83	0.07		0.52	0.88	0.55	0.89
	RT	0.79	0.90	0.06	0.48		0.86	0.54	0.81
	Hunt	0.43	0.61	0.06	0.13	0.14		0.23	0.49
	Nay	0.77	0.76	0.16	0.45	0.46	0.78		0.74
	RLAB	0.49	0.52	0.05	0.11	0.19	0.51	0.26	
Fruit Basket	VK		0.53	0.00	0.00	0.10	0.50	0.33	0.43
	CLAB	0.47		0.00	0.00	0.03	0.47	0.43	0.50
	CLUV	1.00	1.00		0.93	1.00	1.00	1.00	1.00
	LABH	1.00	1.00	0.07		0.53	1.00	0.83	1.00
	RT	0.90	0.97	0.00	0.47		1.00	0.77	0.93
	Hunt	0.50	0.53	0.00	0.00	0.00		0.27	0.50
	Nay	0.67	0.57	0.00	0.17	0.23	0.73		0.70
	RLAB	0.57	0.50	0.00	0.00	0.07	0.50	0.30	
Orchid	VK		0.30	0.17	0.10	0.30	0.77	0.03	0.67
	CLAB	0.70		0.10	0.20	0.10	0.57	0.00	0.50
	CLUV	0.83	0.90		0.83	0.83	0.83	0.47	0.90
	LABH	0.90	0.80	0.17		0.33	0.70	0.13	0.93
	RT	0.70	0.90	0.17	0.67		0.80	0.07	0.77
	Hunt	0.23	0.43	0.17	0.30	0.20		0.00	0.77
	Nay	0.97	1.00	0.53	0.87	0.93	1.00		1.00
	RLAB	0.33	0.50	0.10	0.07	0.23	0.23	0.00	
Musician	VK		0.67	0.07	0.03	0.13	0.50	0.13	0.53
	CLAB	0.33		0.00	0.13	0.00	0.37	0.10	0.47
	CLUV	0.93	1.00		1.00	0.97	1.00	0.97	0.97
	LABH	0.97	0.87	0.00		0.57	1.00	0.70	0.97
	RT	0.87	1.00	0.03	0.43		0.93	0.67	0.87
	Hunt	0.50	0.63	0.00	0.00	0.07		0.20	0.40
	Nay	0.87	0.90	0.03	0.30	0.33	0.80		0.80
	RLAB	0.47	0.53	0.03	0.03	0.13	0.60	0.20	
Candles	VK		0.73	0.07	0.17	0.30	0.53	0.43	0.40
	CLAB	0.27		0.03	0.33	0.27	0.17	0.43	0.47
	CLUV	0.93	0.97		0.97	0.97	0.93	0.93	0.93
	LABH	0.83	0.67	0.03		0.63	0.80	0.53	0.67
	RT	0.70	0.73	0.03	0.37		0.70	0.67	0.67
	Hunt	0.47	0.83	0.07	0.20	0.30		0.43	0.30
	Nay	0.57	0.57	0.07	0.47	0.33	0.57		0.47
	RLAB	0.60	0.53	0.07	0.33	0.33	0.70	0.53	

TABLE E-3. Z-score matrix at the same luminance level

		VK	CLAB	CLUV	LABH	RT	Hunt	Nay	RLAB
Total	VK		0.13	-1.48	-1.48	-0.84	0.18	-0.74	0
	CLAB	-0.15		-1.88	-0.99	-1.28	-0.28	-0.71	-0.05
	CLUV	1.41	1.75		1.48	1.56	1.56	0.99	1.65
	LABH	1.41	0.95	-1.56		0.03	1.13	0.13	1.23
	RT	0.81	1.28	-1.65	-0.05		1.04	0.1	0.84
	Hunt	-0.2	0.25	-1.65	-1.18	-1.08		-0.77	-0.03
	Nay	0.71	0.67	-1.04	-0.13	-0.13	0.74		0.64
	RLAB	-0.03	0.03	-1.65	-1.28	-0.88	0	-0.67	
	SUM	3.96	5.06	-10.91	-3.63	-2.62	4.37	-1.67	4.28
Fruit Basket	VK		0.08	-2.33	-2.33	-1.28	0.00	-0.44	-0.18
	CLAB	-0.10		-2.33	-2.33	-1.88	-0.10	-0.18	0.00
	CLUV	2.33	2.33		1.48	2.33	2.33	2.33	2.33
	LABH	2.33	2.33	-1.56		0.08	2.33	0.95	2.33
	RT	1.28	1.75	-2.33	-0.10		2.33	0.71	1.48
	Hunt	0.00	0.08	-2.33	-2.33	-2.33		-0.64	0.00
	Nay	0.41	0.15	-2.33	-0.99	-0.74	0.61		0.52
	RLAB	0.15	0.00	-2.33	-2.33	-1.56	0.00	-0.52	
	SUM	6.40	6.72	-15.54	-8.93	-5.38	7.50	2.21	6.48
Orchid	VK		-0.52	-0.99	-1.28	-0.52	0.71	-1.88	0.41
	CLAB	0.52		-1.28	-0.84	-1.28	0.15	-2.33	0.00
	CLUV	0.95	1.28		0.95	0.95	0.95	-0.10	1.28
	LABH	1.28	0.84	-0.99		-0.44	0.52	-1.13	1.48
	RT	0.52	1.28	-0.99	0.41		0.84	-1.56	0.71
	Hunt	-0.74	-0.18	-0.99	-0.52	-0.84		-2.33	0.71
	Nay	1.75	2.33	0.08	1.08	1.48	2.33		2.33
	RLAB	-0.44	0.00	-1.28	-1.56	-0.74	-0.74	-2.33	
	SUM	3.84	5.03	-6.44	-1.76	-1.39	4.76	-11.66	6.92
Musician	VK		0.41	-1.56	-1.88	-1.13	0.00	-1.13	0.08
	CLAB	-0.44		-2.33	-1.13	-2.33	-0.36	-1.28	-0.10
	CLUV	1.48	2.33		2.33	1.75	2.33	1.75	1.75
	LABH	1.75	1.08	-2.33		0.15	2.33	0.52	1.75
	RT	1.08	2.33	-1.88	-0.18		1.48	0.41	1.08
	Hunt	0.00	0.33	-2.33	-2.33	-1.56		-0.84	-0.25
	Nay	1.08	1.28	-1.88	-0.52	-0.44	0.84		0.84
	RLAB	-0.10	0.08	-1.88	-1.88	-1.13	0.25	-0.84	
	SUM	4.85	7.84	-14.19	-5.59	-4.69	6.87	-1.41	5.15
Candles	VK		0.61	-1.56	-0.99	-0.52	0.08	-0.18	-0.25
	CLAB	-0.64		-1.88	-0.44	-0.64	-0.99	-0.18	-0.10
	CLUV	1.48	1.75		1.75	1.75	1.48	1.48	1.48
	LABH	0.95	0.41	-1.88		0.33	0.84	0.08	0.41
	RT	0.52	0.61	-1.88	-0.36		0.52	0.41	0.41
	Hunt	-0.10	0.95	-1.56	-0.84	-0.52		-0.18	-0.52
	Nay	0.15	0.15	-1.56	-0.10	-0.44	0.15		-0.10
	RLAB	0.25	0.08	-1.56	-0.44	-0.44	0.52	0.08	
	SUM	2.61	4.56	-11.88	-1.42	-0.48	2.60	1.51	1.33

TABLE E-4. Count Tally sheet at 1/3 luminance level

		VK	CLAB	CLUV	LABH	RT	Hunt	Nay	RLAB
Total	VK		82	10	20	27	69	54	74
	CLAB	34		5	17	14	48	53	38
	CLUV	106	111		110	113	110	94	104
	LABH	96	99	6		53	103	88	98
	RT	89	102	3	63		91	81	96
	Hunt	47	68	6	13	25		46	49
	Nay	62	63	22	28	35	70		68
	RLAB	42	78	12	18	20	67	48	
Fruit Basket	VK		23	0	0	0	18	14	21
	CLAB	6		1	1	0	18	13	13
	CLUV	29	28		29	28	29	28	29
	LABH	29	28	0		13	29	26	29
	RT	29	29	1	16		27	29	28
	Hunt	11	11	0	0	2		15	12
	Nay	15	16	1	3	0	14		17
	RLAB	8	16	0	0	1	17	12	
Orchid	VK		19	7	12	17	10	2	8
	CLAB	10		3	9	8	7	14	4
	CLUV	22	26		26	28	25	12	21
	LABH	17	20	3		14	26	10	22
	RT	12	21	1	15		16	8	21
	Hunt	19	22	4	3	13		2	16
	Nay	27	15	17	19	21	27		27
	RLAB	21	25	8	7	8	13	2	
Musician	VK		18	1	3	2	22	15	19
	CLAB	11		0	0	3	13	12	9
	CLUV	28	29		27	29	29	26	27
	LABH	26	29	2		12	25	26	24
	RT	27	26	0	17		24	21	25
	Hunt	7	16	0	4	5		9	12
	Nay	14	17	3	3	8	20		18
	RLAB	10	20	2	5	4	17	11	
Candles	VK		22	2	5	8	19	23	26
	CLAB	7		1	7	3	10	14	12
	CLUV	27	28		28	28	27	28	27
	LABH	24	22	1		14	23	26	23
	RT	21	26	1	15		24	23	22
	Hunt	10	19	2	6	5		20	9
	Nay	6	15	1	3	6	9		6
	RLAB	3	17	2	6	7	20	23	

TABLE E-5. Normalized matrix at 1/3 luminance level

		VK	CLAB	CLUV	LABH	RT	Hunt	Nay	RLAB
Total	VK		0.71	0.09	0.17	0.23	0.59	0.47	0.64
	CLAB	0.29		0.04	0.15	0.12	0.41	0.46	0.33
	CLUV	0.91	0.96		0.95	0.97	0.95	0.81	0.90
	LABH	0.83	0.85	0.05		0.46	0.89	0.76	0.84
	RT	0.77	0.88	0.03	0.54		0.78	0.70	0.83
	Hunt	0.41	0.59	0.05	0.11	0.22		0.40	0.42
	Nay	0.53	0.54	0.19	0.24	0.30	0.60		0.59
	RLAB	0.36	0.67	0.10	0.16	0.17	0.58	0.41	
Fruit Basket	VK		0.79	0.00	0.00	0.00	0.62	0.48	0.72
	CLAB	0.21		0.03	0.03	0.00	0.62	0.45	0.45
	CLUV	1.00	0.97		1.00	0.97	1.00	0.97	1.00
	LABH	1.00	0.97	0.00		0.45	1.00	0.90	1.00
	RT	1.00	1.00	0.03	0.55		0.93	1.00	0.97
	Hunt	0.38	0.38	0.00	0.00	0.07		0.52	0.41
	Nay	0.52	0.55	0.03	0.10	0.00	0.48		0.59
	RLAB	0.28	0.55	0.00	0.00	0.03	0.59	0.41	
Orchid	VK		0.66	0.24	0.41	0.59	0.34	0.07	0.28
	CLAB	0.34		0.10	0.31	0.28	0.24	0.48	0.14
	CLUV	0.76	0.90		0.90	0.97	0.86	0.41	0.72
	LABH	0.59	0.69	0.10		0.48	0.90	0.34	0.76
	RT	0.41	0.72	0.03	0.52		0.55	0.28	0.72
	Hunt	0.66	0.76	0.14	0.10	0.45		0.07	0.55
	Nay	0.93	0.52	0.59	0.66	0.72	0.93		0.93
	RLAB	0.72	0.86	0.28	0.24	0.28	0.45	0.07	
Musician	VK		0.62	0.03	0.10	0.07	0.76	0.52	0.66
	CLAB	0.38		0.00	0.00	0.10	0.45	0.41	0.31
	CLUV	0.97	1.00		0.93	1.00	1.00	0.90	0.93
	LABH	0.90	1.00	0.07		0.41	0.86	0.90	0.83
	RT	0.93	0.90	0.00	0.59		0.83	0.72	0.86
	Hunt	0.24	0.55	0.00	0.14	0.17		0.31	0.41
	Nay	0.48	0.59	0.10	0.10	0.28	0.69		0.62
	RLAB	0.34	0.69	0.07	0.17	0.14	0.59	0.38	
Candles	VK		0.76	0.07	0.17	0.28	0.66	0.79	0.90
	CLAB	0.24		0.03	0.24	0.10	0.34	0.48	0.41
	CLUV	0.93	0.97		0.97	0.97	0.93	0.97	0.93
	LABH	0.83	0.76	0.03		0.48	0.79	0.90	0.79
	RT	0.72	0.90	0.03	0.52		0.83	0.79	0.76
	Hunt	0.34	0.66	0.07	0.21	0.17		0.69	0.31
	Nay	0.21	0.52	0.03	0.10	0.21	0.31		0.21
	RLAB	0.10	0.59	0.07	0.21	0.24	0.69	0.79	

TABLE E-6. Z-score matrix at 1/3 luminance level

		VK	CLAB	CLUV	LABH	RT	Hunt	Nay	RLAB
Total	VK		0.52	-1.41	-0.95	-0.74	0.23	-0.10	0.33
	CLAB	-0.55		-1.75	-1.08	-1.18	-0.23	-0.13	-0.47
	CLUV	1.34	1.65		1.56	1.88	1.56	0.88	1.23
	LABH	0.92	1.04	-1.65		-0.13	1.18	0.67	0.99
	RT	0.71	1.13	-2.05	0.10		0.77	0.50	0.92
	Hunt	-0.25	0.20	-1.65	-1.23	-0.81		-0.28	-0.20
	Nay	0.08	0.10	-0.92	-0.71	-0.52	0.25		0.20
	RLAB	-0.36	0.44	-1.28	-1.04	-0.95	0.18	-0.23	
	SUM	1.89	5.08	-10.71	-3.35	-2.45	3.94	1.31	3.00
Fruit Basket	VK		0.81	-2.33	-2.33	-2.33	0.31	-0.05	0.58
	CLAB	-0.84		-1.88	-1.88	-2.33	0.31	-0.15	-0.15
	CLUV	2.33	1.75		2.33	1.75	2.33	1.75	2.33
	LABH	2.33	1.75	-2.33		-0.15	2.33	1.23	2.33
	RT	2.33	2.33	-1.88	0.13		1.48	2.33	1.75
	Hunt	-0.33	-0.33	-2.33	-2.33	-1.56		0.03	-0.23
	Nay	0.03	0.13	-1.88	-1.28	-2.33	-0.05		0.20
	RLAB	-0.61	0.13	-2.33	-2.33	-1.88	0.20	-0.23	
	SUM	5.24	6.57	-14.96	-7.69	-8.83	6.91	4.91	6.81
Orchid	VK		0.39	-0.71	-0.23	0.2	-0.41	-1.56	-0.61
	CLAB	-0.41		-1.28	-0.5	-0.61	-0.71	-0.05	-1.13
	CLUV	0.67	1.23		1.23	1.75	1.08	-0.23	0.58
	LABH	0.2	0.47	-1.28		-0.05	1.23	-0.41	0.67
	RT	-0.23	0.58	-1.88	0.03		0.13	-0.61	0.58
	Hunt	0.39	0.67	-1.13	-1.28	-0.15		-1.56	0.13
	Nay	1.48	0.03	0.2	0.39	0.58	1.48		1.48
	RLAB	0.58	1.08	-0.61	-0.71	-0.61	-0.15	-1.56	
	SUM	2.68	4.45	-6.69	-1.07	1.11	2.65	-5.98	1.7
Musician	VK		0.31	-1.88	-1.28	-1.56	0.67	0.03	0.39
	CLAB	-0.33		-2.33	-2.33	-1.28	-0.15	-0.23	-0.50
	CLUV	1.75	2.33		1.48	2.33	2.33	1.23	1.48
	LABH	1.23	2.33	-1.56		-0.23	1.08	1.23	0.92
	RT	1.48	1.23	-2.33	0.20		0.92	0.58	1.08
	Hunt	-0.71	0.13	-2.33	-1.13	-0.95		-0.50	-0.23
	Nay	-0.05	0.20	-1.28	-1.28	-0.61	0.47		0.31
	RLAB	-0.41	0.47	-1.56	-0.95	-1.13	0.20	-0.33	
	SUM	2.96	7.00	-13.27	-5.29	-3.43	5.52	2.01	3.45
Candles	VK		0.67	-1.56	-0.95	-0.61	0.39	0.81	1.23
	CLAB	-0.71		-1.88	-0.71	-1.28	-0.41	-0.05	-0.23
	CLUV	1.48	1.75		1.75	1.75	1.48	1.75	1.48
	LABH	0.92	0.67	-1.88		-0.05	0.81	1.23	0.81
	RT	0.58	1.23	-1.88	0.03		0.92	0.81	0.67
	Hunt	-0.41	0.39	-1.56	-0.84	-0.95		0.47	-0.50
	Nay	-0.84	0.03	-1.88	-1.28	-0.84	-0.50		-0.84
	RLAB	-1.28	0.20	-1.56	-0.84	-0.71	0.47	0.81	
	SUM	-0.26	4.94	-12.20	-2.84	-2.69	3.16	5.83	2.62

TABLE E-7. Count Tally sheet at 3 times luminance level

		VK	CLAB	CLUV	LABH	RT	Hunt	Nay	RLAB
Total	VK		57	6	19	24	60	13	51
	CLAB	59		7	12	39	54	9	59
	CLUV	110	109		111	112	108	80	109
	LABH	97	104	5		73	97	44	93
	RT	92	77	4	43		88	39	91
	Hunt	56	62	8	19	28		16	45
	Nay	103	107	36	72	77	100		102
	RLAB	65	57	7	23	25	71	14	
Fruit Basket	VK		14	1	0	1	21	3	12
	CLAB	15		1	0	3	16	4	15
	CLUV	28	28		28	28	27	24	29
	LABH	29	29	1		20	29	17	28
	RT	28	26	1	9		29	14	28
	Hunt	8	13	2	0	0		2	9
	Nay	26	25	5	12	15	27		27
	RLAB	17	14	0	1	1	20	2	
Orchid	VK		9	2	6	7	17	0	20
	CLAB	20		2	3	20	21	1	23
	CLUV	27	27		28	26	25	5	24
	LABH	23	26	1		13	20	1	22
	RT	22	9	3	16		16	1	19
	Hunt	12	8	4	9	13		1	7
	Nay	29	28	24	28	28	28		29
	RLAB	9	6	5	7	10	22	0	
Musician	VK		15	0	2	6	9	2	6
	CLAB	14		0	2	5	9	0	14
	CLUV	29	29		28	29	29	25	29
	LABH	27	27	1		21	27	16	24
	RT	23	24	0	8		25	13	27
	Hunt	20	20	0	2	4		5	14
	Nay	27	29	4	13	16	24		26
	RLAB	23	15	0	5	2	15	3	
Candles	VK		19	3	11	10	13	8	13
	CLAB	10		4	7	11	8	4	7
	CLUV	26	25		27	29	27	26	27
	LABH	18	22	2		19	21	10	19
	RT	19	18	0	10		18	11	17
	Hunt	16	21	2	8	11		8	15
	Nay	21	25	3	19	18	21		20
	RLAB	16	22	2	10	12	14	9	

TABLE E-8. Normalized matrix at 3 times luminance level

		VK	CLAB	CLUV	LABH	RT	Hunt	Nay	RLAB
Total	VK		0.49	0.05	0.16	0.21	0.52	0.11	0.44
	CLAB	0.51		0.06	0.10	0.34	0.47	0.08	0.51
	CLUV	0.95	0.94		0.96	0.97	0.93	0.69	0.94
	LABH	0.84	0.90	0.04		0.63	0.84	0.38	0.80
	RT	0.79	0.66	0.03	0.37		0.76	0.34	0.78
	Hunt	0.48	0.53	0.07	0.16	0.24		0.14	0.39
	Nay	0.89	0.92	0.31	0.62	0.66	0.86		0.88
	RLAB	0.56	0.49	0.06	0.20	0.22	0.61	0.12	
Fruit Basket	VK		0.48	0.03	0.00	0.03	0.72	0.10	0.41
	CLAB	0.52		0.03	0.00	0.10	0.55	0.14	0.52
	CLUV	0.97	0.97		0.97	0.97	0.93	0.83	1.00
	LABH	1.00	1.00	0.03		0.69	1.00	0.59	0.97
	RT	0.97	0.90	0.03	0.31		1.00	0.48	0.97
	Hunt	0.28	0.45	0.07	0.00	0.00		0.07	0.31
	Nay	0.90	0.86	0.17	0.41	0.52	0.93		0.93
	RLAB	0.59	0.48	0.00	0.03	0.03	0.69	0.07	
Orchid	VK		0.31	0.07	0.21	0.24	0.59	0.00	0.69
	CLAB	0.69		0.07	0.10	0.69	0.72	0.03	0.79
	CLUV	0.93	0.93		0.97	0.90	0.86	0.17	0.83
	LABH	0.79	0.90	0.03		0.45	0.69	0.03	0.76
	RT	0.76	0.31	0.10	0.55		0.55	0.03	0.66
	Hunt	0.41	0.28	0.14	0.31	0.45		0.03	0.24
	Nay	1.00	0.97	0.83	0.97	0.97	0.97		1.00
	RLAB	0.31	0.21	0.17	0.24	0.34	0.76	0.00	
Musician	VK		0.52	0.00	0.07	0.21	0.31	0.07	0.21
	CLAB	0.48		0.00	0.07	0.17	0.31	0.00	0.48
	CLUV	1.00	1.00		0.97	1.00	1.00	0.86	1.00
	LABH	0.93	0.93	0.03		0.72	0.93	0.55	0.83
	RT	0.79	0.83	0.00	0.28		0.86	0.45	0.93
	Hunt	0.69	0.69	0.00	0.07	0.14		0.17	0.48
	Nay	0.93	1.00	0.14	0.45	0.55	0.83		0.90
	RLAB	0.79	0.52	0.00	0.17	0.07	0.52	0.10	
Candles	VK		0.66	0.10	0.38	0.34	0.45	0.28	0.45
	CLAB	0.34		0.14	0.24	0.38	0.28	0.14	0.24
	CLUV	0.90	0.86		0.93	1.00	0.93	0.90	0.93
	LABH	0.62	0.76	0.07		0.66	0.72	0.34	0.66
	RT	0.66	0.62	0.00	0.34		0.62	0.38	0.59
	Hunt	0.55	0.72	0.07	0.28	0.38		0.28	0.52
	Nay	0.72	0.86	0.10	0.66	0.62	0.72		0.69
	RLAB	0.55	0.76	0.07	0.34	0.41	0.48	0.31	

TABLE E-9. Z-score matrix at 3 times luminance level

		VK	CLAB	CLUV	LABH	RT	Hunt	Nay	RLAB
Total	VK		-0.03	-1.65	-0.99	-0.84	0.03	-1.23	-0.18
	CLAB	0.00		-1.56	-1.28	-0.44	-0.10	-1.48	0.00
	CLUV	1.56	1.48		1.65	1.75	1.48	0.47	1.48
	LABH	0.95	1.23	-1.75		0.31	0.95	-0.33	0.84
	RT	0.81	0.41	-1.88	-0.33		0.67	-0.44	0.77
	Hunt	-0.05	0.08	-1.56	-0.99	-0.71		-1.13	-0.31
	Nay	1.18	1.41	-0.50	0.31	0.41	1.08		1.13
	RLAB	0.15	-0.03	-1.56	-0.88	-0.81	0.28	-1.18	
	SUM	4.60	4.55	-10.46	-2.51	-0.33	4.39	-5.32	3.73
Fruit Basket	VK		-0.05	-1.88	-2.33	-1.88	0.58	-1.28	-0.23
	CLAB	0.03		-1.88	-2.33	-1.28	0.13	-1.13	0.03
	CLUV	1.75	1.75		1.75	1.75	1.48	0.92	2.33
	LABH	2.33	2.33	-1.88		0.47	2.33	0.20	1.75
	RT	1.75	1.23	-1.88	-0.50		2.33	-0.05	1.75
	Hunt	-0.61	-0.15	-1.56	-2.33	-2.33		-1.56	-0.50
	Nay	1.23	1.08	-0.95	-0.23	0.03	1.48		1.48
	RLAB	0.20	-0.05	-2.33	-1.88	-1.88	0.47	-1.56	
	SUM	6.68	6.14	-12.36	-7.85	-5.12	8.80	-4.46	6.61
Orchid	VK		-0.5	-1.56	-0.84	-0.71	0.2	-2.33	0.47
	CLAB	0.47		-1.56	-1.28	0.47	0.58	-1.88	0.81
	CLUV	1.48	1.48		1.75	1.23	1.08	-0.95	0.92
	LABH	0.81	1.23	-1.88		-0.15	0.47	-1.88	0.67
	RT	0.67	-0.5	-1.28	0.13		0.13	-1.88	0.39
	Hunt	-0.23	-0.61	-1.13	-0.5	-0.15		-1.88	-0.71
	Nay	2.33	1.75	0.92	1.75	1.75	1.75		2.33
	RLAB	-0.5	-0.84	-0.95	-0.71	-0.41	0.67	-2.33	
	SUM	5.03	2.01	-7.44	0.3	2.03	4.88	-13.13	4.88
Musician	VK		0.03	-2.33	-1.56	-0.84	-0.50	-1.56	-0.84
	CLAB	-0.05		-2.33	-1.56	-0.95	-0.50	-2.33	-0.05
	CLUV	2.33	2.33		1.75	2.33	2.33	1.08	2.33
	LABH	1.48	1.48	-1.88		0.58	1.48	0.13	0.92
	RT	0.81	0.92	-2.33	-0.61		1.08	-0.15	1.48
	Hunt	0.47	0.47	-2.33	-1.56	-1.13		-0.95	-0.05
	Nay	1.48	2.33	-1.13	-0.15	0.13	0.92		1.23
	RLAB	0.81	0.03	-2.33	-0.95	-1.56	0.03	-1.28	
	SUM	7.33	7.59	-14.66	-4.64	-1.44	4.84	-5.06	5.02
Candles	VK		0.39	-1.28	-0.33	-0.41	-0.15	-0.61	-0.15
	CLAB	-0.41		-1.13	-0.71	-0.33	-0.61	-1.13	-0.71
	CLUV	1.23	1.08		1.48	2.33	1.48	1.23	1.48
	LABH	0.31	0.67	-1.56		0.39	0.58	-0.41	0.39
	RT	0.39	0.31	-2.33	-0.41		0.31	-0.33	0.20
	Hunt	0.13	0.58	-1.56	-0.61	-0.33		-0.61	0.03
	Nay	0.58	1.08	-1.28	0.39	0.31	0.58		0.47
	RLAB	0.13	0.67	-1.56	-0.41	-0.23	-0.05	-0.50	
	SUM	2.36	4.78	-10.70	-0.60	1.73	2.14	-2.36	1.71

Appendix F Successive Haploscopic Device

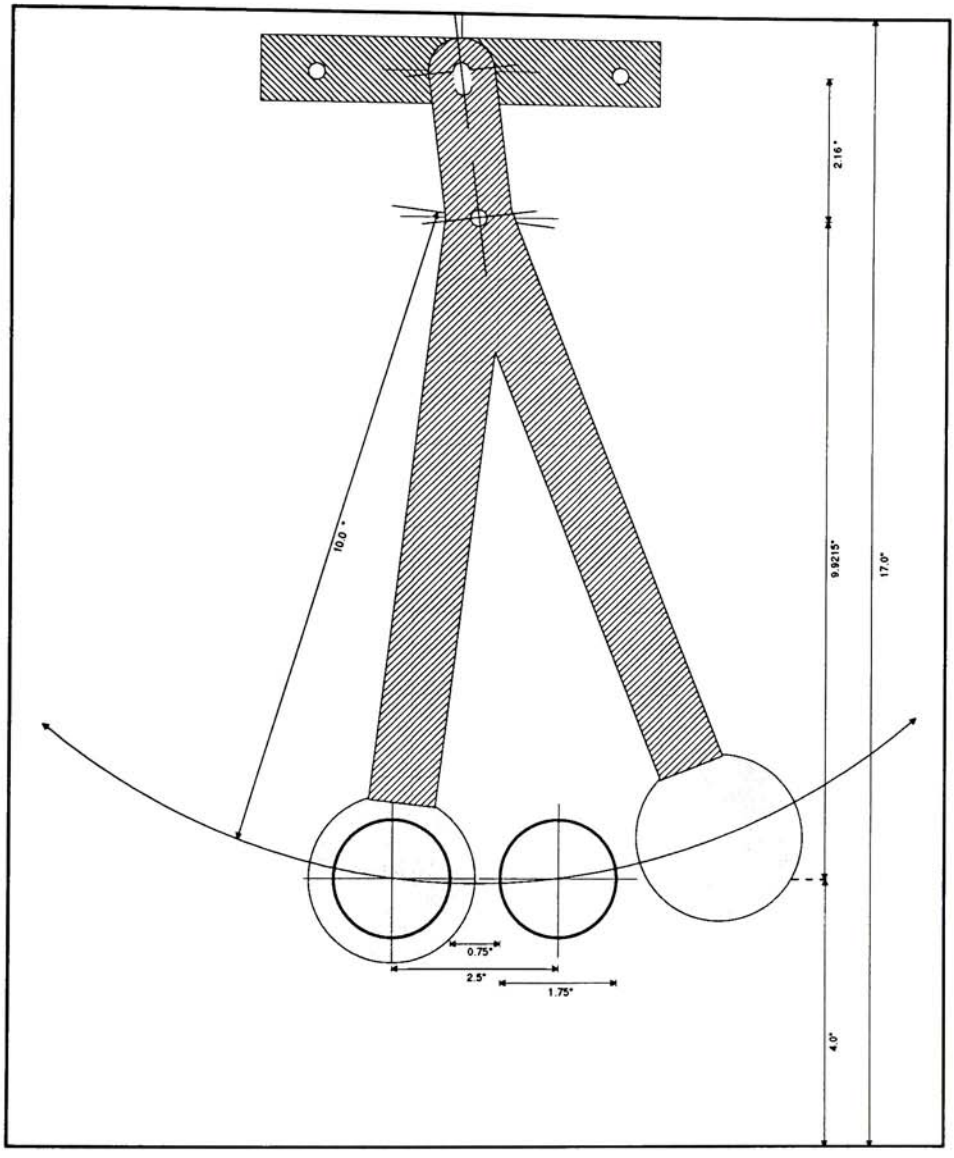

Fig. F-1 Mechanical drawing of successive haploscopic device

Appendix G Z scores of the normal distribution corresponding to proportions (p)

TABLE G-1. Z-scores corresponding to proportions (Gescheider, 1985)

p	*z*	*p*	*z*	*p*	*z*	*p*	*z*
0.01	-2.33	0.26	-0.64	0.51	0.03	0.76	0.71
0.02	-2.05	0.27	-0.61	0.52	0.05	0.77	0.74
0.03	-1.88	0.28	-0.58	0.53	0.08	0.78	0.77
0.04	-1.75	0.29	-0.55	0.54	0.10	0.79	0.81
0.05	-1.65	0.30	-0.52	0.55	0.13	0.80	0.84
0.06	-1.56	0.31	-0.50	0.56	0.15	0.81	0.88
0.07	-1.48	0.32	-0.47	0.57	0.18	0.82	0.92
0.08	-1.41	0.33	-0.44	0.58	0.20	0.83	0.95
0.09	-1.34	0.34	-0.41	0.59	0.23	0.84	0.99
0.10	-1.28	0.35	-0.39	0.60	0.25	0.85	1.04
0.11	-1.23	0.36	-0.36	0.61	0.28	0.86	1.08
0.12	-1.18	0.37	-0.33	0.62	0.31	0.87	1.13
0.13	-1.13	0.38	-0.31	0.63	0.33	0.88	1.18
0.14	-1.08	0.39	-0.28	0.64	0.36	0.89	1.23
0.15	-1.04	0.40	-0.25	0.65	0.39	0.90	1.28
0.16	-0.99	0.41	-0.23	0.66	0.41	0.91	1.34
0.17	-0.95	0.42	-0.20	0.67	0.44	0.92	1.41
0.18	-0.92	0.43	-0.18	0.68	0.47	0.93	1.48
0.19	-0.88	0.44	-0.15	0.69	0.50	0.94	1.56
0.20	-0.84	0.45	-0.13	0.70	0.52	0.95	1.65
0.21	-0.81	0.46	-0.10	0.71	0.55	0.96	1.75
0.22	-0.77	0.47	-0.08	0.72	0.58	0.97	1.88
0.23	-0.74	0.48	-0.05	0.73	0.61	0.98	2.05
0.24	-0.71	0.49	-0.03	0.74	0.64	0.99	2.33
0.25	-0.67	0.50	0.00	0.75	0.67		

Appendix H Hard copy Samples

Note : The pictures included in this section may not represent actual images accurately as used in the experiment due to aging and variability, both of which were not tested.

Samples are in the order of

1. Originals
2. von Kries
3. CIELAB
4. CIELUV
5. HNULAB
6. Reilly-Tannenbaum
7. Hunt
8. Hunt (1/3 luminance level)
9. Hunt (3 times luminance level)
10. Nayatani
11. Nayatani (1/3 luminance level)
12. Nayatani (3 times luminance lelvel)
13. RLAB *(marked as Fairchild 91)*
14. RLAB (1/3 luminance level) *(marked as Fairchild 91 (1/3X))*
15. RLAB (3 times luminance level) *(marked as Fairchild 91 (3X))*

ORIGINAL

von Kries

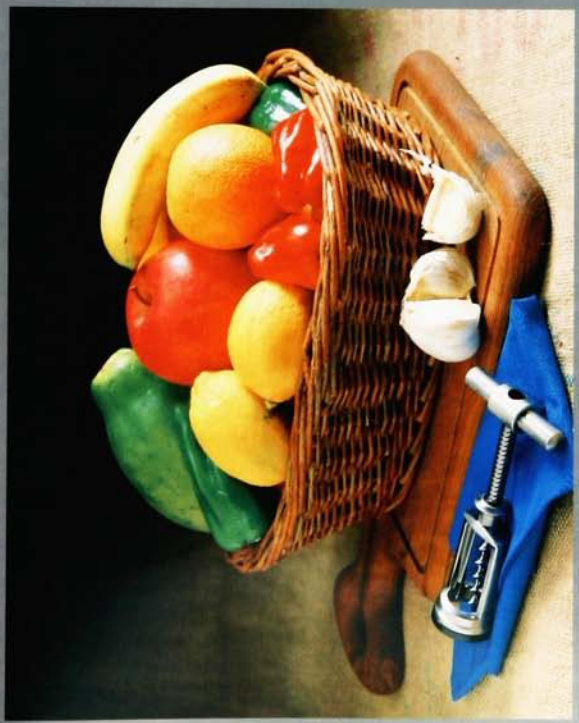

CIELAB

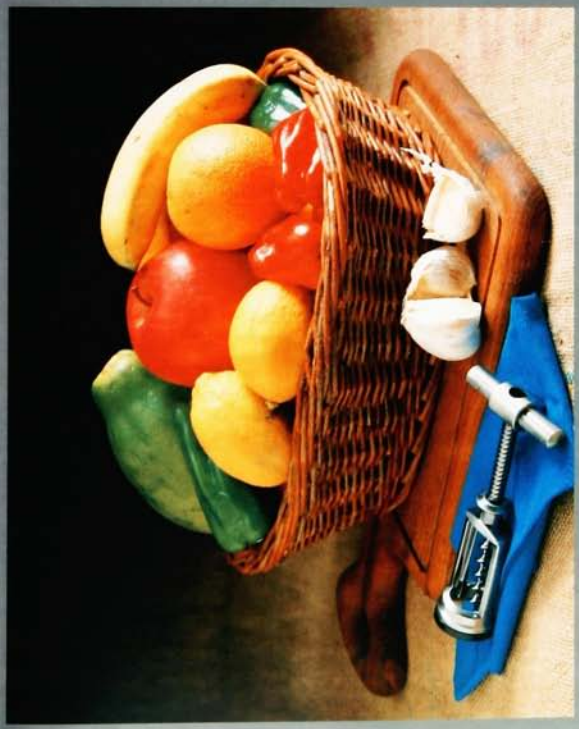

CIELUV

Hunt

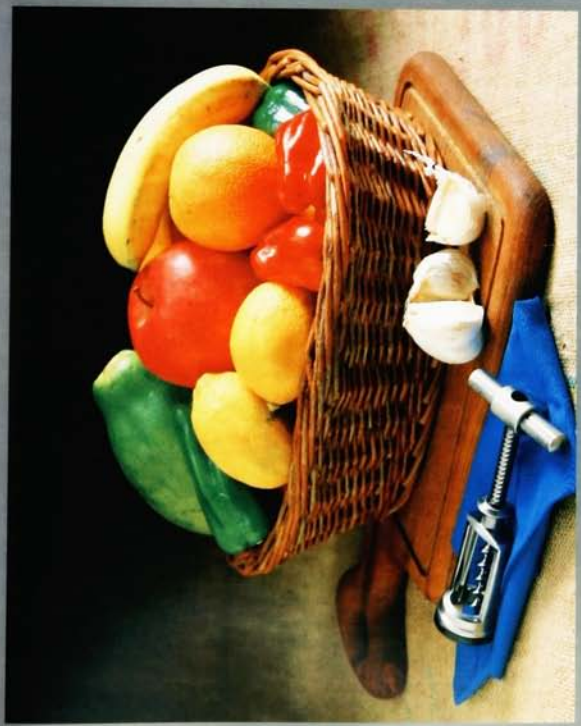

HNULAB

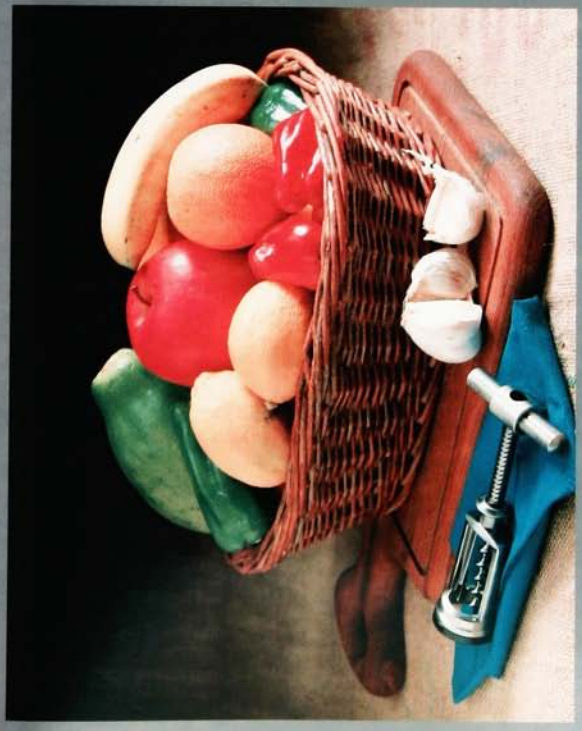

Reilly-Tannenbaum

Hunt

Hunt (1/3x)

Hunt (3x)

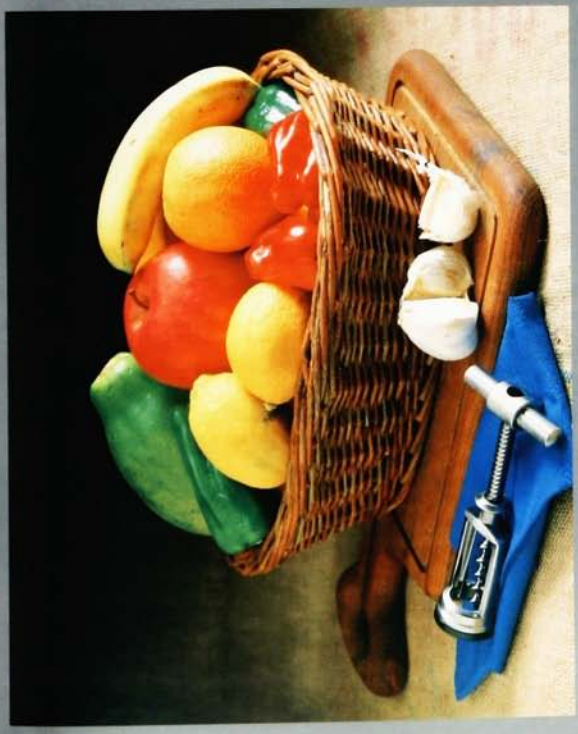

Nayatani

Nayatani (1/3x)

Nayatani (3x)

Fairchild 91

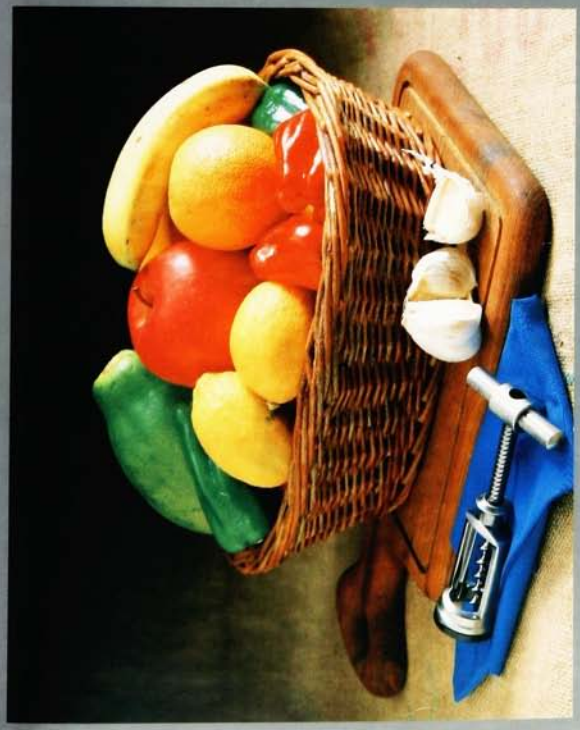

Fairchild 91 (1/3x)

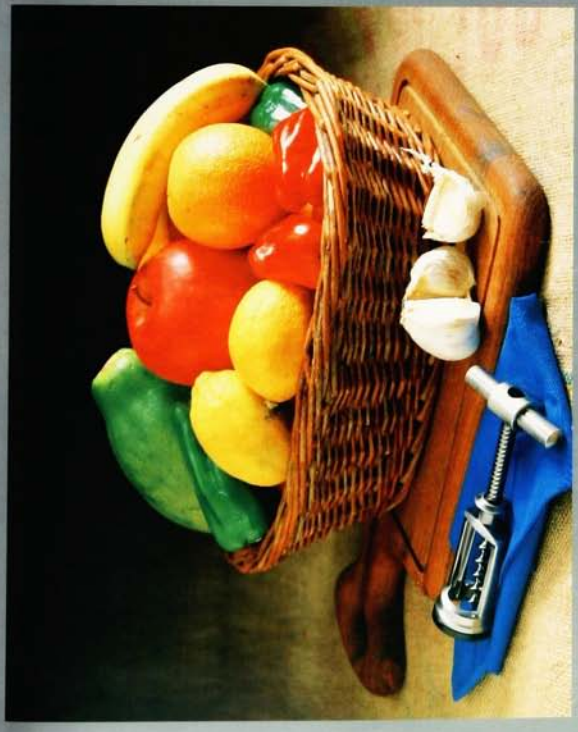

Fairchild 91 (3x)